Development of bispecific antibodies for selective stimulation of the CD95 death receptor on malignant and normal activated B-cells

Dissertation

der Mathematisch-Naturwissenschaftlichen Fakultät
der Eberhard Karls Universität Tübingen
zur Erlangung des Grades eines
Doktors der Naturwissenschaften
(Dr. rer. nat.)

vorgelegt von
M.Sc. Kristina Nalivaiko
aus Jurbarkas, Litauen

Tübingen
2016

Gedruckt mit Genehmigung der Mathematisch-Naturwissenschaftlichen Fakultät der Eberhard Karls Universität Tübingen.

Tag der mündlichen Qualifikation:	01.12.2016
Dekan:	Prof. Dr. Wolfgang Rosenstiel
1. Berichterstatter	Prof. Dr. Hans-Georg Rammensee
2. Berichterstatter	Prof. Dr. Gundram Jung

Summary

Treatment of oncological and autoimmune diseases still remains a considerable challenge to modern medicine. Current therapy options such as chemotherapy and radiotherapy in oncology and glucocorticoids or other conventional immunosuppressive drugs for autoimmune diseases are often of limited efficacy. They suffer from a lack of specificity, with respect to the eradication of tumour and immune cells, respectively. The use of monoclonal antibodies in oncology allowed in some instances specific targeting of tumour cells and thus, improved this situation in the last decades. Some antibodies, such as anti-CD20 antibody Rituximab, targeting normal and malignant B-cells, are meanwhile firmly established in oncological treatment regimes. Interestingly, over the last years the anti B-cell activity of Rituximab was used in addition in numerous studies for the treatment of autoimmune diseases.

Many strategies have been developed to further improve therapeutic activity of monoclonal antibodies. One of them is the development of bispecific antibodies recognising target cell antigens and effector cells or effector molecules at the same time. The "bispecific concept" used in this work is the target cell restricted stimulation of the death receptor CD95 (APO-1/Fas) with bispecific antibodies as described by Jung et al. in 2000. Whereas initial experiments were performed using chemically hybridised bispecific antibodies with CD20×CD95 specificity, the goal of this thesis was the generation of recombinant antibodies within a suitable format.
To this end, a recombinant CD20×CD95 molecule in the so called FabSc format, designated BS9520 was developed and characterised in various *in vitro* and *in vivo* assays. It was found that the capability of this antibody to suppress the growth of malignant B-cells *in vitro* and *in vivo* and to specifically deplete normal, activated B-cells from PBMC cultures was superior to that achieved with monospecific clinically established anti-CD20 antibodies including a newly developed third generation Fc-optimized CD20 antibody. Moreover, the bispecific antibody was the only reagent capable of significantly suppressing IgG production by activated B-cells *in vitro*. These findings imply that the bispecific CD95×CD20 antibody might become an attractive reagent for the treatment of B-cell malignancies as well as B-cell mediated autoimmune diseases.

In the second part of this work a completely new approach for the stimulation of the CD95 death receptor on antigen specific B-cells was evaluated. For proof of principle, the CD20 part in the BS9520 antibody was replaced by antigen fragments (tetanus or diphtheria toxoid derivatives). We named these fusion proteins BS95TT and BS95DT, respectively. Such protein should bind to B-cell receptor via their toxoid part and with the CD95 antibody part to CD95 receptor on activated TT-specific B-cells. Thereby, apoptosis is induced only in an antigen-specific fashion. This approach could be used for the treatment of autoimmune diseases if the antigen inducing auto-antibody production is known (such as *Myasthenia gravis*, multiple sclerosis and others).

Zusammenfassung

Die Behandlung von onkologischen und Autoimmunerkrankungen ist nach wie vor eine große Herausforderung für die moderne Medizin. Aktuelle Therapieoptionen wie Chemotherapie und Strahlentherapie in der Onkologie und Glukokortikoide oder andere immunsuppressive Medikamente für Autoimmunerkrankungen sind aufgrund ihrer eingeschränkten Spezifität oft nicht effektiv genug. Durch die Verwendung von monoklonalen Antikörpern in der Onkologie konnte bei einigen Erkrankungen spezifisches Targeting und damit eine verbesserte Therapie in den letzten Jahrzehnten erreicht werden. Außerdem werden einige Antikörper, die bereits für die Immuntherapie von Krebs existieren (z. B. anti-CD20-Antikörper Rituximab), zusätzlich in zahlreichen Studien für die Behandlung von Autoimmunerkrankungen verwendet.

In den letzten Jahrzehnten wurden viele Strategien entwickelt um die Wirksamkeit von monoklonalen Antikörpern zu verbessern. Eine dieser Strategien liegt in der Entwicklung bispezifischer Antikörper, welche Zielzellen und Effektorzellen oder Effektormoleküle gleichermaßen erkennen. Das in dieser Arbeit angewendete "Bispezifische Konzept" beruht auf der Stimulierung des CD95 Todesrezeptores mit bispezifischen Antikörpern (beschrieben von Jung et al. in 2000). Während die ersten Experimente mit chemisch-hybridisierten bispezifischen CD20×CD95 Antikörpern durchgeführt wurden, war das Hauptziel dieser Arbeit die Entwicklung von rekombinanten bispezifischen Antikörpern in einem geeigneten Format.
Dazu wurde in der ersten Teil dieser Arbeit ein rekombinanter CD95×CD20 Antikörper BS9520 im FabSc Format entwickelt und in unterschiedlichen *in vitro* und *in vivo* Untersuchungen charakterisiert. Es wurde festgestellt, dass die Lyse von humanen CD20 exprimierenden Lymphomzellen *in vitro* und *in vivo* durch BS9520 effizienter ausgelöst wurde als durch monospezifische CD20 Antikörper. Dies schließt einen neu entwickelten Fc-optimierten CD20 Antikörper ein. BS9520 war auch in der Lage normale, aktivierte B-Zellen selektiv zu depletieren und, im Gegensatz zu monospezifischen CD20 Antikörpern, die Antikörperproduktion *in vitro* effizient zu unterdrücken. Diese Ergebnisse bedeuten, dass der bispezifische CD95×CD20 Antikörper ein prototypisches Reagenz zur Behandlung von B-Zell-vermittelten Autoimmunerkrankungen werden kann.

Im zweiten Teil dieser Arbeit wurde ein völlig neuer Ansatz für die Stimulation der CD95 Todesrezeptoren auf Antigen-spezifischen B-Zellen untersucht. Als prinzipieller Beweis für die Wirksamkeit dieser Technik wurde der CD20 Teil im bispezifischen BS9520 Antikörper durch Antigen-Fragmente ersetzt (Tetanus oder Diphtherie Toxoid Derivate). Diese Fusionsproteine wurden als BS95TT und BS95DT bezeichnet. Ein solches Protein sollte an B-Zell Rezeptoren über den Toxoid-Teil und mit dem CD95-Antikörper an CD95-Rezeptoren auf aktivierten B-Zellen binden. Auf diese Weise sollte Apoptose nur in Antigen-spezifischen aktivierten B-Zellen induziert werden. Dieser Ansatz könnte für die Behandlung von Autoimmunerkrankungen eingesetzt werden, bei denen das Auto-Antikörper induzierende Antigen bekannt ist (z.B. *Myasthenia gravis*, Multiple Sklerose (MS) und andere).

Own publications

Publication:

Nalivaiko, K., Hofmann, M., Kober, K., Teichweyde, N., Krammer, P.H., Rammensee, H.-G., Grosse-Hovest, L., Jung, G. (2016). A recombinant bispecific CD20 × CD95 antibody with superior activity against normal and malignant B-cells. *Molecular Therapy*, 24(2):298–305.

Poster presentations:

- **Kristina Nalivaiko**, Martin Hofmann, Ludger Grosse-Hovest, Hans-Georg Rammensee and Gundram Jung.
  Selective killing of activated B-cells and inhibition of antibody production with bispecific CD20 × CD95 antibodies
  11th CIMT Annual Meeting, Mainz, 2013; 15th International Congress of Immunology, Milan, 2013.

- **Kristina Nalivaiko**, Martin Hofmann, Ludger Grosse-Hovest, Hans-Georg Rammensee and Gundram Jung.
  Development of recombinant bispecific antibodies for selective stimulation of the CD95 death receptor on activated B-cells and lymphoma cells
  12th CIMT Annual Meeting, Mainz, 2014; 4th Translational Immunology School (TIS), Potsdam, 2015; PEGS Europe, Lisbon, 2015.

Contents

List of Figures

List of Tables

Chapter 1

Introduction

With more than 3 million new cases and 1.7 million deaths each year (WHO/Europe, 2016), cancer is the most important cause of death and morbidity in Europe after cardiovascular diseases. A significant part of cancer diseases consists of haematological malignancies – tumours affecting the blood, bone marrow, and lymphatic system. Surgical treatment is obviously not possible and therapy, including hematopoietic stem cell transplantation, is often of limited success,whereas side effects and treatment costs are high.
Autoimmune diseases affect approximately 1 of 12 individuals living in the Western Hemisphere, representing a significant cause of morbidity, chronic disability and health-care burden (Li et al., 2015). The National Institutes of Health (NIH) estimates, that up to 23.5 million Americans suffer from autoimmune diseases with rising prevalence. This diverse group encompasses more than 100 diseases, including type-1 diabetes, multiple sclerosis (MS), rheumatoid arthritis (RA), Crohn's disease and systemic lupus erythematosus (SLE). Although autoimmune diseases do not cause high mortality, they are responsible for more than $ 100 billion in direct health care costs annually in the US (AARDA, 2016). Thus, autoimmune diseases are among the most expensive health disorders society has to face.

1.1 Haematological malignancies

Haematological malignancies are derived from one of the two major blood cell lineages: myeloid and lymphoid cells. The myeloid cell line produces granulocytes, erythrocytes, thrombocytes, macrophages and mast cells; the lymphoid cell line B-, T-, NK and plasma cells. Lymphomas, lymphocytic leukaemias, and myeloma derive from lymphoid precursors, whereas acute and chronic myelogenous leukaemia, myelodysplastic syndromes and myeloproliferative diseases are myeloid in origin (Vardiman et al., 2009). The proposed WHO classification of haematologic malignancies stratifies these neoplastic disorders primarily according to lineage: myeloid neoplasms, lymphoid neoplasms, mast cell disorders, and histiocytic neoplasms. Within each category, distinct diseases are defined according to a combination of morphology, immunophenotype, genetic features, and clinical syndromes (Harris et al., 2000).
B-cell malignancies belong to the group of lymphoid neoplasms. They represent a diverse collection of diseases, including most non-Hodgkin's lymphomas (NHL), some leukaemias and myelomas. Examples include B-cell acute lymphoblastic leukaemia (B-ALL) accounting for 80-85% of childhood ALL (American cancer society, 2016), chronic lymphocytic leukaemia (CLL), follicular lymphoma, mantle cell lymphoma (MCL) and diffuse large B-cell lymphoma (DLBCL) (Zelenetz et al., 2013). B-cell malignancies can be divided into 2 clinically relevant categories: indolent and aggressive. Indolent malignancies, such as follicular lymphoma, small lymphocytic lymphoma and marginal zone lymphoma, are characterised by slow growth and a high initial response rate, followed by a relapsing and progressive disease course (Guerard and Bishop, 2012; Vidal et al., 2012). Aggressive lymphomas, such as DLBCL, MCL and Burkitt's lymphoma, are characterised by rapid growth and lower initial response rates, with shorter overall survival (Dotan et al., 2010; Vidal et al., 2012). B-ALL is characterised by its aggressiveness and short latency (Sanjuan-Pla et al., 2015).

Current therapy strategies for B-cell malignancies include radiation therapy, chemotherapy and immunotherapy. Radiation therapy (also known as external beam radiation) is used in early-stage limited disease, as consolidative therapy in aggressive lymphomas that respond to chemotherapy and to manage some complications. Chemotherapy, which kills rapidly-dividing cells, is used as a curative as well as palliative intervention. Some of the chemotherapeutic drugs commonly used to treat lymphoma include alkylating agents (Cyclophosphamide), platinum drugs (Cisplatin, Carboplatin, Oxaliplatin), anti-metabolites (Methotrexate) and others like Doxorubicin and Vincristine. In principle both, radiotherapy and chemotherapy affect proliferating cells rather unspecifically, that is, not specific for tumour cells. Small-molecule kinase inhibitors such as Ibrutinib promised improved specificity due to their defined mode of action. Ibrutinib inhibits Bruton's tyrosine kinase (BTK) – a key component of B-cell receptor (BCR) signalling that functions as an important regulator of cell proliferation and cell survival in various B-cell malignancies. Ibrutinib treatment leads to inhibition of downstream BCR signaling and cell apoptosis. However, BTK is also involved in signalling pathways downstream of many other receptors, including G protein-coupled chemokine receptors and Toll-like receptors (TLRs) (Hendriks et al., 2014).
In contrast to conventional chemotherapy, cancer immunotherapy promises an increased specificity. It's goal is to induce or enhance immune responses to support the immune system in defeating cancer. Cell-based therapy, useful for the treatment of B-cell malignancies, includes hematopoietic stem cell transplantation (Bhatt and Vose, 2014), adoptive transfer of NK-cells (Ljunggren and Malmberg, 2007) or chimeric antigen receptors (CAR)-modified T-cells (Porter et al., 2011). Therapy with biological agents consists mostly of therapeutic antibodies (Alemtuzumab, Rituximab) and cytokines such as interferon-α (Kirkwood, 2002). Newer therapeutic agents for lymphomas and lymphocytic leukaemias such as nucleic acids (O'Brien et al., 2005; Badros et al., 2005) and peptide vaccines (Kowalewski et al., 2015) are still in the research phase.

1.2 B-cell mediated autoimmune diseases

A century ago Paul Ehrlich proposed that immune reactivity against self, which he called *"horror autotoxicus"*, and which is now called autoimmunity, would be incompatible with life because of potentially devastating consequences for the host. But this view was proven wrong after the demonstration of auto-antibodies and the emergence of a theoretical basis for autoreactivity (Burnet, 1976). In the 1960s, it was believed that all self-reactive lymphocytes were eliminated during their development in the bone marrow and thymus and that a failure to eliminate these lymphocytes led to autoimmune consequences. Since the late 1970s, a broad experimental evidence has countered that belief, revealing that not all self-reactive lymphocytes are deleted during T-cell and B-cell maturation. Normal healthy individuals have been shown to possess mature, recirculating, self-reactive lymphocytes. Due to the fact that the presence of such cells in the peripheral blood does not inevitably result in autoimmune reactions, their activity must be regulated in healthy individuals through clonal anergy or clonal suppression. A breakdown of this regulation can lead to ac-

tivation of self-reactive clones of T- or B-cells, generating humoral or cell-mediated responses against self antigens (Goldsby, 2003).
Very often the autoimmune damage of cells or organs is caused by auto-antibodies, produced by activated B-cells (Table 1.2). A number of viruses and bacteria can induce nonspecific polyclonal B-cell activation. Gram-negative bacteria, cytomegalovirus and Epstein-Barr virus (EBV) are all known to be such polyclonal activators, inducing the proliferation of numerous clones of B-cells. If autoreactive B-cells are activated by this mechanism, auto-antibodies can appear. For instance, during infectious mononucleosis, which is caused by EBV, a variety of auto-antibodies are produced, including those reactive to T- and B-cells, rheumatoid factors, and antinuclear antibodies (Wucherpfennig, 2001). Similarly, B-cells from patients with SLE produce large quantities of IgM in cell culture, suggesting that lymphocytes have been polyclonally activated. Many patients suffering from acquired immune deficiency syndrome (AIDS) also show high levels of auto-antibodies such as anti-cardiolipin, anti-β2 GPI (β2-glycoprotein I), anti-DNA, anti-small nuclear ribonucleoproteins (snRNP), anti-thyroglobulin, anti-thyroid peroxidase, anti-myosin, and anti-erythropoietin antibodies (Zandman-Goddard and Shoenfeld, 2002).
In some autoimmune diseases, antibodies act as agonists, binding to hormone receptors replacing the normal ligand and stimulate inappropriate activity. This usually leads to an overproduction of mediators or cell proliferation. Conversely, auto-antibodies may act as antagonists, binding hormone receptors but blocking receptor function rather than stimulating it. This generally causes impaired secretion of mediators and gradual atrophy of the affected organ. For example, in autoimmune thyroid disease (AITD) auto-antibodies bind to the thyroid stimulating hormone receptor (TSHR) and can act as either agonists, mimicking the biological activity of TSH, or as antagonists inhibiting the action of TSH (Sanders et al., 2010).
One representative example of a systemic autoimmune disease is SLE. Affected individuals may produce auto-antibodies to a vast array of tissue antigens, such as DNA, histones, red blood cells (RBCs), platelets, leukocytes, and clotting factors; interaction of these auto-antibodies with their specific antigens produces various symptoms. Auto-antibodies specific for RBCs and platelets may lead to complement-mediated lysis, resulting in haemolytic anaemia or thrombocytopenia, respectively. When immune complexes of auto-antibodies with various nuclear antigens are deposited along the walls of small blood vessels, a type III hypersensitive immune reaction develops. The antigen-antibody complexes activate the complement system by generating membrane-attacking complexes which damage the wall of the blood vessel, resulting in vasculitis and glomerulonephritis (SK Mohanty, 2008). Many individuals with rheumatoid arthritis produce a group of auto-antibodies called rheumatoid factors that are reactive towards determinants of the Fc region of IgG. The classic rheumatoid factor is an IgM antibody. Such auto-antibodies bind to normal circulating IgG, forming IgM-IgG complexes that are deposited in the joints. These immune complexes can activate the complement cascade, and, as in the situation described before, result in a type III hypersensitive reaction, which leads to chronic inflammation of the joints (Leadbetter et al., 2002).
Current therapies for B-cell mediated autoimmune diseases include treatment with immunosuppressive drugs or monoclonal antibodies which interact with some components specifically involved in an autoimmune reaction.

Table 1.1: **Selected autoimmune diseases in humans**
(Adapted from (Goldsby, 2003))

Disease	**Self-antigen**	**Immune response**
ORGAN-SPECIFIC AUTOIMMUNE DISEASES		
Addison's disease	Adrenal cells	Auto-antibodies
Autoimmune hemolytic anemia	RBC membrane proteins	Auto-antibodies
Goodpasture's syndrome	Renal and lung basement membranes	Auto-antibodies
Graves' disease	Thyroid-stimulating hormone receptor	Auto-antibody (stimulating)
Hashimoto's thyroiditis	Thyroid proteins and cells	T_{DTH} cells, auto-antibodies
Idiopathic thrombocyopenia purpura	Platelet membrane proteins	Auto-antibodies
Insulin-dependent diabetes mellitus	Pancreatic beta cells	T_{DTH} cells, auto-antibodies
Myasthenia gravis	Acetylcholine receptors	Auto-antibodies
Pernicious anemia	Gastric parietal cells; intrinsic factor	Auto-antibodies
Poststreptococcal glomerulonephritis	Kidney	Antigen-antibody complexes
Spontaneous infertility	Sperm	Auto-antibodies
SYSTEMIC AUTOIMMUNE DISEASES		
Ankylosing spondylitis	Vertebrae	Immune complexes
Multiple sclerosis	Brain or white matter	T_H1 cells, T_C cells, auto-antibodies
Rheumatoid arthritis	Connective tissue, IgG	Auto-antibodies, immune complexes
Scleroderma	Nuclei, heart, lungs, gastrointestinal tract, kidney	Auto-antibodies
Sjogren's syndrome	Salivary gland, liver, kidney, thyroid	Auto-antibodies
Systemic lupus erythematosus (SLE)	DNA, nuclear protein, RBC and platelet membranes	Auto-antibodies, immune complexes

In general, introduction of antibody-based therapies in the last decades have demonstrated promising results in oncology as well as in autoimmune diseases.

1.3 Antibody-based immunotherapy

The first therapeutic monoclonal antibody approved by FDA was the anti-CD3 antibody Muromonab (1986) used to prevent acute organ rejection (Emmons and Hunsicker, 1987). It happened more than a decade after the development of the hybridoma technology (Köhler and Milstein, 1975). As a result of technological breakthroughs in the field of molecular biology and cloning, progress in the therapeutic antibody field developed very fast in the 1980-1990ies. Currently antibody-based therapeutics enjoy unprecedented success. There are more than 40 monoclonal antibodies approved for clinical use in the European Union or United States (Antibody Society, 2015) and hundreds are in clinical trials for treatment of various diseases including cancer, immune disorders and infections.

1.3.1 Antibodies: structure and function

Antibodies, also known as immunoglobulins (Ig), are large (150 kDa – 900 kDa), Y-shape proteins produced by plasma cells. They are used by the immune system to identify and neutralize pathogens such as bacteria and viruses. An antibody monomer contains two light chains and two heavy chains, which are linked by multiple disulphide bonds (Fig. 1.1 a).

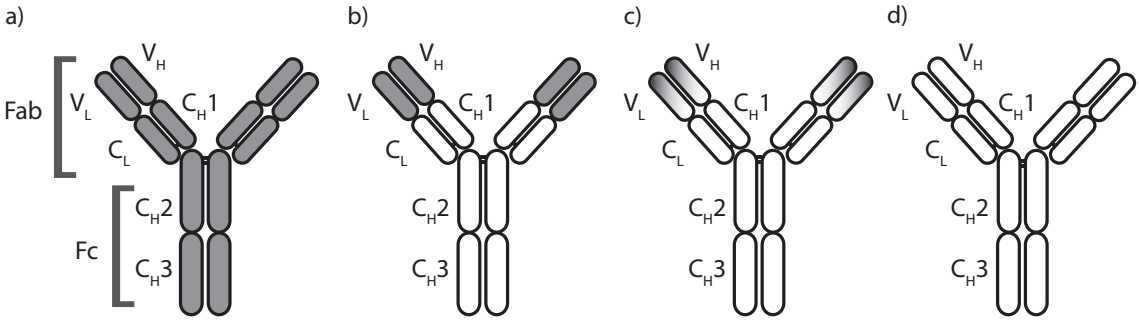

Figure 1.1: **Structure of an IgG antibody with various humanized isoforms** a) murine antibody: V_L and C_L are variable light and constant light domains, respectively, V_H and C_H are variable heavy and constant heavy domains, respectively; Fc part – fragment crystallizable, Fab – fragment antigen-binding b) chimeric antibody: mouse constant domains were exchanged to human constant domains; c) humanized antibodies: mouse constant domains and framework regions (FRs) were exchanged to human sequences; d) fully human antibody

In mammals, antibodies can be subdivided into five main classes or isotypes – IgA, IgD, IgE, IgG and IgM according to the heavy chain they contain – α, δ, ϵ, γ or μ respectively. They differ in the sequence and number of constant domains, hinge structure and the valency of the antibody. IgA, for instance, is typically found as a dimer and IgM as a pentamer. Antibody light chains fall into two classes in

mammals, κ and λ (Cruse and Lewis, 2010). Most of the therapeutic antibodies derive from IgG κ isotype.
An antibody recognises an antigen via complementarity-determining regions (CDRs). These are short, hypervariable amino acid sequences found in the variable domains of both light and heavy chains. Due to the fact, that those parts are the only responsible for antigen binding, the remaining part of the antibody molecule can be manipulated by *in vitro* genetic engineering approaches to reduce its immunogenicity. Fig. 1.1 a depicts a normal murine antibody, the exchange of the murine constant domains to human results in a chimeric antibody (Fig. 1.1 b) and exchange of the all murine sequences except CDRs results in a humanised antibody (Fig. 1.1 c). Fully *human antibodies* (Fig. 1.1 d) can be obtained using phage display (McCafferty et al., 1990), transgenic animals (Mendez et al., 1997; Lonberg et al., 1994) or single cell cloning (Traggiai et al., 2004) technology.
After binding to a target, the Fc part of the antibody molecule can recruit effector cells such as natural killer cells, macrophages, or neutrophils, and/or activate the complement components in serum to destroy the target cells. These properties, referred to as "antibody-dependent cellular cytotoxicity" (ADCC) (Wisloff et al., 1974) , "antibody-dependent cellular phagocytosis" (ADCP) (Krauss et al., 1994) and "complement-dependent cytotoxicity" (CDC) (Ross, 1989), are fundamental aspects of natural antibody biology that are being manipulated to create therapeutics with more potent biological activity and longer half-life. In addition to ADCC, ADCP and CDC activities, the Fc region of an antibody is also responsible for the long half-life of the molecule through its interaction with the neonatal receptor FcRn (Roopenian and Akilesh, 2007).

1.3.2 Targets for antibody therapy

A key challenge of antibody-based cancer therapy is to identify antigens/targets that are suitable for antibody-based therapeutics. They should be overexpressed, mutated or selectively expressed on malignant cells compared to normal tissues. Once a suitable target is identified, one can decide which mechanism of action will be appropriate to achieve the desired therapeutic effect.

1.3.2.1 Targets for leukaemia/lymphoma

Cancer cells differ from normal cells due to genomic mutations in oncogenes and/or tumour suppressor genes (Chow, 2010). Once the integrity of the genome is compromised, cells are more likely to aquire additional genetic defects, some of which may give rise to tumour-associated antigens (overexpressed on tumour cells, but also present on normal cells) (Sensi and Anichini, 2006). Leukaemias and lymphomas have less mutations compared to other cancer types such as melanoma, lung and bladder cancer (Lawrence et al., 2013). Thus it is particularly challenging to find appropriate targets for monoclonal antibody (mAb)-based therapy expressed exclusively on leukaemic cells. Most of the antigens targeted in leukaemia and lymphoma are cell surface proteins also found on normal cells of the haemotopoietic system.

The main targets for B-cell malignancies are currently CD20 and CD19 lymphocyte antigens. The **CD20** molecule is expressed on all stages of B-cell development except the first and last. It is a 297 amino acid phosphoprotein with four transmembrane domains. CD20 is found on B-cell lymphomas, hairy cell leukemia and B-cell chronic lymphocytic leukemia making it a suitable biomarker for immunotherapy targeting B-cell derived diseases. Rituximab was the first anti-CD20 monoclonal antibody approved by the FDA for treatment of B-cell malignancies, and it is perhaps the most extensively investigated drug in this field. It was first approved in 1997 for the treatment of low grade B-cell lymphoma, and subsequently was shown to improve cure rates when added to the standard CHOP ((C)yclophosphamide, (H)ydroxydaunorubicin, (O)ncovin, (P)rednisone) chemotherapy regimen for patients with diffuse large B-cell lymphoma (Lim and Levy, 2014).
In order to decrease immunogenicity and improve antitumour activity, new generations of anti-CD20 monoclonal antibodies are being developed (Cang et al., 2012). Second-generation anti-CD20 antibodies (humanised molecules) include a fully human type I anti-CD20 antibody Ofatumumab (Arzerra®) (Coiffier et al., 2008), a humanised type I anti-CD20 antibody Veltuzumab (with complementarity-determining regions (CDRs) identical to Rituximab, except for a single amino acid change, Asp101 instead of Asn101 (Stein et al., 2004; Goldenberg et al., 2010)) and humanised type I anti-CD20 antibody Ocrelizumab differing from Rituximab at several amino acid positions within the CDRs of the light chain and heavy chain variable regions (Morschhauser et al., 2010).
The third-generation humanized anti-CD20 antibodies have an engineered Fc region to increase their binding affinity for the FcγRIIIa receptor and thus, enhanced ADCC activity. Those include type II anti-CD20 antibody Obinutuzumab (Gazyva®, GA-101) approved by FDA in 2013 (Goede et al., 2014), Ocaratuzumab (AME-133v, LY2469298) (Ganjoo et al., 2015) and PRO131921 (Casulo et al., 2014) currently undergoing active clinical development. Recent studies with CLL patients showed superiority of GA-101 over Rituximab (Goede et al., 2014; Goede et al., 2015).
CD19 is an antigen expressed on B-cells from earliest detectable B-lineage cells during development to B-cell blasts but is lost on maturation to plasma cells. It is maintained on more than 95% B-cell malignancies (Ramos et al., 2014), making this molecule an attractive target for antibody therapy. CD19 antibody is also benefiting from the Fc-optimisation described above: a humanized CD19 monoclonal antibody with an engineered Fc region (also known as XmAb5574 or MOR00208) just completed Phase 1 clinical trial in patients with relapsed or refractory CLL (Woyach et al., 2014) and Phase 2 clinical trial study is currently recruiting participants (ClinicalTrials.gov Identifier: NCT02005289). Moreover, CD19 antibody is part of bispecific CD19×CD3 antibody Blinatumomab (Bargou et al., 2008) and also the first antibody used within chimeric antigen receptors (CAR) engineered T-cells (Porter et al., 2011).
Anti-CD22 antibody Epratuzumab binds to the glycoprotein CD22 of mature and malignant B-cells and is used in adult acute lymphoblastic leukaemia and DLBCL therapy. Brentuximab vedotin is an antibody-drug conjugate directed to the protein **CD30** expressed in in classical Hodgkin lymphoma and systemic anaplastic large cell lymphoma. Alemtuzumab is a monoclonal antibody that binds to **CD52** present on the surface of mature lymphocytes. It is used in the treatment of CLL, cutaneous

T-cell lymphoma (CTCL) and T-cell lymphoma under the trade name Campath®. Campath® was withdrawn from the markets in the US and Europe in 2012 to prepare for a higher-priced relaunch of the same antibody under the trade name Lemtrada for the treatment of multiple sclerosis (Thompson et al., 2013).

1.3.2.2 Targets for autoimmune diseases

Due to the fact that autoimmune disorders cover a plethora of diseases, it comes as no surprise that research covers a wide range of approaches and therapeutic targets. These approaches range from gene therapy to vaccines and a variety of cytokines. Among these approaches, antibody therapy is most rapidly expanding, owing to the favorable efficacy and safety profiles of these drugs and the better understanding of the initial targets of altered immune regulation and activity in various diseases (Rosman et al., 2013). The major targets for antibody therapy in autoimmune diseases can be divided in inflammatory cytokines, B-cells and co-stimulating molecules.

Anti-cytokines include **anti-tumour necrosis factor antibodies** (anti-TNF), used to treat inflammatory conditions such as rheumatoid arthritis (RA), psoriatic arthritis, juvenile arthritis, inflammatory bowel disease (Crohn's and ulcerative colitis), ankylosing spondylitis and psoriasis (Feldmann, 2002). In many cases these drugs are able to reduce inflammation and stop disease progression. This effect can be achieved with monoclonal antibodies such as Infliximab (Remicade®), Adalimumab (Humira®), Certolizumab pegol (Cimzia®), and Golimumab (Simponi®) or fusion proteins containing soluble TNF receptor such as Etanercept (Enbrel®).
Anti-BAFF antibody Belimumab (Benlysta®), previously known as LymphoStat-B, is another drug addressing B-lymphocyte hyperactivity. It inhibits B-cell activating factor (BAFF) (Bossen and Schneider, 2006), also known as B-lymphocyte stimulator (BLyS) (Kaveri et al., 2010) overexpressed in SLE. Belimumab binds to BAFF, preventing BAFF from binding to B-cells. Without the survival factor BAFF, B-cells get disrupted, and no longer contribute to the autoimmune damage of SLE.
Anti-interleukin-6 (IL-6) agents include drugs blocking this proinflammatory cytokine. Tocilizumab (Actemra) is a humanized antibody directed against the IL-6 receptor and Siltuximab (Sylvant™) and Sirukumab are antibodies directed against soluble IL-6 itself. Tocilizumab has been approved by the FDA in 2010 for rheumatoid arthritis and Sirukumab just entered into a Phase III clinical study for the treatment of adults with moderately to severely active RA. Sirukumab is expected to reduce the signs and symptoms of RA in patients with active RA who are refractory or intolerant to anti-TNFα agents (ClinicalTrials.gov Identifier: NCT01606761).
The **Anti-interleukin-12** (IL-12) antibody ABT-874 just finished Phase III clinical trials (ClinicalTrials.gov Identifier: NCT00570986) for psoriasis and Phase II trials for Crohn's disease (ClinicalTrials.gov Identifier: NCT00562887). ABT-874 has previously been developed for the treatment of multiple sclerosis; however, by May 2007, development for this indication was discontinued (Ding et al., 2008).
An alternative approach to specifically inhibit B-cell activity in autoimmune diseases is the depletion of B-cells using monoclonal antibodies recognising the surface molecules CD19, CD20 and CD22. Compared to immunomodulation by cytokine blockade this approach seems to be more specific. B-cell directed **anti-CD20** an-

tibodies such as Rituximab (chimeric), Obinutuzumab (humanized), Ofatumumab (human), and Ocrelizumab (humanized) are established reagents in this field. **Anti-CD19** afucosylated human monoclonal antibody MEDI-551 is able to deplete all B-cell subtypes from pro-B-cell stage to plasma cell (Herbst et al., 2010). **Anti-CD22** antibody Epratuzumab depletes mature $CD27^+$ B-cells. All of these antibodies show potential not only in oncology, but also in treatment of inflammatory autoimmune disorders (Ramos-Casals et al., 2012).

Other targets for autoimmune disorders are the cell adhesion molecules α**4-integrin** and α**1-integrin** (CD11a). Natalizumab (Tysabri®) used for treatment of MS and Crohn's disease binds α4-integrin, which may heterodimerize with integrin β1 to form $\alpha4\beta1$ integrin (also known as VLA-4), or with integrin β7 to form $\alpha4\beta7$ integrin; both $\alpha4\beta1$ and $\alpha4\beta7$ are present on T- and B-cells and serve as attachment ligands for VCAM (vascular cell adhesion molecules) on endothelial cells. Natalizumab prevents $\alpha4\beta1$ binding to VCAM and $\alpha4\beta7$ binding to mucosal addressin cellular adhesion molecule-1 (MAdCAM-1) and thus prevents T-cell extravasation into the brain or gut, respectively. Because both MS and Crohn's disease feature inflammatory T-cells as a significant part of the disease pathology, preventing access of these cells to target organs should have substantial clinical effects (Kappos et al., 2007; Major, 2010). Another humanized monoclonal antibody, Efalizumab (Raptiva®) used in psoriasis patients, binds the α1 integrin molecule CD11a on T- and B- cells, blocking attachment to the ICAM (intercellular adhesion molecules) on endothelial cells and infiltration into the layers of the skin (Vugmeyster et al., 2004). Unfortunately, despite therapeutic success patients treated with Natalizumab and Efalizumab have a higher risk to develop progressive multifocal leukoencephalopathy (PML) (Major, 2010). Due to the risk of PML, Efalizumab was withdrawn from the market in 2009. Natalizumab was withdrawn from the market by its manufacturer in 2004, but after a review of safety information and no further deaths, the drug was re-approached for the US market in 2006.

1.3.3 Bispecific antibodies

Most therapeutic antibodies today are full length unconjugated IgG molecules. Thus, they exert their activity via ADCC, CDC or by blocking molecules with unwanted biological activity. Bispecific antibodies comprise two different binding specificities fused to a single molecule. It opens up new opportunities for therapeutic applications by redirecting potent effector systems to diseased areas or by increasing neutralizing or stimulating activities of antibodies. Bispecific antibodies are thus able to improve efficacy and selectivity of natural effector functions and to expand effector functions to those not exerted by natural immunoglobulins (Fanger et al., 1992; Cao and Suresh, 1998).

The concept of dual targeting with bispecific antibodies is based on the binding of multiple disease-modifying molecules within one drug. In contrast to a combination of different therapeutic antibodies, bispecific antibodies make development less complex because manufacturing, preclinical and clinical testing is reduced to a single, bispecific molecule. Therapy with a single dual-targeting drug rather than combinations should also be less complicated for patients (Kontermann, 2012).

1.3.3.1 Generation of bispecific antibodies

The first chemically hybridized bispecific F(ab')$_2$ molecule was prepared by Brennan et al. in 1985. They described the preparation of bispecific antibodies by chemical combination of monoclonal IgG1 fragments (Brennan et al., 1985). To dissociate reduced immunoglobulin half-molecules under mild conditions, they used pepsin hydrolysis method described by Nisonoff et al. (Nisonoff and Mandy, 1962). After that, the authors reduced F(ab')$_2$ to F(ab'), stabilized them and fused different specificities in one antibody molecule. In 1991 Jung et al. reported important simplifications of the published procedures for the chemical generation of bispecific and trispecific F(ab')-hybrid fragments (Jung et al., 1991). They achieved reduction and subsequent modification of purified F(ab')$_2$ fragments in one step without the need to stabilize F(ab') groups.
An alternative and more effective method for the generation of bispecific antibodies is to generate cell lines constantly producing bispecific antibodies. Milstein and Cuello in 1983 were the first in this field. They described hybrid hybridomas, producing bispecific antibodies. When two myeloma cells producing monoclonal antibodies are fused, the derived hybrids are capable of co-dominantly expressing the antibody genes of both parents (Milstein and Cuello, 1983). However, this procedure produces a mixture of hybrid antibodies with various assortments of chains, which must be fractionated to yield the desired bispecific molecules.
The dominant production platform for antibody therapeutics nowadays relies on recombinant antibody technology capable of generating bispecific antibodies in various formats (Jeong et al., 2011; Huston and George, 2001). Development of bispecific antibodies for clinical applications have mainly focused on the retargeting of different effector cells of the immune system to tumour cells, although various other therapeutic strategies have been evaluated. However, such antibodies differ from the usual IgG structure of monoclonal antibodies and their development is therefore challenging so that progress is only slow, as reflected by the fact that as yet only two bispecific antibodies has been approved by the FDA. Developments in the field of antibody engineering have resulted in new approaches to improve the efficacy and safety of therapeutic antibodies. This had a substantial impact on the generation of novel bispecific antibody formats and led to a progress in the field. More than 45 different bispecific formats have been established in the past two decades (Kontermann, 2012). Fig. 1.2 and table 1.2 summarise modern scaffolds used for generating of bispecific antibodies. ScFv molecules, as an universal building block, are often fused to the N-terminus or the C-terminus of the of the heavy or light chain of an antibody. Generally this modification does not compromise productivity, although issues regarding antigen-binding activity or stability and aggregation arise.

1.3.3.2 Mechanisms of action of bispecific antibodies

Engaging T-cells

Cytotoxic T lymphocytes (CTLs) are considered to be the most potent killer cells of the immune system. Under physiological conditions, recognition and killing of a target cell is a highly controlled process involving antigen-specific binding of the T-

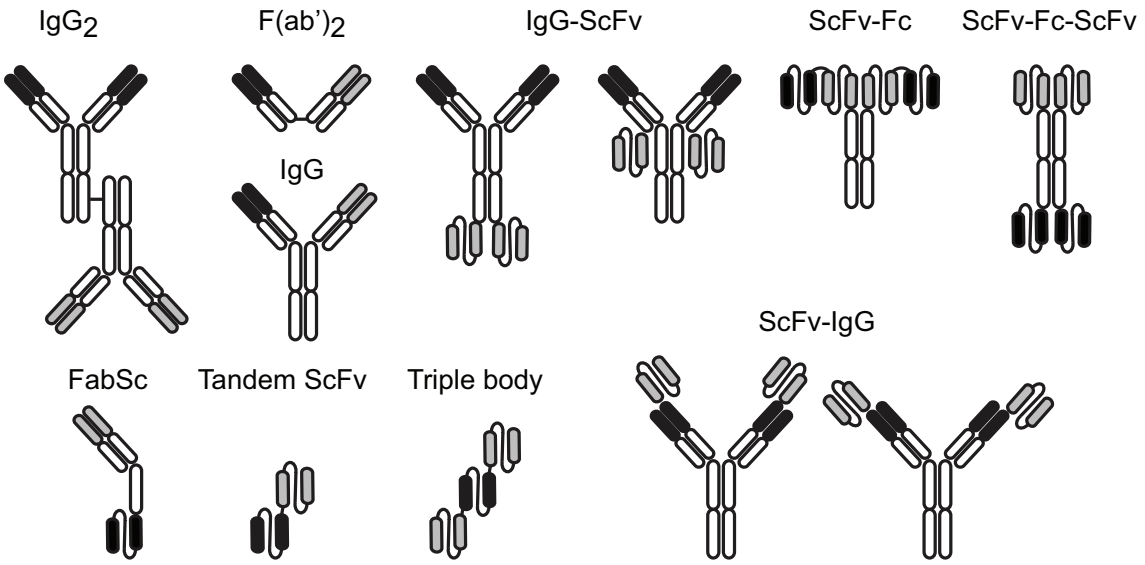

Figure 1.2: **Selected bispecific antibody formats.**
Black and grey are indicating different antibody specificities. Antibody constant domains are shown in white ellipses (Adapted from (Kontermann, 2012)).

Table 1.2: **Physiological properties of selected antibody formats**
Summary of salient properties of intact antibodies, enzymatic fragments, recombinant fragments and smaller scaffolds. Adapted from (Freise and Wu, 2015)

Format	**Composition**	**MW (kDa)**	**Serum $t_{1/2}$**	**Clearance route**	**Reference**
Intact IgG	$(V_H + V_L)_2$	150-160	1-3 weeks	Hepatic	(Ogasawara et al., 2013)
$F(ab')_2$	$(V_H C_H 1 + V_L C_L)_2$	110	8-10 h	Hepatic	(Lütje et al., 2014)
Minibody	$(scFv + C_H 3)_2$	75	5-10 h	Hepatic	(Tavaré et al., 2014)
Fab	$V_H C_H 1 + V_L C_L$	50-55	12-20 h	Renal	(Chakravarty et al., 2014)
Diabody	$(scFV)_2$	50	3-5 h	Renal	(Tavaré et al., 2014)
scFv	$V_H + V_L$	28	2-4 h	Renal	(Kim et al., 2014)
Nanobody	V_H (Camelid)	12-15	30-60 min	Renal	(Bannas et al., 2014)
Affibody	Z domain of protein A	7	30-60 min	Renal	(Strand et al., 2014)

cell receptor to major histocompatibility complexes (MHCs) on target cells. In order to be fully activated, CTLs need a second stimulus mainly provided by interaction of membrane-bound CD80/CD86 molecules with CD28 on T lymphocytes during the process of T-cell activation by antigen-presenting cells.
Bispecific antibodies used for the retargeting of CTLs have the advantage of bypassing MHC-restricted target-cell recognition by CTLs, a process that is often inadequate due to downregulation or loss of MHC molecules on tumour cells (Bubeník, 2003). Most bispecific antibodies developed for the retargeting of CTLs are directed against CD3, which is a multi-subunit complex associated with the T-cell receptor (TCR), but other trigger molecules such as CD2 or the TCR itself have also been evaluated (Fanger et al., 1992). The first successful bispecific antibody Blinatumomab, approved by the FDA in 2014 for the treatment of acute lymphoblastic leukemia (ALL), combines two binding sites: a CD3 site for T-cells and a CD19 site for the target B-cells (Bargou et al., 2008).
Other studies have shown that binding of certain monoclonal antibodies to CD28 can induce CTL-mediated cytotoxicity without the need for a first activation through the TCR complex (Tacke et al., 1997). These supraagonistic antibodies bind to a particular epitope (60–65 a.a.) on CD28 different from the region that interacts with B7 (99–104 a.a.) (Lühder et al., 2003). A nonsupraagonistic anti-CD28 antibody was used to construct a bispecific tandem ScFv molecule directed against the melanoma-associated glycoprotein (Grosse-Hovest et al., 2003). This antibody, r28M, was able to induce efficient tumour cell killing *in vitro* and *in vivo* in a CD3-independent way (Grosse-Hovest et al., 2005).

Engaging NK cells and Fc receptors

Another group of effector cells consists of those naturally recruited by binding to Fc receptors. These include natural killer (NK) cells, monocytes/macrophages and polymorphonuclear leukocytes (PMNs) (e. g. neutrophils). Consequently, bispecific antibodies have been generated for the retargeting of these effector cells by binding to Fc receptors such as FcγRI (CD64), FcγRIII (CD16), and FcαR (CD89).
Bispecific antibodies directed against Fc receptors are able to extend ADCC to cells normally not or only inefficiently recruited by conventional antibodies, such as PMNs or monocytes and macrophages. These cells are retargeted by binding to CD89 or CD64, respectively, and eliminate target cells directly through cytotoxicity or phagocytosis (Deo et al., 1998; Sundarapandiyan et al., 2001). In addition, since some Fc receptors such as CD64 are also present on antigen-presenting cells, bispecific antibodies can indirectly enhance antitumour immunity by increased antigen presentation (van Spriel et al., 2000).

Both, CTLs and NK cells kill target cells by the perforin/granzyme pathways. The granule exocytosis pathway utilizes perforin to traffic the granzymes to appropriate locations in target cells, where they cleave critical substrates that initiate DNA fragmentation and apoptosis; granzymes A and B induce death via alternate, nonoverlapping pathways. The CD95/CD95L system is responsible for activation-induced cell death but also plays an important role in lymphocyte-mediated killing under certain circumstances (Russell and Ley, 2002).

1.4 Apoptosis and other types of cell death

Apoptosis is the most common form of eukaryotic cell death and occurs in embryogenesis, metamorphosis, tissue atrophy, and tumour regression (Wyllie et al., 1980). It plays a central role for cell differentiation, removal of the damaged cells and the homoeostasis of the immune system. Two major pathways leading to apoptosis are now well established: the *extrinsic pathway*, that is mainly executed via death receptors on the cell surface promoting recruitment and activation of caspase-8 and caspase-10 within membrane receptor complexes (Wilson et al., 2009), and the *intrinsic pathway*, which involves the activation of BH3-only proteins which promote caspase activation by permeabilizing the mitochondrial outer membrane leading to cytochrome c release and the formation of the Apaf-1/caspase-9 apoptosome (Nagata, 1999; Peter et al., 2007; Peter and Krammer, 2003; Strasser et al., 2009). In both pathways (Fig. 1.3), activation of upstream initiator caspases (either caspase-8 or caspase-9) leads to a cascade of additional caspase activation events that collectively dismantles the cell to produce the apoptotic phenotype (Martin et al., 2012; Taylor et al., 2008).
Members of the caspase family of cysteine proteases target several hundred proteins for restricted proteolysis leading to cell shrinkage, membrane blebbing, DNA fragmentation, chromatin condensation and, finally, cell destruction (Nicholson, 1999; Creagh et al., 2003). Multiple membrane alterations, most notably the externalization of phosphatidylserine, have been detected on apoptotic cells. These membrane alterations trigger the terminal event of the demolition phase – the recognition and consumption of the dead cell by phagocytes and perhaps the most important aspect of the entire process (Fadok et al., 1992; Martin et al., 1995; Savill and Fadok, 2000). Because apoptotic cells are typically recognised and engulfed by macrophages before leakage of their intracellular contents, they appear to be capable of attracting the attention of such cells by secreting molecules with chemotactic properties such as a chemoattractant lipid, lysophosphatidylcholine (Lauber et al., 2003) or S19 ribosomal protein and aminoacyl-tRNA synthetases (Horino et al., 1998; Wakasugi and Schimmel, 1999) that would not normally be present in the extracellular space. Therefore, apart from limiting direct cell damage caused by the release of cytoplasmic contents, one of the main benefits of controlled cell death through apoptosis is to prevent unwanted immune responses (Taylor et al., 2008).
Activation-induced cell death (AICD) belongs to apoptotic programmed cell death caused by the interaction of Fas receptor (Fas, CD95) and Fas ligand (FasL, CD95 ligand). It occurs as a result of repeated stimulation of specific T-cell receptors (TCR) and it eliminates activated T-cells no longer needed after the immune response to maintain the peripheral immune tolerance (Kabelitz and Janssen, 1997). In T-cell dependent humoral responses, AICD of B-cells is known to be initiated by Fas ligand on T-cells stimulating Fas receptor on B-cells (Figgett et al., 2013). Therefore an alteration of the process may lead to autoimmune diseases (Zhang et al., 2004). In conclusion: AICD is a negative regulator for activated lymphocytes.
Before the details of apoptotic cell death and signalling will be discussed more thoroughly, it is worth to mention other types of regulated cell death.
Immunogenic cell death or immunogenic apoptosis is a form of cell death caused by some cytostatic agents such as anthracyclines, oxaliplatin and bortezomib, or

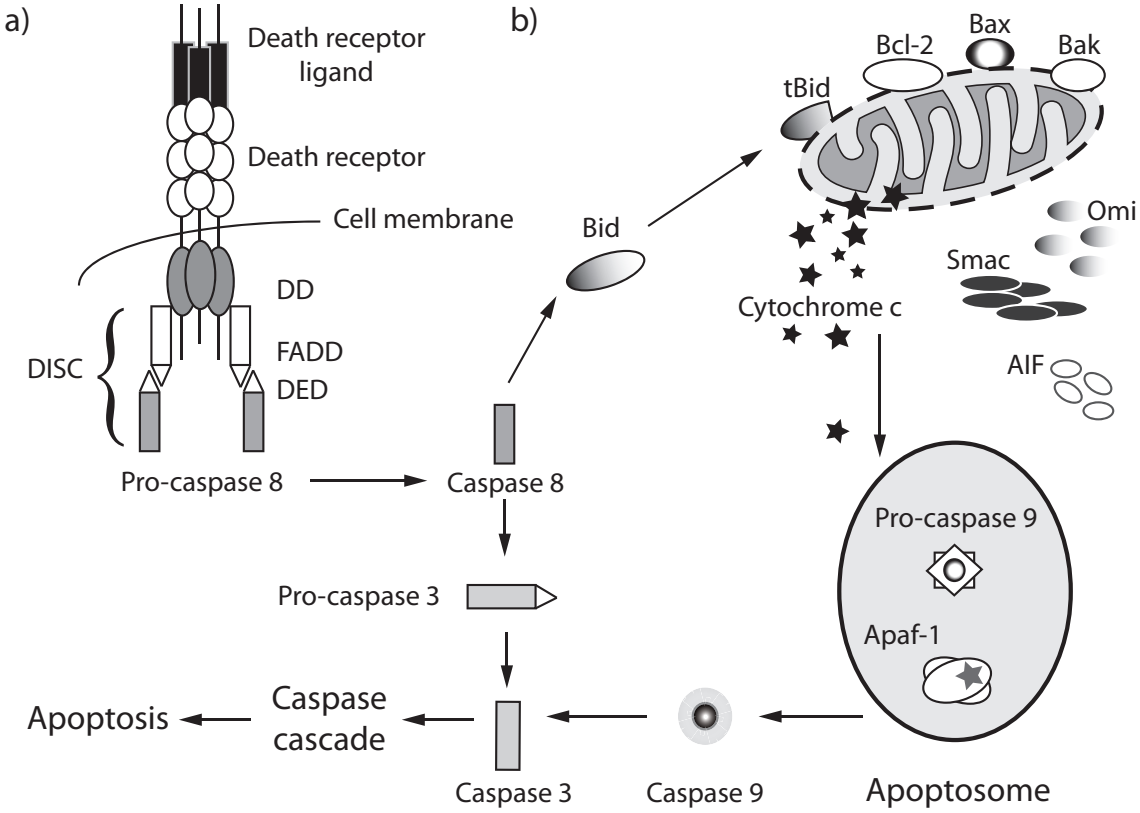

Figure 1.3: **Schematic representation of the molecular pathways leading to apoptosis**
In the extrinsic pathway (a) upon ligand binding to specific receptors the DISC complex is formed and caspase 8 activated. In the intrinsic pathway (b) release of cytochrome c from the mitochondria result in the formation of the apoptosome and activation of caspase 9. Caspase 8 and 9 then activate downstream caspases such as caspase 3 resulting in cell death. The two pathways are connected through the cleavage of the BH3-only protein Bid. (Adapted from (Favaloro et al., 2012) and (Wehrli et al., 2000))
Abbreviations: **DISC** – death-inducing signalling complex, **DD** – death domain, **FADD** – Fas-associated protein with death domain, **DED** – death effector domain, **Bid** – BH3 interacting-domain, **tBid** – truncated Bid, **Bcl-2** – B-cell lymphoma 2, **Bax** – Bcl-2-associated X protein, **Bak** – Bcl-2 homologous antagonist/killer, **Smac** – second mitochondria-derived activator of caspases, **Omi** – serine protease HtrA2, **AIF** – apoptosis-inducing factor, **Apaf-1** – Apoptotic protease activating factor 1.

radiotherapy and photodynamic therapy. At the molecular level, it has been shown that the immunological silhouette of these cell death pathways is defined by a set of molecules called 'damage-associated molecular patterns (DAMPs)' (Garg et al., 2010). Unlike normal apoptosis, which is mostly nonimmunogenic or even tolerogenic, immunogenic apoptosis of cancer cells can induce an effective antitumour immune response through activation of dendritic cells (DCs) and consequently activation of specific T-cell response (Spisek and Dhodapkar, 2007).

Autophagy, sometimes referred to as Type II cell death, is the basic catabolic mechanism that involves degradation of unnecessary or dysfunctional cellular components through the actions of lysosomes (Lin et al., 2013). Autophagy allows the degradation and recycling of cellular components (Lin et al., 2013). During this process, targeted cytoplasmic constituents are isolated from the rest of the cell within a double-membraned vesicle known as an autophagosome. The autophagosome then fuses with a lysosome and its cargo is degraded and recycled (Patel et al., 2012). There are three different forms of autophagy that are commonly described, namely macroautophagy, microautophagy and chaperone-mediated autophagy (Peracchio et al., 2012).

Necroptosis is a recently described regulated form of necrotic cell death. Necrotic death is generally a result of an overwhelming cytotoxic insult, and requires no specific molecular events in order to occur. However, in the last decade, a regulated form of it has been characterized and termed necroptosis, because it shares features of apoptosis and necrosis. Like apoptosis, a defined molecular cascade controls necroptosis. Like necrosis, necroptosis is characterized by swelling of the cell and its organelles leading to cell rupture. Rupture results in the release of cellular contents, a number of which serve as damage-associated molecular patterns (DAMPs) such as mitochondrial DNA (mtDNA), high mobility group protein B1 (HMGB1), IL-33, IL-1α or S100 calcium-binding protein A9 (S100a9), which can potentiate inflammation (Kaczmarek et al., 2013).

Pyroptosis was first described in 2001 (Cookson and Brennan, 2001). It is a pro-inflammatory caspase 1-dependent programmed cell death, triggered by various pathological stimuli, such as stroke, heart attack or cancer, and is crucial for controlling microbial infections (for example, *Salmonella*, *Francisella* and *Legionella*) (Bergsbaken et al., 2009). In this process, immune cells use a range of mechanisms to sense intracellular and extracellular 'danger' signals generated by invading pathogenic microorganisms or by the host in response to tissue injury (Matzinger, 2002). Toll-like receptors (TLRs) initiate a signalling cascade that leads to cellular activation and production of inflammatory cytokines, such as tumour necrosis factor (TNF), IL-6, IL-8 and type I interferons (IFNs), in response to extracellular signals (Kawai and Akira, 2007). Nod-like receptors (NLRs) function in the recognition of danger signals introduced into the host cell cytosol (Kufer and Sansonetti, 2007). This leads to caspase 1-dependent pyroptosis and release of the inflammatory cytokines IL-18 and IL-1β. The mechanism and outcome of this form of cell death are distinctly different from these aspects of apoptosis, which actively inhibits inflammation (Fink and Cookson, 2005).

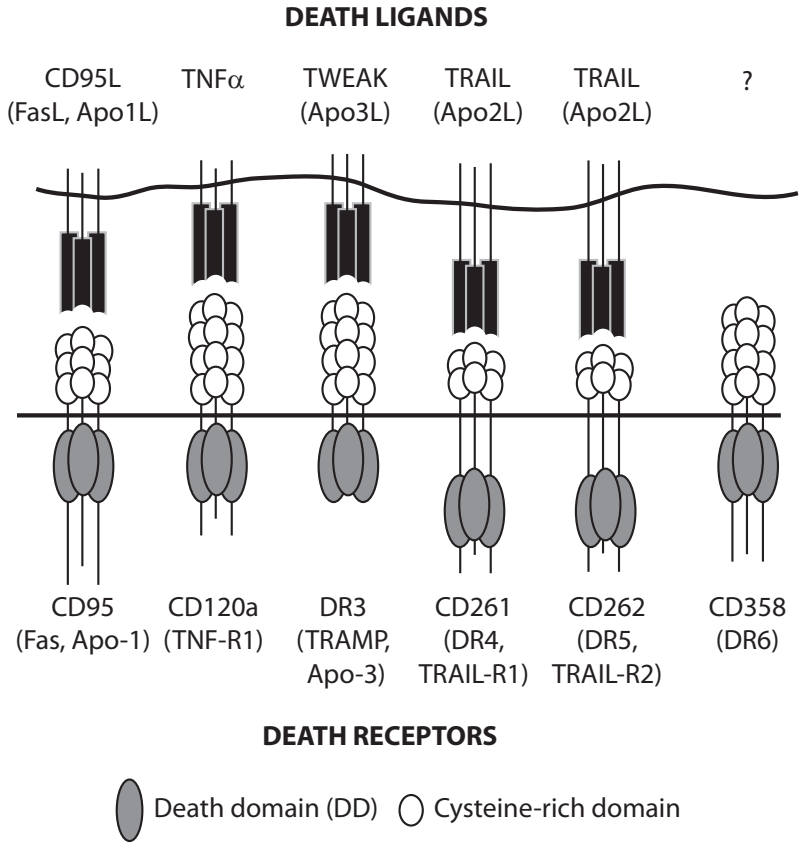

Figure 1.4: **Death receptors and their respective ligands:**
six human death receptors (CD95, CD120a, DR3, CD261, CD262, CD358), are known to date. All are type I membrane proteins that contain two to four cysteine-rich extracellular domains and a cytoplasmic sequence named 'death domain' (DD). The known ligands for these death receptors are shown. DR6 is at present an orphan receptor. Adapted from (Wehrli et al., 2000)

1.4.1 Apoptosis receptors and their ligands

In many immune cells, and particularly in lymphocytes, cell death can be triggered by the specific engagement of a subset of the tumor necrosis factor (TNF) receptor family. The best characterized ligands of these receptors to date are soluble or membrane-bound FasL and TNF-α. This form of cell death plays a critical role in the deletion of auto-reactive immune cells to limit inflammatory responses (Lalaoui et al., 2015).

However, FasL and TNF-α are not the only molecules responsible for triggering and induction of apoptosis. In general, apoptosis can be induced through the activation of death receptors including CD95 (Fas, APO-1), CD120a (TNFR1, p55/p60 TNFR), TRAMP (WSL-1, APO-3, DR-3, LARDDR3), CD261 (TRAIL-R1, DR4) and CD262 (TRAIL-R2, DR5, APO-2, TRICK-2, KILLER). These receptors are activated by their respective ligands which belong to the TNF Superfamily (SF) of cytokines, namely CD95L (FasL, APO-1L), TRAIL (APO-2L), TNF and TL1A (Fig. 1.4).

All of the mentioned death receptors are type I membrane proteins that contain two

to four cysteine-rich extracellular domains and a cytoplasmic sequence named 'death domain'. Death receptor ligands usually initiate signalling via receptor oligomerisation, which in turn results in the recruitment of specialized adaptor proteins and activation of caspase cascades. For DR6 (also known as TNFRSF21), the sixth DD-containing receptor, a specific amino-terminal cleavage fragment of the β-amyloid precursor protein (APP), N-APP, was recently described as a ligand. No ligand for DR6 belonging to the TNF SF has been identified, at least so far, and caspase-8 does not seem to be involved in this signalling (Nikolaev et al., 2009).

1.4.2 The CD95 death receptor

In 1989, Trauth et al. described the discovery of an apoptosis inducing receptor. They named this receptor APO-1, anticipating that it might be the first of a series receptors of this kind (Trauth et al., 1989). At the same time Yonehara et al. described a cell surface molecule, termed Fas, that could be triggered to induce apoptosis by an agonistic monoclonal antibody (Yonehara et al., 1989). Sequencing and cloning of the APO-1/Fas proteins and cDNAs, respectively, showed that APO-1 and Fas were identical (Itoh et al., 1991; Oehm et al., 1992). Later the 5^{th} Workshop on Leukocyte Typing (Schlossman, 1995) suggested the name CD95 for this receptor. The significance of CD95 mediated apoptosis was shown in experiments with mice which carried mutations in the genes encoding either for CD95 receptor or for CD95 ligand. These animals developed massive lymphadenopathy and lymphoproliferative syndromes (Watanabe-Fukunaga et al., 1992; Takahashi et al., 1994; Rieux-Laucat et al., 2003). CD95 messenger RNA (mRNA) is expressed in the thymus, heart, lung and ovary (Watanabe-Fukunaga et al., 1992). CD95 receptor is also very important in the liver. It is expressed in the developing (French et al., 1996) and mature liver tissue (Leithauser et al., 1993). A physiological role of CD95 in maintaining liver homeostasis has been suggested since mice deficient in CD95 develop increased cellularity and substantial liver hyperplasia (Adachi et al., 1995).
CD95/Apo-1/Fas is a transmembrane molecule and a member of the TNF/nerve growth factor receptor superfamily and serves as the prototypic death receptor in and outside the immune system. CD95-dependent apoptosis is triggered by the CD95 ligand (CD95L) which induces clustering of surface CD95 (Fig. 1.5 a). Oligomerisation initiates the recruitment of the 'CD95 (Fas) associated protein with death domain' (FADD) and procaspase-8 to form the 'death-inducing signaling complex' (DISC). Procaspase-8 undergoes autocatalytic cleavage in the DISC resulting in the generation of active caspase-8, which dissociates from the DISC to proceed with the activation of the caspase cascade that leads to apoptotic cell death (Krammer et al., 2007; Strasser et al., 2009).

1.4.3 Ambivalence of CD95-mediated apoptosis

In case of cancer cells, the function of CD95 is ambivalent. It was found that most malignant cells express CD95 receptor, but appear to be refractory to CD95-induced cell death. Undermining the immune system and suppressing the anti-tumour response are essential events during oncogenesis allowing tumour formation (Hanahan and Weinberg, 2011). In this context, the CD95/CD95L system can

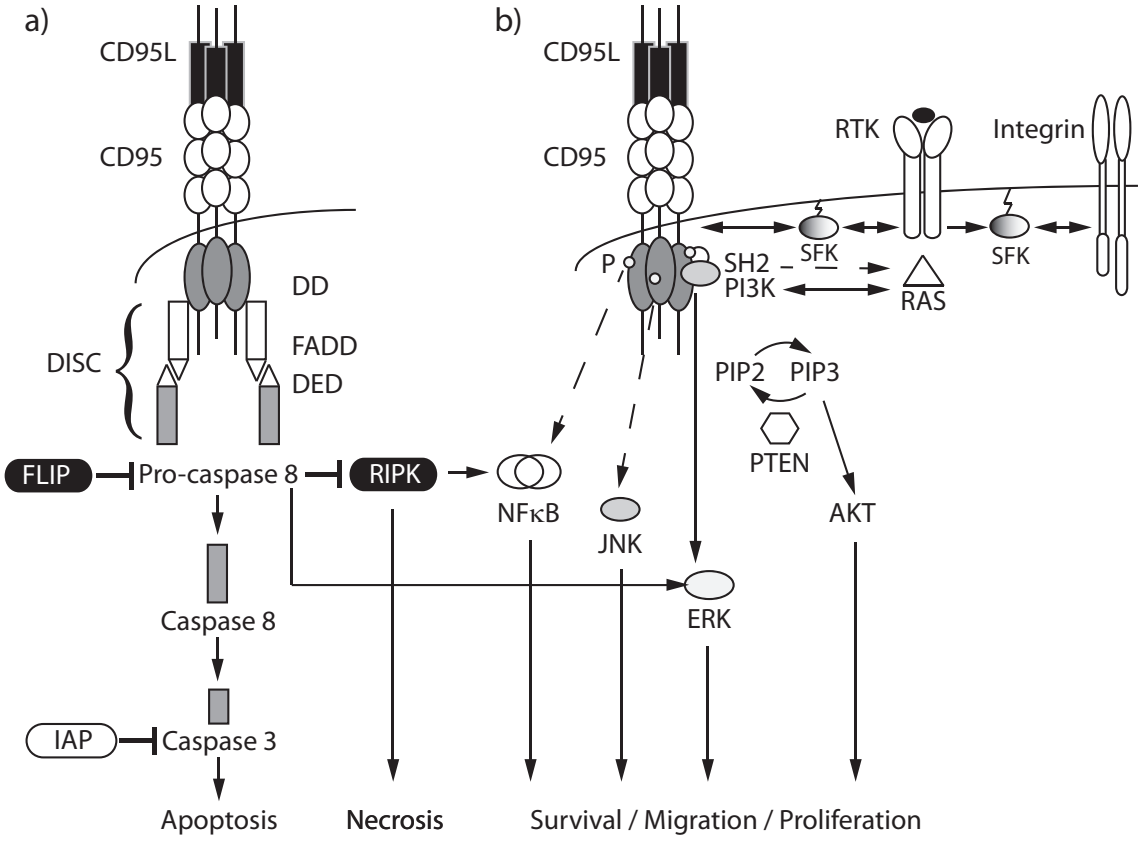

Figure 1.5: **The simplified CD95 signaling pathway**
a) Apoptosis and programmed necrosis. Upon binding of the trimerized CD95L, FADD is recruited to the DD of CD95. Procaspase-8 subsequently binds FADD through its DED to form the DISC, which is inhibited in the presence of FLIP. DISC formation prevents RIPK activation and programmed necrosis. Autoproteolytic cleavage of procaspase-8 at the DISC leads to apoptosis, whereas procaspase-8 phosphorylation leads to ERK activation. Active caspase-8 cleaves caspase-3, which is inhibited in the presence of IAP. b) Nonapoptotic pathways. Activation of CD95 (or cross-activation through RTKs or integrins) leads to the phosphorylation of the DD through SFKs. The phosphorylated DD can serve as a docking site for SH2 adaptors, including the p85 subunit (not shown) of PI3K. PI3K-dependent activation of AKT, which is inhibited by PTEN, induces migration and survival. PI3K might also lead to ERK activation in a Ras-dependent or -independent manner. CD95 also leads NFB activation, probably through RIPK, and to JNK activation through a yet unknown mechanism ultimately increasing proliferation (Adapted from (Tang et al., 2011) and (Martin-Villalba et al., 2013)).
Abbreviations: **CD95L** - CD95Ligand; **FADD** - Fas-associated protein with death domain; **FLIP** - FLICE-like inhibitory protein; **IAP** - inhibitor of apoptosis , **RIPK** - receptor-interacting protein kinase; **ERK** - extracellular signal-regulated kinase; **NFκB** - nuclear factor κB; **JNK** - c-jun N-terminal kinase; **PTEN** - phosphatase and tensin homolog; **P** - phosphotyrosine; **PI3K** - phosphoinositide 3-kinase; **PIP2** - phosphatidylinositol 4,5-bisphosphate; **PIP3** - phosphatidylinositol (3,4,5)-trisphosphate; **SH2** - src homology domain 2; **SFK** - src-family kinase; **RAS** - rat sarcoma; **RTK** - receptor tyrosine kinase.

elicit both tumourigenic and tumour suppressing roles in the pathogenesis of cancer (Ehrenschwender and Wajant, 2009).

The molecular mechanisms mediating CD95-resistance are complex and involve both post-receptorial and pre-receptorial events (Inaba et al., 1999). Post-receptorial resistance mechanisms are known to include expression of truncated CD95 receptor lacking the intracytoplasmic signaling domain (Cascino et al., 1996), over-expression of bcl-2 (Itoh et al., 1993) and bcl-X_L proteins (Boise et al., 1995), expression of caspase regulators such as FLICE-like inhibitory protein (FLIP) (Irmler et al., 1997) and inhibitor of apoptosis proteins (IAP) (Deveraux et al., 1998; Inaba et al., 1999) (See Fig. 1.5 a). Pre-receptorial resistance can be mediated by the soluble CD95 (sCD95) protein, which antagonizes both anti-CD95 antibody and CD95L killing in a dose-dependent manner (Cheng et al., 1994; Papoff et al., 1996). sCD95 was found to be elevated in the serum from patients with B- and T-cell leukaemias (Knipping et al., 1995) and nonhaematopoietic malignancies such as melanoma, breast cancer, and colon cancer (Midis et al., 1996). In addition to the full-length CD95 mRNA, those cells expresses alternatively spliced mRNA variants coding for sCD95 proteins (Cheng et al., 1994). To date, eight mRNA variants of CD95 receptor have been described, which are translated into seven isoforms of the protein. Another example of pre-receptorial resistance the downregulation/loss of CD95 expression has been found in a variety of malignancies (e.g., pulmonary adenocarcinomas, esophageal cancer, melanoma) (Leithauser et al., 1993; Hahne et al., 1996; Shin et al., 1999).

Work by Marcus Peter's laboratory using cells from breast, ovary, skin, lung, and kidney tumours showed that not only apoptotic signaling is blocked and that CD95 activation increases motility and invasion (Martin-Villalba et al., 2013; Barnhart et al., 2004). There is evidence that, in addition to inducing cell death, in at least some cell lines CD95 can mediate other activation signals, including increased proliferation in human T-cells (Alderson et al., 1993) and fibroblasts (Aggarwal et al., 1995).

Collectively, these observations indicate that CD95-mediated signaling is not limited to the induction of cell death. Indeed, there are CD95-dependant pathways responsible for survival, migration and proliferation (Fig. 1.5 b) and the regulation of this pathway is still not completely clear.

1.4.4 Therapeutic stimulation of CD95 death receptor

Despite the dichotomy described above, the use of programmed cell death for clinical purpose e.g. against cancer is being discussed as attractive therapeutic option since development of agonistic antibodies against the CD95 receptor in 1989 (Trauth et al., 1989; Yonehara et al., 1989). First it was shown that single i.v. injection of agonistic mouse anti-human CD95 antibodies (IgG3) into *nu/nu* mice carrying a xenotransplant of human B-cell tumour induced regression of this tumour (Trauth et al., 1989). However, the therapeutic use of anti-CD95 antibodies is precarious, since this receptor is expressed also on normal cells, in particular hepatocytes. In principle, there are two fundamental problems of using CD95 antibodies: a specificity and a sensitivity problem:

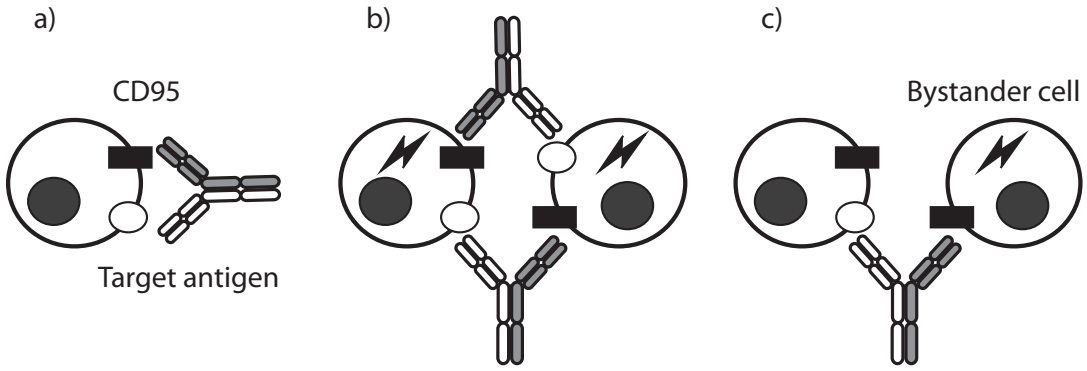

Figure 1.6: **Bispecific antibodies**
directed to two different antigens on the same cell may bind in a monocellular (a) or bicellular (b) way. Mutual cross-linking of both antigens induces apoptosis if the antibody binds in bi-cellular way. Bystander lysis (c) may occur in the presence of target cells if the bystander cell carries CD95 but not the target antigen.
(Adapted from (Herrmann et al., 2008))

- A systemically application of hamster anti-mouse CD95 antibody (clone JO2, IgG2 λ) induces apoptosis of hepatocytes and an acute hepatic failure in normal mice (constitutes the specificity problem) (Ogasawara et al., 1993).
- Primary tumour cells are often refractory to CD95 stimulation. The reason may be the absence of CD95 expression or defective receptor-associated signalling (constitutes the sensitivity problem) (Hammond et al., 2007).

With respect to the solution of the specificity problem, it was shown that bispecific TA×CD95 antibodies (against **T**arget **A**ntigen and CD95) induce apoptosis selectively on antigen positive tumour cells (Wajant, 2006; Jung et al., 2001). Fig. 1.6 illustrates possible binding mechanisms of bispecific antibody in mono- (a) or bicellular (b) way. Effective crosslinking of CD95 on the cell surface requires *trans* engagement of CD95 and the target antigen (bicellular binding) (Herrmann et al., 2008) and thus bystander killing of cells not expressing the target antigen may occur, but only in the vicinity of target antigen and CD95 expressing cells Fig. 1.6 b.
Target cell restricted CD95 activation as outlined above solves the specificity but not the sensitivity problem: many tumour cells have lost their susceptibility to CD95-mediated cell death either by down-regulation of CD95 or by regulation of proapoptotic and antiapoptotic intracellular proteins towards resistance (Bullani et al., 2002; Xerri et al., 1998). This problem is now well recognised and numerous compounds have been described which are capable of enhancing the susceptibility of tumour cells towards apoptotic cell death. The presence of sensitizing reagents such as cycloheximide and various cytostatic drugs could enhance CD95-mediated killing of the tumour cells (Herrmann et al., 2008).

1.5 The objectives of the thesis

Whereas chemically hybridized bispecific F(ab')$_2$-fragments targeting CD20 and the death receptor CD95 were already shown to selectively kill B-cell lymphoma cells carrying both antigens (Jung et al., 2001), the main goal of this work was to develop recombinant bispecific CD95×CD20 antibodies. They should be able to trigger apoptosis specifically on malignant B-cells as well as on normal activated B-cells carrying CD20 and CD95 on their surface. These therapeutic agents should be suitable for production and purification from eukaryotic cell cultures in pharmaceutical quality and quantity.
The therapeutic effect of these recombinant molecules on malignant and normal activated B-cells should be compared to monospecific clinically established anti-CD20 antibodies. These antibodies include parental monospecific CD20 antibody 2H7 (used for the generation of commercial antibody Ocrelizumab) and FDA-approved anti-CD20 antibody Rituximab widely used for lymphoma therapy as well as for the treatment of some autoimmune diseases. Additionally, recombinant bispecific CD95×CD20 should be compared to the improved monospecific "third generation" therapeutic antibodies against CD20 that are carrying optimisation in antibody Fc-part for enhancement of the therapeutic efficacy.

In the second part of this work a concept for bispecific CD95×Ag fusion proteins able to trigger apoptosis specifically on antigen-specific B-cells should be developed. For the proof of principle antigen fragments from Tetanus (TT) and Diphtheria (DT) toxoids (as a control) were coupled to CD95 antibodies to check whether those proteins are able to deplete Tetanus specific B-cells in PBMC cultures from freshly immunized donors.

Chapter 2

Materials and methods

2.1 Materials

2.1.1 Instruments

ÄKTAprime chromatography system	Amersham Biosciences AB, Uppsala, Sweden
ÄKTApure chromatography system	GE Healthcare Bio-Scieces, Uppsala, Sweden
Balance PT600	Sartorius AG, Göttingen
Biosafety cabinet Technoflow 3F150-IIGS	Integra Biosciences Deutschland GmbH, Fernwald
Cell-harvester	Inotech Biosystems International, Inc., Rockville, USA
Centrifuge Heraeus Biofuge fresco	Thermo Electron Corporation, Waltham, USA
Centrifuge Heraeus Megafuge 1.0	Thermo Electron Corporation, Waltham, USA
Centrifuge Sorvall RC5C Plus	Thermo Fisher Scientific, Inc., Schwerte
CO_2 incubator	BINDER GmbH, Tuttlingen
Diaphragm vacuum pump type MD 4C	Vacuubrand GmbH & Co. KG, Wertheim
Dionex™ UltiMate™ 3000 BioRS system	Thermo Fisher Scientific, Inc., Germering
Elektrophoresis Power Supply EPS 600 & 3500	Pharmacia LKB Biotechnology, Uppsala, Sweden
ELISA reader Spectra Max 340	Molecular devices, LLC., Sunnyvale, USA
FACS Calibur flow cytometer	BD Biosciences, Heidelberg
FACS Canto™ II flow cytometer	BD Biosciences, Heidelberg
FPLC system	Pharmacia LKB Biotechnology, Uppsala, Sweden
Freezer (-80°) E 80-450 S	Colora Messtechnik GmbH, Lorch
Heating bath circulator Julabo 19	Julabo Labortechnik GmbH & Co. KG, Staufen
Incubated Shaker Multitron	Infors AG, Bottmingen, Switzerland
Magnetic stirrer RTC Basic	IKA®-Werke GmbH & Co. KG, Staufen
Microplate counter 2450 MicroBeta^{2}™	PerkinElmer, Inc., Rodgau
Microscope Axiovert 25	Carl Zeiss AG, Oberkochen
Microwave oven Super Crousty 1100 W	Krups GmbH, Offenbach
Multichannel Pipette DV12-200C	Abimed GmbH, Langenfeld
Nanodrop™ 1000 spectrophotometer	Thermo Fisher Scientific, Inc., Schwerte
pH electrode InLab Expert Pro	Mettler Toledo GmbH, Albstadt
Refrigerator Liebherr Premium	Liebherr Hausgeräte Ochsenhausen GmbH, Ochsenhausen
Peristaltic pump P-1	Pharmacia LKB Biotechnology, Uppsala, Sweden
Platform shaker Duomax 1030	Heidolph Instruments GmbH & Co. KG, Schwabach
Pipetboy acu	Integra Biosciences Deutschland GmbH, Fernwald

PIPETMAN® Pipettes P10, P20, P200, P1000	Gilson, Inc., Middleton, USA
SMART® System	Pharmacia Biotech AB, Uppsala, Sweden
Thermocycler PTC-100	MJ Research, Inc., St. Bruno, Canada
Thriller Thermoshaker Incubator	PEQLAB Biotechnologie GmbH, Erlangen
UV Transilluminator FLX-20M and TFX-20M	Vilber Lourmat Deutschland GmbH, Eberhardzell
Vortex mixer VF2	IKA®-Werke GmbH & Co. KG, Staufen

2.1.2 Plastic and glass supply

15 mL polystyrene conical tubes	BD Biosciences, Heidelberg
50 mL polypropylene conical tubes	Greiner Bio One International GmbH, Frickenhausen
Amicon Ultra-4 Centrifugal Filter Units MWCO 10 kDa and 30 kDa	Merck Millipore Corporation, Schwalbach
Beakers (Duran® glass)	Schott AG, Mainz
Beakers (plastic)	Vitlab GmbH, Grossostheim
Bottletop Filter (0.22 μm)	Merck Millipore Corporation, Schwalbach
Broome style mouse restrainer	Kent Scientific Corporation, Torrington, USA
Chromacol™ Amber Glass Crimp/Snap Top Vials (03-FIRV(A))	Thermo Fisher Scientific, Inc., Schwerte
Chromacol™ Cap snap cap polyethylene 11 mm	Thermo Fisher Scientific, Inc., Schwerte
Cell culture multiwell plates (6, 24, 96 well Format)	Greiner Bio One International GmbH, Frickenhausen
Cell Culture Treated TripleFlasks™	Nunc™, Thermo Fisher Scientific, Inc., Denmark
Cellstar® Cell Culture Flasks (25 cm^2, 75 cm^2 and 175 cm^2)	Greiner Bio One International GmbH, Frickenhausen
Centrifuge bottles 250 mL nalgene™	Thermo Fisher Scientific, Inc., Schwerte
Combitips	Eppendorf AG, Hamburg
Cryovials	Greiner Bio One International GmbH, Frickenhausen
Dialysis tubing visking, cellulose type 27/32 & 8/32 inch, MWCO 14 kDa	Carl Roth GmbH + Co. KG, Karlsruhe
Electroporation cuvettes (4 mm electrode gap)	PEQLAB Biotechnologie, Erlangen
ELISA plates (Maxisorp)	Nunc™ & Thermo Fisher Scientific, Inc., Langenselbold
Eppendorf tubes (0.5 mL, 1.5 mL, 2 mL)	Eppendorf AG, Hamburg
Erlenmeyer Flasks	Schott AG, Mainz
Erlenmeyer shape Duran® filtering flask with KECK™ assembly set	Schott AG, Mainz

FACS tubes 0.5 mL 38 mm×6.5 mm polystyrene	Sarstedt AG & Co., Nürmbrecht
FACS tubes 5 mL, 12 mm×75 mm polystyrene	BD Biosciences, Heidelberg
Filtermate A, printed	PerkinElmer, Inc., Rodgau
Glass bottles Duran® (0.5 L, 1 L, 2 L)	Schott AG, Mainz
Measuring cylinders (Duran® glass)	Schott AG, Mainz
Millex® Syringe-driven Filter unit (0,22 μm)	Merck Millipore Corporation, Schwalbach
Nalgene™ Cryo 1° Freezing Container	Thermo Fisher Scientific, Inc., Schwerte
Needles 27 G×1/2 in.	BD Biosciences, Heidelberg
Neubauer cell counting chamber	Brand GmbH & Co., Weinheim
Pasteur Pipettes (Long size)	Ulbrich Wilhelm GdbR, Bamberg
PCR Softtubes 0.5 mL	Biozym Scientific GmbH, Hessisch Oldendorf
Petri dishes	Greiner Bio One International GmbH, Frickenhausen
Pipette tips (10 μL, 200 μL, 1000 μL)	Starlab GmbH, Hamburg
Pipette tips with plug barrier SafeSeal-Tips	Biozym Scientific, Hessisch Oldendorf
Safety-Multifly® Needles 21 G×3/4 in.	Sarstedt AG & Co., Nürmbrecht
Serological pipets, BD Falcon™ polystyrene (2 mL, 5 mL, 10 mL, 25 mL)	BD Biosciences, Heidelberg
Serological pipets Costar (50 mL)	Corning Incorporated, Amsterdam, Netherlands
Syringes BD Luer-Lok™ (5 mL, 20 mL, 50 mL)	BD Biosciences, Heidelberg
Syringe SubQ 1 mL	BD Biosciences, Heidelberg

2.1.3 Chemicals and reagents

Acetic acid	Carl Roth GmbH & Co. KG, Karlsruhe
Agarose NEEO Ultra	Carl Roth GmbH & Co. KG, Karlsruhe
Ampicillin	Carl Roth GmbH & Co. KG, Karlsruhe
Ampuwa water	Fresenius Kabi GmbH & Co. KG, Bad Homburg
β-mercaptoethanol	Carl Roth GmbH & Co. KG, Karlsruhe
Bacto Agar	Becton Dickinson GmbH, Heidelberg
Bacto yeast extract	Becton Dickinson GmbH, Heidelberg
Bacto tryptone	Becton Dickinson GmbH, Heidelberg
Bovine serum albumin (BSA)	Carl Roth GmbH & Co. KG, Karlsruhe
Calcium chloride	Sigma-Aldrich Chemie, Steinheim
Chloroform	Merck KGaA, Darmstadt
Diethyl ether	Merck KGaA, Darmstadt
Dimethyl sulfoxide (DMSO)	Merck KGaA, Darmstadt
Disodium phosphate	Merck KGaA, Darmstadt

Disposable PD-10 Desalting Columns	GE Healthcare Bio-Scieces, Uppsala, Sweden
DTNB (5,5'-Dithiobis (2-nitrobenzoic acid))	Sigma-Aldrich Chemie, Steinheim
DTT (1,4-dithiothreitol)	Sigma-Aldrich Chemie, Steinheim
Dulbecco's Phosphate Buffered Saline (DPBS) 10×	Bio Whittaker Lonza, Verviers, Belgium
Diphtheria toxin[Glu^{52}]	Sigma-Aldrich Chemie GmbH, Steinheim
Ethylenediaminetetraacetic acid (EDTA)	Sigma-Aldrich Chemie GmbH, Steinheim
Ethanol	Merck KGaA, Darmstadt
Ethidium bromide	Carl Roth GmbH & Co. KG, Karlsruhe
G418	Biochrom AG, Berlin
Glycine	Carl Roth GmbH & Co. KG, Karlsruhe
Glycerol	Carl Roth GmbH & Co. KG, Karlsruhe
HiLoad™ 16/60 Superdex™ 200 prep grade column	GE Healthcare Bio-Scieces, Uppsala, Sweden
Hydrochloric acid	Merck KGaA, Darmstadt
Kanamycin sulfate	Carl Roth GmbH & Co. KG, Karlsruhe
KappaSelect 1 mL HiTrap column	GE Healthcare Bio-Scieces, Uppsala, Sweden
KappaSelect Sepharose	GE Healthcare Bio-Scieces, Uppsala, Sweden
Magnesium chloride	Merck KGaA, Darmstadt
Manganese(II) chloride	Sigma-Aldrich Chemie GmbH, Steinheim
Methanol	Merck KGaA, Darmstadt
Mini-PROTEAN® TGX™ Precast Gels	Bio-Rad Laboratories GmbH, München
MOPS (3-(N-morpholino)propanesulfonic acid)	Carl Roth GmbH & Co. KG, Karlsruhe
Phosphoric acid	Merck KGaA, Darmstadt
Phenol/Chloroform/Isoamylalkohol (25/24/1)	Carl Roth GmbH & Co. KG, Karlsruhe
Pokeweed mitogen (PWM)	Sigma-Aldrich Chemie GmbH, Steinheim
Potassium chloride	Merck KGaA, Darmstadt
Potassium acetate	Merck KGaA, Darmstadt
Protein A Sepharose	GE Healthcare Bio-Scieces, Uppsala, Sweden
Protein L, biotinylated	Thermo Fisher Scientific, Inc., Schwerte
Sodium acetate	Carl Roth GmbH & Co. KG, Karlsruhe
Sodium azide	Merck KGaA, Darmstadt
Sodium Dihydrogen Phosphate Monohydrate	Merck KGaA, Darmstadt
Streptavidin-polyHRP (horseradish peroxidase)	Immunotools, Friesoythe
Superdex 200™ increase 10/300 GL column	GE Healthcare Bio-Scieces, Uppsala, Sweden
Superdex 200 PC3.2/30 column	GE Healthcare Bio-Scieces, Uppsala, Sweden

Tetagam P	CSL Behring GmbH, Marburg
Tetanus toxoid purified	Statens serum institute, Copenhagen, Denmark
Tetanus toxoid	Astarte biologics,Bothell, USA
Thymidine, [Methyl-^{3}H]	Hartman analytic GmbH, Braunschweig
TMB Microwell Peroxidase Substrate system (2-C)	KPL Inc., Gaithersburg, USA
Tris-Base	Sigma-Aldrich Chemie GmbH, Steinheim
Tris-HCl	Sigma-Aldrich Chemie GmbH, Steinheim
Trypan blue	Sigma-Aldrich Chemie GmbH, Steinheim
Tween-20	Merck KGaA, Darmstadt
Ultima Gold™	PerkinElmer, Rodgau

2.1.4 Enzymes

Calf Intestinal phosphatase (CIP)	New England Biolabs GmbH, Frankfurt
Pepsin (from porcine gastric mucosa)	Merck KGaA, Darmstadt
Restriction endonucleases	New England Biolabs GmbH, Frankfurt or Thermo Fisher Scientific, Inc., Vilnius, Lithuania
T4 DNA Ligase	Thermo Fisher Scientific, Inc., Vilnius, Lithuania

2.1.5 Markers and DNA ladders

1 kb Plus DNA Ladder	New England Biolabs GmbH, Frankfurt
100 bpDNA Ladder	New England Biolabs GmbH, Frankfurt
PageRuler® Prestained Protein Ladder, 10 to 180 kDa	Thermo scientific, Vilnius, Lithuania

2.1.6 Solutions and buffers

2.1.6.1 Commercial solutions for cell culture

Dulbecco's Phosphate buffered saline (DPBS)	Lonza Group Ltd, Basel, CH
Fetal calf serum (FCS)	Biochrom AG, Berlin
Iscove's Modified Dulbecco's Medium (IMDM)	Lonza Group Ltd, Basel, CH
L-Glutamine (100x)	Lonza Group Ltd, Basel, CH
LSM 1077 Lymphocyte	PAA Laboratories GmbH, Pasching, Austria
MEM non-essential amino acids (100x)	PAA Laboratories GmbH, Pasching, Austria
Sodium pyruvate (100 mM)	PAA Laboratories GmbH, Pasching, Austria

Penicillin-Streptomycin Solution (100x)	PAA Laboratories GmbH, Pasching, Austria
RPMI 1640 medium	Lonza Group Ltd, Basel, CH
Trypan-Blue-Solution	Sigma-Aldrich Chemie GmbH, Steinheim
Accutase® solution	Sigma-Aldrich Chemie GmbH, Steinheim
Panexin NTS	PAN-Biotech GmbH, Aidenbach

2.1.6.2 Media for cell culture

Freezing medium	90% (v/v) FCS 10% (v/v) DMSO
IMDM Complete medium	IMDM medium 10% (v/v) FCS L-Glutamine (1x) MEM non-essential amino acids (1x) Sodium pyruvate (1 mM) Penicillin (100 U/mL) Streptomycin (100 μg/mL) 50 μM β-mercaptoethanol
IMDM Pan medium	IMDM medium 10% (v/v) PANEXIN NTS L-Glutamine (1x) MEM non-essential amino acids (1x) Sodium pyruvate (1 mM) Penicillin (100 U/mL) Streptomycin (100 μg/mL) 50 μM β-mercaptoethanol
RPMI 1640 Complete medium	RPMI 1640 Medium 10% (v/v) FCS L-Glutamine (1x) MEM non-essential amino acids (1x) Sodium pyruvate (1 mM) Penicillin (100 U/mL) Streptomycin (100 μg/mL) 50 μM β-mercaptoethanol

2.1.6.3 Chromatography buffers

Acetate buffer pH 4	0.06 M Sodium acetate 0.07 M Acetic acid 0.1 M NaCl pH adjusted with 37% HCl

0.1 M Glycine/0.1 M Citrate-Buffer pH 2.4 and pH 4.2	0.05 M Trisodium citrate dihydrate 0.05 M Citric acid 0.1 M Glycine 0.15 M NaCl in ddH_2O pH adjusted with HCl
0.1 M Glycine-Buffer pH 2.3	0.1 M Glycine in ddH_2O pH 2.3 adjusted with HCl
0.1 M Phosphate-Buffer pH 7.2-7.3	0.07 M Disodium phosphate 0.03 M Sodium Dihydrogen Phosphate Monohydrate 0.1 M NaCl in ddH_2O pH 7.2-7.3 adjusted with NaOH
0.01 M NaOH	1% (v/v) 1M NaOH buffer in ddH_2O
20% ethanol	20% (v/v) of 100% ethanol in ddH_2O

2.1.6.4 Buffers for SDS-PAGE

10x Tris/Glycine/SDS Buffer	Bio-Rad Laboratories GmbH, München
Laemmli Sample Buffer	Bio-Rad Laboratories GmbH, München
Roti®-Blue 5x colloidal coomassie staining solution	Carl Roth GmbH & Co. KG, Karlsruhe

2.1.6.5 Buffers for flow cytometry

7-AAD Viability staining solution	BioLegend GmbH, Fell
FACS-Buffer	DPBS 0.02% (w/v) Sodium azide 1% (v/v) FCS

2.1.6.6 Buffers for ELISA

Blocking buffer	10% (v/v) BSA in ddH_2O

Wash buffer	0,05% Tween-20 in DPBS
Stop solution	1 M Phosphoric acid (H_3PO_4)

2.1.6.7 Buffers and chemicals for molecular biology

Ampicillin stock solution (100 mg/m)]	Ampicillin in ddH_2O
Kanamycin stock solution (100 mg/mL)	Kanamycin in ddH_2O
dNTP-stock solution (10 mM)	dATP, dCTP, dGTP, dTTP (each 10 mM) in ddH_2O
Gel Loading Dye, Purple (6 x)	New England Biolabs GmbH, Frankfurt
LB-Medium	10 g Bacto-tryptone 5 g Bacto-yeast extract 5 g NaCl ad 1 L ddH_2O pH 7
LB-Plates	10 g Bacto-tryptone 5 g Bacto-yeast extract 5 g NaCl 15 g Bacto-Agar ad 1 L ddH_2O
LB-Amp-Plates	10 g Bacto-tryptone 5 g Bacto-yeast extract 5 g NaCl 15 g Bacto-Agar ad 1 L ddH_2O pH 7 1 mL ampicillin stock solution
LB-Kan-Plates	10 g Bacto-tryptone 5 g Bacto-yeast extract 5 g NaCl 15 g Bacto-Agar ad 1 L ddH_2O pH 7 1 mL kanamycin stock solution
TAE-Puffer	40 mM Tris-Base 20 mM acetic acid 1 mM EDTA in ddH_2O
TfbI	30 mM potassium acetate

	50 mM $MnCl_2$ 100 mM KCl 10 mM $CaCl_2$ 15% (w/v) Glycerine adjusted with 0.2 M acetic acid to pH 5.8 sterile-filtered
TfbII	10 mM MOPS pH 7 75 mM $CaCl_2$ 10 mM KCl 15% (w/v) Glycerol sterile-filtered

2.1.7 Cell lines and bacteria strains

All cell lines in this work used are listed in the table 2.13.

Table 2.13: **Cell lines**

Name	**Cell type, reference**	**Source**
SP2/0 Ag14	mouse myeloma, (Shulman et al., 1978)	LGC Standards GmbH, Wesel
Jurkat	human acute T-cell-leukemia cell line (Schneider et al., 1977)	D. Schendel, München
Daudi	human Burkitt's Lymphoma cell line (Klein et al., 1968)	P. Fisch, Freiburg
SKW 6.4	human B lymphoblast cell line (Saiki and Ralph, 1983)	P. Krammer, Heidelberg
C1R-B7	human B lymphoblast cell line (Storkus et al., 1989)	W. Walter, Mainz
Raji	human Burkitt's lymphoma cell line (Pulvertaft, 1964)	European Collection of Cell Cultures (ECACC)
JY	human B lymphoblastoid cell line (Swaroop and Xu, 1993)	European Collection of Cell Cultures (ECACC)
SK-Mel-63	human malignant melanoma (Fogh et al., 1977)	B. Gückel, Tübingen

Bacteria strain *E.coli* DH5-α used in this work was purchased from MBI Fermentas, St. Leon Rot
Genotype:
$F^-(\Phi 80d\Delta(lacZ)M15)recA1\ endA1\ gyrA96\ thi\text{-}1hsdR17(r^-{}_\kappa m^+{}_\kappa)\ supE44\ relA1\ deoR\ \Delta(lacZYA\text{-}argF)U169$

2.1.8 Antibodies

Monoclonal and polyclonal antibodies listed in the tables 2.14 and 2.15 were used for analytical methods (flow cytometry, ELISA and Western-blot) and for functional immunobiological assays.

Table 2.14: **Unconjugated antibodies**

Name	Special feature	Specificity	Isotype	Species	Source
2H7		human CD20	Igγ1/κ	Mouse	BioLegend GmbH, Fell
2H7 korr		human CD20	Igγ1/κ	Chim. mouse/human Ab	N. Teichweyde, Tübingen
2H7 SDIE	SDIE opt.	human CD20	Igγ1/κ	Chim. mouse/human Ab	L. Grosse-Hovest, Tübingen
anti-Tetanus Hc	Rabbit serum	C fragment of Tetanus toxin	polyclonal	Rabbit	Novus Biologicals, Littleton, USA
anti-Diphtheria	Rabbit serum	Diphtheria toxin	polyclonal	Rabbit	Abcam, Cambridge, UK
APO-1		human CD95	Igγ2a/κ	Mouse	P. Krammer, Heidelberg
APO-1 hum		human CD95	Igγ2a/κ	Chim. mouse/human Ab	L. Grosse-Hovest, Tübingen
EGFR		human EGFR	Igγ1/κ	Chim. mouse/human Ab	L. Grosse-Hovest, Tübingen
EGFR SDIE	SDIE opt.	human EGFR	Igγ1/κ	Chim. mouse/human Ab	E. Pyz, Tübingen
Flebogamma	human Ab	polyclonal	Igγ	Human	Grifols international S.A.
Goat anti-mouse Igγ		mouse Igγ	polyclonal	Goat	Dianova GmbH, Hamburg
Goat anti-human Igγ		human Igγ	polyclonal	Goat	Dianova GmbH, Hamburg
Rituximab		human CD20	Igγ1/κ	Chim. mouse/human Ab	Hoffmann-La Roche AG, Basel
UCHT-1		human CD3	Igγ1/κ	Chim. mouse/human Ab	L. Grosse-Hovest, Tübingen
χ9.2.27-DE		human CSPG4	Igγ1/κ	Chim. mouse/human Ab	L. Grosse-Hovest, Tübingen

Table 2.15: **Conjugated antibodies**

Name	Conjugation	Specificity	Isotype, Fragment	Species	Source
anti-Mouse Igγ Fc-RPE	RPE	Mouse Igγ Fc specific	polyclonal $F(ab')_2$-Fragment	Goat	Dianova GmbH, Hamburg
anti-Mouse Igγ + Igμ (H+L) -RPE	RPE	Mouse Igγ und Igμ H + L specific	polyclonal $F(ab')_2$-Fragment	Goat	Dianova GmbH, Hamburg
anti-Human Igγ Fc-RPE	RPE	human Igγ Fc specific	polyclonal $F(ab')_2$-Fragment	Goat	Dianova GmbH, Hamburg
anti-Human Igγ Fc-APC	APC	human Igγ Fc specific	polyclonal $F(ab')_2$-Fragment	Goat	Dianova GmbH, Hamburg
anti-Human $F(ab')_2$-Biotin	Biotin	$F(ab')_2$-Fragment specific	polyclonal whole IgG	Goat	Dianova GmbH, Hamburg
anti-Rabbit Igγ-APC	APC	IgG (H+L) specific	polyclonal Igγ $F(ab')_2$-Fragment	Donkey	Dianova GmbH, Hamburg
anti-Human CD4	FITC	human CD4	Igγ1/κ	Mouse	own production, Tübingen
anti-Human CD8a	APC	human CD8	Igγ1/κ	Mouse	BioLegend GmbH, Fell
anti-Human CD14	FITC	human CD14	Igγ1/κ	Mouse	BioLegend GmbH, Fell
anti-Human CD19	Pacific Blue	human CD19	Igγ1/κ	Mouse	BioLegend GmbH, Fell
anti-Human CD19	PE	human CD19	Igγ1/κ	Mouse	BioLegend GmbH, Fell
anti-Human CD56	BV421	human CD56	Igγ1/κ	Mouse	BioLegend GmbH, Fell
anti-Human CD138	PE	human CD138	Igγ1/κ	Mouse	BioLegend GmbH, Fell
Mouse Igγ1 κ FITC	FITC	Isotype control	Igγ1/κ	Mouse	BioLegend GmbH, Fell
Mouse Igγ1 κ PE	PE	Isotype control	Igγ1/κ	Mouse	BioLegend GmbH, Fell
Mouse Igγ1 κ APC	APC	Isotype control	Igγ1/κ	Mouse	BioLegend GmbH, Fell
Mouse Igγ1 κ Pacific Blue	Pacific Blue	Isotype control	Igγ1/κ	Mouse	BioLegend GmbH, Fell

2.1.9 Kits

Anti-Tetanus Toxoid ELISA (IgG)	Euroimmun, Lübeck
BD® CompBead Anti-mouse Ig κ	Becton Dickinson GmbH, Heidelberg
cDNA Synthesis system	Roche, Basel, Switzerland
CloneJET PCR Cloning Kit	Thermo Fisher Scientific, Inc., Vilnius, Lithuania
Cytoplasmic and Nuclear RNA Purification Kit	Norgen Biotec Corp., Ontario, Canada
KAPA HiFi PCR Kit	KAPA Biosystems, Cape Town, South Africa
NucleoSpin® Gel and PCR Clean-up	Macherey-Nagel, Düren
QIAprep® Spin Miniprep Kit	Qiagen GmbH, Hilden
QIAGEN® Plasmid Maxi Kit	Qiagen GmbH, Hilden
QIAquick® Gel Extraction Kit	Qiagen GmbH, Hilden
QIFIKIT®	DAKO Deutschland GmbH, Hamburg

2.1.10 DNA sequences

2.1.10.1 Oligonucleotides

All oligonucleotides used for sequencing or cloning were purchased from Sigma-Aldrich Chemie GmbH (München), Biomers GmbH (Ulm) or Eurofins Genomics (Ebersberg).

Oligonucleotides for cloning of bispecific CD20×CD95 antibodies in the FabSc format

2H7 SpeI-rev	5'-tataactagt[1]ttatcatttcagctccagcttggtcccagcaccgaacgtggg-3'
BspEI CD20 HL-hin	5'-aaaatttccgga[2]caggcttatctacagcagtctggggctgag-3'

Oligonucleotides for cloning of CD95-Ag fusion proteins

CRM197$_{C186G}$-hin	5'-catggcccaggccggc[3]gccggcaacagag-3'
CRM197$_{C186G}$-rev	5'-ctctgttgccggcgcc[3]ggcctgggccatg-3'
CRM197$_{C201G}$-hin	5'-gcagctccctgagcggc[3]atcaacctgg-3'
CRM197$_{C201G}$-rev	5'-ccaggttgatgcc[3]gctcagggagctgc-3'
CRM197$_{R173Q}$-hin	5'-gacaagaggcaagcag[4]ggccaggacgc
CRM197$_{R173Q}$-rev	5'-gcgtcctggccctg[4]cttgcctcttgtc-3'
CRM197$_{R193Q}$-hin	5'-caacagagtgcgacaa[4]tctgtgggcag-3'
CRM197$_{R193Q}$-rev	5'-ctgcccacagattg[4]tcgcactctgttg-3'

[1]SpeI restriction site
[2]BspEI restriction site
[3]Mutation Cys→Gly
[4]Mutation Arg→Gln

Diph-C-hin	5'-catttatccgga[5]ggcgctgacgacgtgg-3'
Diph-R-rev	5'-gccgggactagt[6]tatcaggacttgatctcg-3'
Diph-T-hin	5'-tttaatccgga[5]tctgtgggcagctccctgag-3'
Diph-T-rev	5'-ctgggactagt[6]tatcaaaaaggctgggtcttg-3'
TetC-$_{1-451}$-hin	5'-cagccctccgga[5]aagaacttgg-3'
TetC-$_{80}$-hin	5'-cagccctccgga[5]aacgatatgttcaataac-3'
TetC$_{271}$-rev	5'-ctgattcctgtagcgtcttgataactagt[6]cccag-3'
TetC$_{451}$-rev	5'-ctgggactagt[6]tatcaatcg-3'

Oligonucleotides for sequencing

Kons1-hin	5'-gggtgcaaaagagcggccttctagaag-3'
Kons1-rev	5'-tgcagggtcccaaggcagtgctgggtg-3'
Kons2-hin	5'-ccagactcaaacttaccctacctttatc-3'
Kons2-rev	5'-ggtctgttatgccaagctctgtctatg-3'
Kons3-hin	5'-tgtgacatagaagctgcaatagtcag-3'
Kons3-rev	5'-ccaggatattaaccaatgagtgta-3'
CH2-hin	5'-caaaacccaaggacaccctc-3'
pA-rev	5'-ggaggtaggtgtcagagtcc-3'
mRNA-hin1	5'-acatatgtacaatgtcctcaccacag-3'
kmRNA-hin	5'-atgagccacacaaactcagggaaagctcg-3'
pJET 1.2 Forw	5'-cgactcactatagggagagcggc-3'
pJET 1.2 Rev	5'-aagaacatcgattttccatggcag-3'
T7 promoter	5'-taatacgactcactataggg-3'
Intron-rev	5'-gattcccgtttgcagagaatcttgg-3'
M13-hin	5'-gtaaaacgacggccagt-3'
M13-rev	5'-aacagctatgaccatg-3'

2.1.10.2 DNA sequences

CD20 V_H-V_L	L. Grosse-Hovest, Tübingen GenBank: #AJ937362.1
CSPG4 V_H-V_L	L. Grosse-Hovest, Tübingen GenBank: #AJ459797.1 and #AJ459796.1
APO-1 V_H and V_L	L. Grosse-Hovest, Tübingen (See Appendix 6.3, page 125)
Tetanus Hc Fragment (GenBank: #1AF9_A)	Eurofins MWG Operon, Ebersberg
Diphtheria Toxoid CRM197 (GenBank: #1007216A)	GeneArt®, Regensburg

[5]BspEI restriction site
[6]SpeI restriction site

2.1.10.3 Plasmids for the cloning of nucleic acids

pJET1.2/blunt was used for standard manipulation of PCR products and DNA fragments prior to insertion into expression vectors according to the manufacturer instructions. For mapping and manipulation of the insert, the pJET1.2/blunt cloning vector multiple cloning site contains two BglII recognition sequences that flank the insertion site. The vector contains a lethal restriction enzyme gene that is disrupted by ligation of a DNA insert into the cloning site. As a result, only bacterial cells with recombinant plasmids are able to form colonies. In addition, the vector contains a T7 promoter for *in vitro* and *in vivo* transcription. Sequencing of the insert was performed with the sequencing primers of the kit. Further details and genetic elements of this vector are described in the Fig. 2.1.
NF-CU-N297Q expression vector generated by M. Durben (Durben et al., 2015) was used as a starting material for cloning of bispecific CD95×CD20 antibodies in the FabSc format. Further details and genetic elements of this vector are provided in Fig. 2.2.

2.1.10.4 Expression vectors

Two types of vectors were used for the expression of antibodies and antibody-fusion proteins in the mouse myeloma cell line Sp2/0:

- For the expression of the antibody κ-light chain, a vector based on pPCR-Script-vector was used. The lacZ promoter- and termination sequence were removed. Further details and genetic elements of this vector are described in the Fig. 2.3.

- For the expression of the antibody heavy chain, a vector based on fusion vector pcDNA × pPCR (L. Grosse-Hovest, Tübingen) was used. The CMV promoter was replaced by a promoter for the mouse IgG heavy chain and the termination sequence for bovine growth hormone was removed. Further details and genetic elements of this vector are provided in the Fig. 2.4.

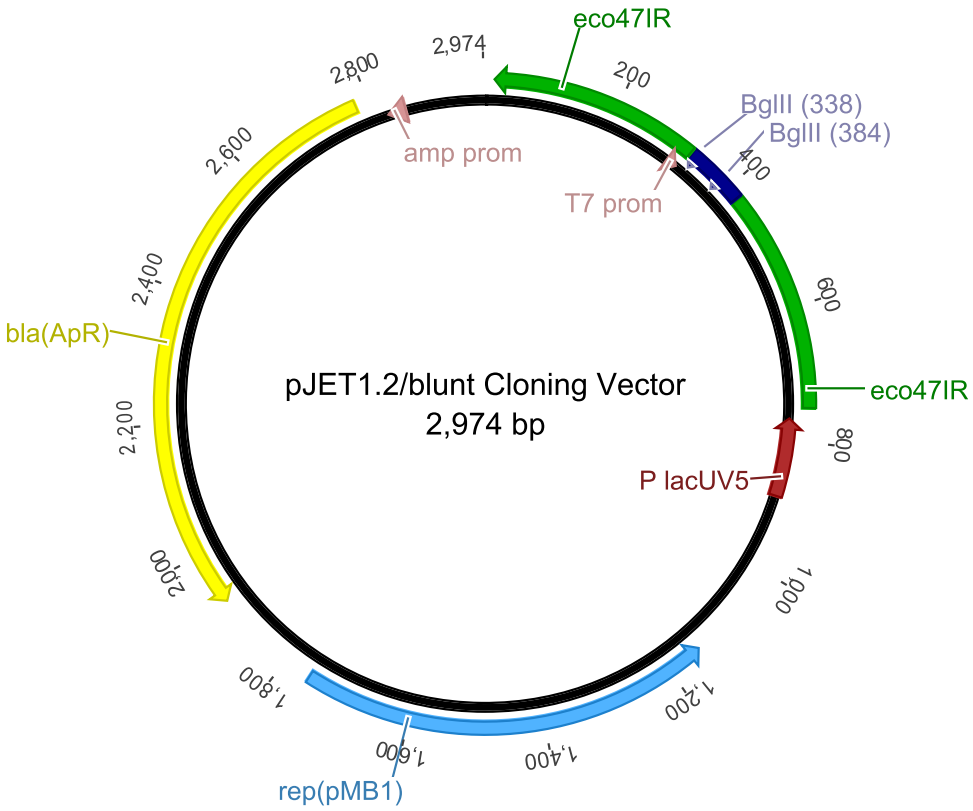

Figure 2.1: **Genetic elements of the pJET1.2/blunt cloning vector** rep (pMB1) – replicon (rep) from the pMBI plasmid responsible for the replication of pJET1.2 (1762 bp – 1148 bp); replication start (1162± 1); *bla*Ap^R – β-lactamase gene conferring resistance to ampicillin (2782 bp – 1922 bp); *eco47IR* – lethal gene *eco47IR* enabling positive selection of the recombinants (753 bp – 16 bp); P$_{lacUV5}$ – modified promoter for expression of the *eco47IR* gene at a level sufficient to provide positive selection (892 bp – 769 bp); T7 promoter – T7 RNA polymerase promoter for*in vitro* transcription of the cloned insert (305 bp – 324 bp); Multiple cloning site (MSC) – mapping, screening and excision of the cloned insert (422 bp - 328 bp); insertion site (coloured in blue) – blunt DNA ends for ligation with insert (371 bp – 372 bp).

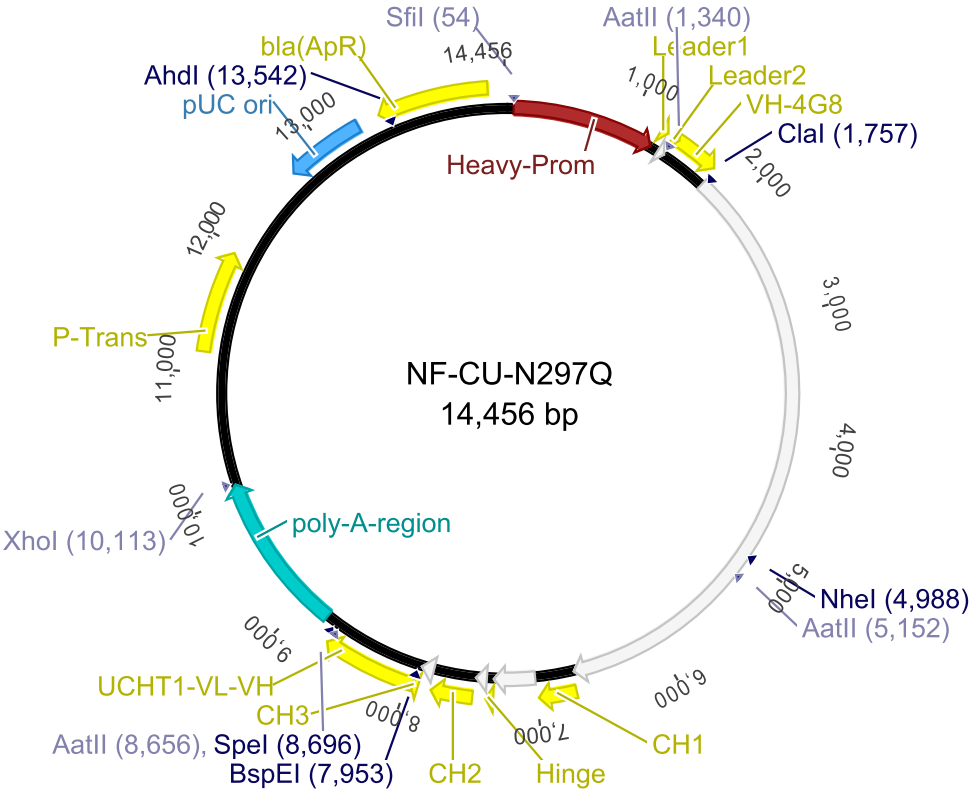

Figure 2.2: **Genetic elements of the NF-CU$_{N297Q}$ heavy chain vector**
Major parts of the vector:
This vector is based on the backbone of the fusion vector pcDNA × pPCR. It contains a promoter sequence for mouse IgG-heavy chain (53 bp – 1230 bp). The leader sequence segmented by one intron, which is coded between promoter sequence and variable domain (V_H). The V_H domain coding for the FLT3 (clone 4G8) antibody is flanked by AatII and ClaI restriction sites. V_H domain and first constant region of the heavy chain (C_H1) are separated by intron containing μ-enhancer-element. C_H1 domain is followed by a modified C_H2 domain of human IgG1 and the ScFv-fragment of CD3 antibody (UCHT1). Modification of the C_H2 domain of human IgG1 consists of the amino acid substitutions and deletions (EU-index) C226S; C229S; E233P; L234V; L235A; ΔG236; D265G; N297Q; A327Q; A330S). The coding section for ScFv on the C-terminus is flanked by BspEI and SpeI restriction sites. Promoter, introns and poly-A-region are obtained from genomic sequence from mouse C57BL/6 antibody locus (GenBank #AJ487681). Coding sequences for constant domains are from human Igγ1-chain. The vector contains a *bla*Ap^R - β-lactamase gene and a phosphotransferase-gene (P-Trans) sequences for ampicillin and neomycin resistance.

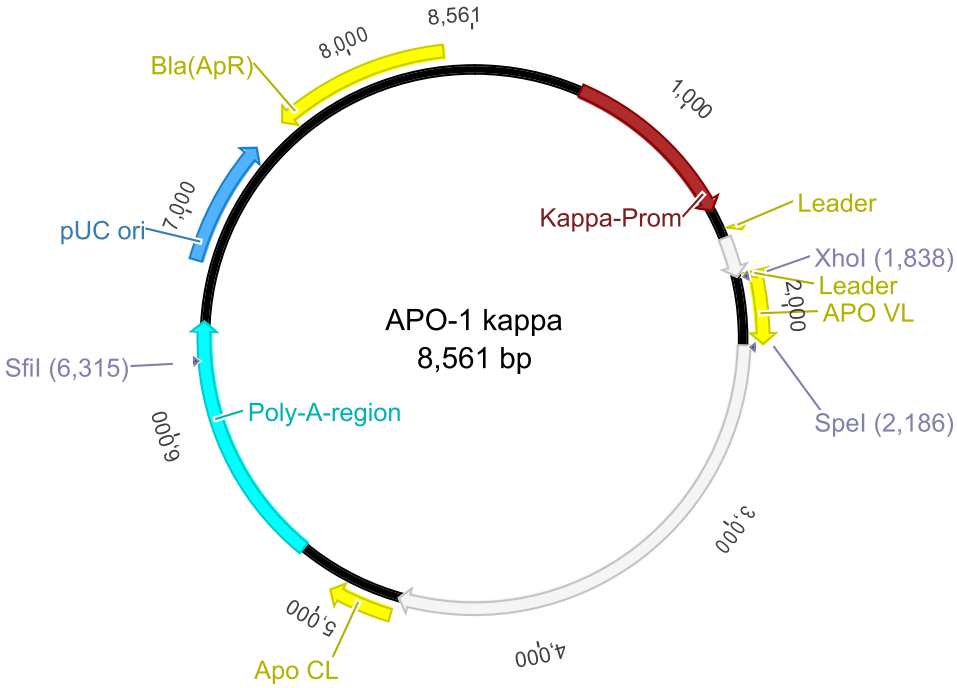

Figure 2.3: **Genetic elements of the APO-1 κ-chain vector**
This vector is based on the backbone of the *pPCR-Script*^{TM} *AmpSK(+)Cloning-Vector,* without LacZ promoter- and termination sequence. It contains the promoter sequence from mouse κ-chain (K-Prom) gene. The leader sequence segmented by one intron is coded between promoter sequence and variable domains (V_L). The V_L domain is flanked by XhoI and SpeI restriction sites. V_L domain and constant region of the light chain (C_L) are separated by intron containing κ-enhance -element. The vector contains *bla*Ap^R – β-lactamase gene conferring resistance to ampicillin. Promoter, introns and poly-A-region are obtained from genomic sequence from mouse C57BL/6 light chain antibody locus (GenBank #AJ487682).

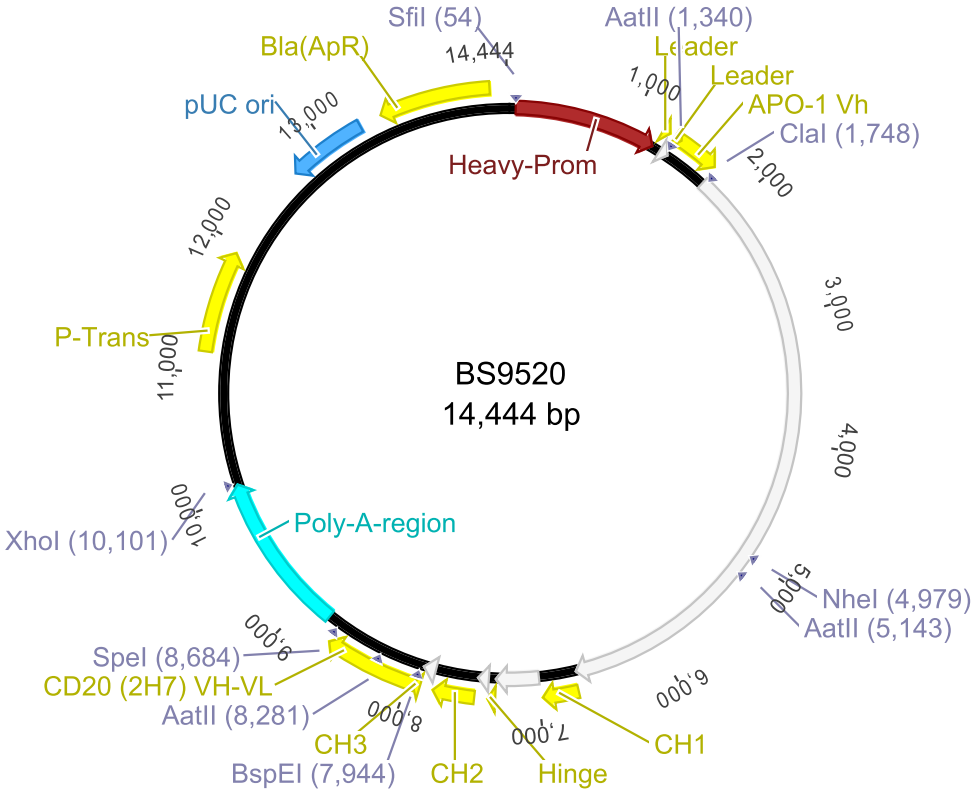

Figure 2.4: **Genetic elements of the BS9520 heavy chain vector**
Major parts of the vector:
This vector is based on the backbone of NF-CU-N297Q heavy chain expression vector depicted on the Fig. 2.2. The V_H domain for a mouse APO-1 antibody is flanked by AatII and ClaI restriction sites. The coding sequences for constant domains are from human IgG-chain. CD20 ScFv (V_H-V_L) at the C-terminus is flanked by BspEI and SpeI restriction sites. In case of control antibody BS95Mel the CD20 ScFv element was exchanged by a CSPG4 specific ScFv (V_H-V_L) antibody fragment.

2.2 Molecular biology methods

2.2.1 Isolation and purification of nucleic acids

2.2.1.1 Isolation of Plasmid-DNA from bacteria cultures

Isolation of Plasmid-DNA from bacterial cultures was performed using commercial kits from Qiagen. Depending on the required amount of DNA different kits were used. Isolation was performed according to the QIAprep® Spin Plasmid-DNA Miniprep Kit or QIAGEN® Plasmid-DNA Maxiprep Kit manufacturer's instructions. QIAGEN plasmid purification protocols are based on a modified alkaline lysis procedure (Bimboim and Doly, 1979).

2.2.1.2 Isolation of cytoplasmic RNA and cDNA synthesis

Mature, cytoplasmic RNA from antibody producing transfected Sp2/0 cells was isolated to verify the RNA sequence for potential splicing sites using Cytoplasmic & Nuclear RNA Purification Kit. Isolation was performed according to the manufacturer's instructions. Isolated RNA was applied to cDNA synthesis using cDNA synthesis system, according to the manufacturer's protocol. ssDNA was subsequently proceeded to polymerase chain reaction (PCR) using mRNA-hin1 and pA-rev oligonucleotides to amplify DNA sequences, coding for antibody heavy chain (PCR is described in the section 2.2.2.4).

2.2.1.3 Purification of DNA from the agarose gel

Gel purification was used to isolate and purify DNA fragments based on size. The procedure starts with standard agarose gel electrophoresis, which separates DNA by their length. Following electrophoresis, DNA bands were cut out of the agarose gel. DNA fragments were purified using commercial gel purification kits according to the manufacturer's instructions. For the fragments $\geq$10 kb NucleoSpin® Gel and PCR clean up Kit was used. Smaller fragments ($\leq$10 kb) were purified using Qiaquick® Gel Extracion Kit.

2.2.1.4 Phenol-chloroform extraction and precipitation of DNA

The Phenol-chloroform extraction was performed to purify the expression vectors after preparative digestion (linearization) with restriction endonucleases. DNA solution was mixed with an equal volume of ready-to use Phenol/Chloroform/Isoamylalcohol (25/24/1) mixture and vortexed vigorously to mix the liquid phases. After centrifugation of the sample the upper aqueous phase was removed carefully into the new 1.5 mL tube to avoid transfer of any proteins, concentrated in the interface. The sample was extracted two more times with an equal volume of chloroform to remove trace amounts of phenol.
For the precipitation of nucleic acids 10% (v/v) of 3 M sodium acetate solution pH 5.2 and 2.5 volumes of the absolute ethanol were added to the aqueous phase. The sample was frozen at -80° C for 20 min and centrifugated at 4° C and 17900 $\times$ g in the microcentrifuge for 20 min. The supernatant was carefully decanted and the

DNA pellet was air dried on the clean bench. Subsequently the DNA was dissolved in 40-50 μL ddH_2O.

2.2.2 Handling of nucleic acids

2.2.2.1 Digestion of DNA with restriction endonucleases

Restriction enzymes of Type II and Type IV were used in this work. The most common Type II enzymes cut DNA at defined positions close to or within their recognition sequences. Cleavage leaves a 3'-hydroxyl on one end of each cut and a 5'-phosphate on the other end. Type IV enzymes recognize and cleave modified, typically methylated DNA (DpnI).
Restriction digestion was used for analysis or preparation of DNA fragments. Analytical restriction digestion was performed as follows:

1 μg	DNA
1 μL	10 $\times$ Reaction buffer
2 U	Restriction endonuclease
ad 10 μL	ddH_2O

DNA was subjected to digestion for 1 h at appropriate temperature recommended by manufacturer.
Preparation of larger amounts of DNA (for cloning or transfection) was performed as follows:

30 μg	DNA
10 μL	10 $\times$ Reaction buffer
40 U	Restriction endonuclease
ad 100 μL	ddH_2O

DNA was subjected to digestion for 3-4 h at appropriate temperature recommended by manufacturer.

2.2.2.2 Dephosphorylation of 5' and 3' ends of DNA

Plasmids were treated with Calf intestinal phosphatase (CIP) before performing ligation of dsDNA fragments with blunt or sticky ends to form recombinant DNA plasmids. In this step 5'-phosphate is removed to ensure that the vector does not recirculate during ligation. 1000 U CIP was added to the DNA mixture after restriction digestion and incubated for 1 h at 37° C.

2.2.2.3 Ligation of nucleic acid fragments

Ligation was used to join dsDNA fragments with blunt or sticky ends to insert DNA fragments into the plasmids or expression vectors.

Ligation of DNA fragments into pJET1.2/blunt vector

1 μL	pJET1.2/blunt clonig vector
1 : 3 molar ratio over vector	DNA-Insert (Blunt-End)
10 μL	2 $\times$ reaction buffer
1 μL	T4 DNA Ligase (5 U/μL)
Total volume	20 μL

The reaction mix was incubated at room temperature for 10 min – 30 min.

Ligation of DNA into Expression vectors

50-100 ng	Plasmid
1 : 5 molar ratio over vector	Insert
2 μL	10 $\times$ ligation buffer
1 μL	T4 DNA Ligase (5 U/μL)
Total volume	20 μL

The reaction mix was incubated at room temperature for 10 min.

2.2.2.4 Polymerase chain reaction

Polymerase chain reaction was used for amplification and mutagenesis of specific DNA fragments *in vitro*. For the amplification of DNA fragments specific *sense*- and *anti-sense* primers complementary to the 3' end of the sense and anti-sense DNA sequences were generated (Kleppe et al., 1971; Mullis and Faloona, 1987). PCR reaction was performed in 3 steps using KAPA HiFi DNA polymerase and following cycling parameters:

Initial denaturation	95°C	5 min
Denaturation	98° C	20 sec
Primer annealing	$T_m \pm 10$°C	15 sec
Extension	72° C	30 sec/kb
Final extension	72° C	5 min
Cooling	4° C	Hold

Inverse PCR reaction with the same polymerase and the same cycling parameters was used for site-directed mutagenesis. Using this approach with a circular fully methylated plasmid as template and oligonucleotide pairs (approx. 30 bp in length) containing the desired mutation in the middle, a linearised un-methylated vector is created that incorporates the mutation. The linearised vector was re-circulated via PCR. After that reaction mixture was subjected to DpnI digestion to destroy the methylated and hemi-methylated DNA template. Chemically competent *E. coli* were transformed with 10 μL of this mixture (Bacterial transformation is described in the section 2.3.1.2 on page 46).

2.2.3 Analysis of nucleic acids

2.2.3.1 Agarose gel electrophoresis

Agarose gel electrophoresis was used to separate DNA by size (e.g. length in base pairs) for visualization and purification. Agarose gels were commonly used in concentrations of 1% to 1.5% depending on the size of DNA fragments. The required amount of agarose powder was mixed with the TAE buffer and heated in a microwave oven for 1-3 min (until the agarose was completely dissolved). Agarose solution was cooled for 5 min and ethidium bromide (EtBr) was added to a final concentration of 0.5-1 μg/mL. The DNA-samples were mixed with 1/6 volume of the loading buffer before running an agarose gel. A molecular weight ladder (100 bp or 1 kb Plus) was loaded with the samples for determination of size of the DNA-fragments. Agarose gel electrophoresis was performed using TAE buffer at 80-150 V. DNA fragments were visualized using UV light (254 nm).

2.2.3.2 Nucleic acid quantification

Concentration of nucleic acids in aqueous solution was determined by spectrophotometric analysis at the wave length 230 nm, 260 nm and 280 nm using Nanodrop™ 1000 UV-Vis spectrophotometer. An Absorbance (A) of 1 corresponds to a concentration of 50 μg/mL for double-stranded DNA (dsDNA), 40 μg/mL for RNA and 33 μg/mL for single-stranded DNA (ssDNA). The ratio of absorbance at 260 and 280 nm was used to assess the purity of DNA and RNA. A ratio of ≈ 1.8 was accepted as "pure" for DNA; a ratio of ≈ 2.0 was accepted as "pure" for RNA. If the ratio is appreciably lower in either case, it may indicate the presence of protein, phenol or other contaminants that absorb strongly at or near 280 nm.

2.3 Microbiology and cell biology methods

2.3.1 Bacteria

2.3.1.1 Preparing chemically competent cells

E. coli DH5α bacteria were plated out on LB plates without antibiotics the day before starting the liquid culture for the competent cells. The plate straight from 37°C was used to start the cultures. 5 mL of LB medium were inoculated with 1 clone of *E. coli* DH5α and incubated overnight at 250 rpm and 37°C. In the morning, the overnight culture was diluted to at least 1:100 in 100 mL and incubated for further 1-2 h at 250 rpm and 37°C until the optical density (O.D.) of the culture reached 0.2-0.3 at 550 nm. The cells were centrifuged for 10 min at $1619 \times g$ and 4°C. Supernatant was discarded, the pellet resuspended in 20 mL of ice-cold TfbI buffer and incubated on ice for 20-30 min. The cells were centrifuged again for 5 min at $719 \times g$ and 4°C. Supernatant was discarded and the pellet was resuspended in 4 mL of ice-cold TfbII buffer. Aliquots with 100 or 200 μL of this suspension were frozen in 1.5 mL tubes and stored immediately at -80°C.

2.3.1.2 Transforming chemically competent *E. coli* DH5α with plasmid-DNA

For the transformation of chemically competent bacteria, the required number of aliquots was thawed on ice, mixed with plasmid DNA ($\leq 1\mu$g) or the ligation reaction mix (see Ligation 2.2.2.3 on the page 43) and incubated on ice for 45 min. Subsequently, a heat shock was performed for 1 min at 42°C. The tubes were placed on ice immediately. 300 μL LB medium was added to each tube and incubated for 1 h at 37°C and 250 rpm. 100 μL of each suspension was plated out on LB plates containing the appropriate antibiotic. The plates were incubated overnight at 37°C.

2.3.1.3 Cultivation of bacteria

Bacteria were cultivated for amplification of plasmid DNA. Single bacteria colonies from a selective plate were picked with a sterile pipette tip and transferred to a new selective master-plate. Pipette tip was then dropped into a tube with 1-5 ml LB medium containing 100 μg/mL of the appropriate selective antibiotic to inoculate the culture.
For the isolation of plasmid DNA with QIAGEN® Plasmid-DNA Miniprep Kit, the cultures were incubated for 12-16 h at 37°C with vigorous shaking.
For the isolation of plasmid-DNA with QIAGEN® Plasmid-DNA Maxiprep Kit, the cultures were incubated at the same conditions for 6 h and then diluted 1/1000 into 200 mL of LB medium containing the appropriate antibiotic. Erlenmeyer flasks with bacteria cultures were incubated for 12-16 h at 37°C with vigorous shaking.

2.3.2 Eukaryotic Cells

All cell lines and human peripheral blood mononuclear cells (PBMC) were maintained at 37°C and 5% CO_2 (for RPMI medium) or 7% CO_2 (for IMDM medium) in a cell incubator.

2.3.2.1 Thawing cryopreserved cells

Cryovials containing frozen cells were removed from liquid nitrogen or -80°C freezer and thawed rapidly ($\leq$1 min) in a 37°C water bath. The cell suspension was slowly diluted with pre-warmed IMDM or RPMI complete medium and centrifuged at $200 \times g$ for 5 min. After the centrifugation, the supernatant was decanted without disturbing the cell pellet. The cells were gently re-suspended in complete growth medium, and transferred into the appropriate culture vessel and environment.

2.3.2.2 Subculturing mammalian cells

Adherent cells were detached from the culture flask before subcultivation. To this end, the medium was aspirated from the cell culture flask. The cell layer was rinsed once with 10 mL DPBS and 2.5 - 5 mL Accutase® was added to the flask to cover the cell layer. The flask was incubated at room temperature (RT) for 5 to 10 min up to a maximum of 1 h. Subsequently the cells were gently dispersed and an aliquot of the detached cells was added to fresh medium in new flasks.

Suspension cells were diluted with fresh medium in new flasks with desired cell density.

2.3.2.3 Viability measurement and cell count

Viability of the cells was determined by Trypan blue exclusion. The cell sample was diluted 1:2 or 1:10 (depending on cell density) in Trypan blue solution. The cell suspension was transferred into a hemacytometer and examined immediately under a microscope.
The number of viable cells in the chamber was used to calculate the cell concentration in the sample. The number of cells in the 0.1 mm^3 chamber multiplied by the factor of 10^4 and with the dilution factor results in cell concentration per 1 mL medium.

2.3.2.4 Cryopreservation of cells

Cells were pelleted by centrifugation at $250 \times g$ and the supernatant was discarded. The cells were re-suspended in freezing medium in a concentration of 10^6 - 10^7 cells/mL and aliquoted into cryovials. Cells were frozen slowly 1°C/min. This was done by placing vials in a freezing container placed in a -80°C. After 24 h frozen cells were transferred to liquid nitrogen storage.

2.3.2.5 Stable transfection of eukaryotic cells

For stable transfection 2×10^7 Sp2/0-Ag14-cells were washed three times with 50 mL ice-cold IMDM medium without supplements. Centrifugation was performed at $200 \times g$. The cell pellet was resuspended in 200 μL IMDM, mixed with linearized expression vectors and transferred into a cold electroporation cuvette with 0.4 cm gap width. Electroporation was performed at 230 V und 975 μF. The cells were then transferred immediately into 12 mL of warm IMDM complete medium and, after serial dilution, seeded into 96-well plates (50 μL/well).
Selection for stable transfected cells was accomplished by adding the antibiotic G418 (end concentration: 1 mg/mL) 24 h after transfection. 7-10 days after transfection cells were monitored for antibiotic-resistant clones. 14-20 days after transfection cell culture supernatants from growing clones were tested for the presence of recombinant antibodiesby flow cytometry.

2.3.2.6 Cultivation of antibody-producing transfected cells

Antibody-producing Sp2/0 cells were cultivated in IMDM complete medium supplemented with 1 mg/mL G418. The cells were kept at a density of $2\text{-}3 \times 10^5$ cells/mL. Cell were expanded in 175 cm^2 cell culture flasks to the final volume of 1-2 liter and cultivated until approx. 50% of all cells were dead. Cell culture supernatant was harvested by centrifugation at $6000 \times g$, supplemented with 0.02% (w/v) NaN_3 and filtrated using 0.22 μm bottletop filter. Depending on the purification strategy the supernatant was adjusted to pH 7.6 (KappaSelect) or pH 8 (Protein A) and stored at 4°C.

2.3.2.7 Cultivation of antibody-producing hybridoma cell lines

Antibody-producing Sp2/0 hybridoma cells were cultivated in IMDM Pan medium (IMDM supplemented with chemically defined serum substitute for suspension cells PANEXIN NTS) at a cell density of $2\text{-}3 \times 10^5$ cells/mL. Cells were expanded in TripleFlask™ cell culture flasks to a final volume of 1 - 2 L. Afterwards the cells were kept in culture until approx. 50% of all cells were dead. Finally cell culture supernatant was harvested by centrifugation at $6000 \times g$, supplemented with 0.02% (w/v) NaN_3 and filtrated using 0.22 μm bottletop filter. For purification with Protein A the supernatant was adjusted to pH 8 and stored at 4°C.

2.3.2.8 Isolation of human PBMC from whole blood

Human PBMCs were separated from heparinised blood by a density gradient centrifugation method using Ficoll-Hypaque solution.
To this end heparinised blood was diluted 1:2 with DPBS and 25 mL of diluted cell suspension was carefully layered over 15 mL Ficoll-Hypaque solution in a 50 mL conical tube. The cells were centrifuged at $561 \times g$ for 30 min in a swinging-bucket rotor without brake. The layer of mononuclear cells was carefully transferred from the interphase to a new 50 mL conical tubes, washed by adding DPBS to 50 ml and centrifugation $300 \times g$ for 10 min. Supernatant was removed completely. For removal of platelets, the cell pellet was resuspended in 50 mL of DPBS and centrifuged at $200 \times g$ for 10 min. The cell pellet was resuspended in the appropriate amount of RPMI complete medium or DPBS.

2.3.2.9 Isolation of human PBL using red blood cell lysis

RBC lysis buffer containing ammonium chloride was used to remove red blood cells (RBC) from whole blood and bone marrow samples. To this end, 10× RBC lysis buffer was diluted prior to use to 1× working concentration with room temperature bidist. water. For purification of human peripheral blood leukocytes (PBL) 15 volumes of 1× RBC lysis buffer were added to the cell sample, gently vortexed and incubated for 10-15 minutes at the room temperature. As soon as the cell suspension became clear, the cells were centrifuged at $350 \times g$ for 5 minutes. Supernatant was aspirated without disturbing pellet, the cells were washed at $350 \times g$ for 5 minutes with DPBS and resuspended in the appropriate buffer depending on following experiments.

2.4 Protein biochemistry and analytical methods

2.4.1 Chromatography

2.4.1.1 Affinity chromatography

The principle of affinity chromatography is based on a reversible interaction between a protein and a specific ligand coupled to a chromatography matrix. In this work two types of ligands were used. Antibodies containing a complete Fc part (mouse

IgG, chimeric IgG) were purified using Protein A media and chimeric antibodies without C_H3-domain were purified using KappaSelect media.

Protein A affinity chromatography
Protein A is a bacterial protein purified from *Staphylococcus aureus*. The basis for purification of IgG is the high affinity of protein A for the Fc region of polyclonal and monoclonal IgG antibodies.
Cell culture supernatants prepared and filtered as described in 2.3.2.7 on page 48 were applied to the column (equilibrated with 0.1 M phosphate buffer pH 8) at the flow rate of 50 mL/h using a peristaltic pump. All unbound material was removed by washing with at least 10 column volumes and determined by UV absorbance at 280 nm.
Protein A is also able to bind bovine IgG. However, binding of bovine IgG to Protein A is weaker than binding of chimeric (mouse/human) IgG. To avoid contamination with bovine IgG containing FCS, elution buffers with different pH-values were used. Bovine IgG was eluted using 0.1 M glycine / 0.1 M citrate buffer at pH 4.2 and chimeric antibodies at pH 2.5. After elution the column was re-equilibrated with binding buffer, washed with ddH_2O and stored in 20% ethanol at 4°C. Collected eluate was dialysed against DPBS using dialysis tubing or disposable PD-10 columns.

KappaSelect affinity chromatography
The KappaSelect ligand is a camelbody directed against the constant domain (C_L) of human Igκ and is useful for purification of constructs lacking the Fc region.
Cell culture supernatants prepared and filtered as described in section 2.3.2.6 on page 47 were applied to the DPBS equilibrated KappaSelect column at the flow rate of 50 mL/h using a peristaltic pump or at the flow rate of 2 mL/min using an ÄKTAprime system. All unbound material was washed out using DPBS. Antibodies were eluted with 0.1 M glycine buffer pH 2.5, the column was re-equilibrated with DPBS, washed with ddH_2O and stored in 20% ethanol at 4°C.

2.4.1.2 Size-exclusion chromatography

Two types of size exclusion chromatography were applied in this work. FPLC system (Pump-type P500, control unit LCC501, single channel UV-monitor UV-1, fraction collector FRAC-100) or ÄKTA pure system were used for the preparative separation of proteins. For analytical gelfiltration SMART® System or Dionex™ UltiMate™ 3000 BioRS system were used.

Preparative size-exclusion chromatography
Preparative size-exclusion chromatography was used to separate monomeric antibody fraction from multimers, aggregates and smaller protein fragments or salts. Max. 4 mL protein solution was injected in a 5 mL loop, and loaded onto Superdex™ 200 Prep Grade 16/60 HiLoad column and separated at a flow rate 50 mL/h. DPBS or 0.1 M phosphate buffer were used as a running buffer. Separated proteins were detected by UV absorbance at 280 nm and collected in prepared tubes filling fraction collector.

Analytical size-exclusion chromatography
Analytical size exclusion chromatography was used to characterize purified antibodies with respect to their approx. molecular weight, aggregation and contamination. SMART® System equipped with Superdex 200 PC3.2/30 column or Dionex™ UltiMate™ 3000 BioRS system equipped with a Superdex200™ increase 10/300 GL column were used for these experiments.
For analysis 10 μg protein was diluted in 50 μL DPBS and applied onto the columns. Separated proteins were detected by UV absorbance at 280 nm and 220 nm. Molecular weight was determined using absorption profiles of calibration proteins.
The peak retention volume of the calibration proteins listed in the table 2.25 was used as a standard for the SMART® System. The void volumes of the columns were determined using blue dextran.

Table 2.25: **Calibration proteins for SMART®**

Protein	Molecular weight (kDa)
Catalase	232 kDa
Aldolase	158 kDa
Albumin	67 kDa
Ribonuclease A	13.7 kDa

The peak retention time of the calibration proteins listed in the table 2.26 was used as a standard for the Dionex™ UltiMate™ 3000 BioRS system.

Table 2.26: **Calibration proteins for Dionex™ UltiMate™ 3000 BioRS**

Protein	Molecular weight (kDa)
Thyroglobulin (bovine)	670 kDa
γ-globulin (bovine)	158 kDa
Ovalbumin (chicken)	44 kDa
Myoglobin (horse)	17 kDa
Vitamin B_{12}	1,35 kDa

2.4.2 Generation of antibody F(ab')-fragments

Antibodies were digested with pepsin at a ratio of 30 μg pepsin for 1 mg antibody in a 0.1 M sodium acetate buffer (pH 4.0) containing 0.1 M sodium chloride. $F(ab')_2$ fragments were purified from the intact antibodies and pepsin using preparative size exclusion chromatography (Superdex™ 200 Prep Grade 16/60 HiLoad column). Reduction and subsequent modification of purified $F(ab')_2$ fragments were achieved in one step through reaction with a mixture of 10 mM DTT (1,4-Dithiothreitol) and 40 mM Ellmans reagent DTNB (5,5'-Dithiobis (2-nitrobenzoic acid)) for 24 h.

F(ab') fragments were purified from the $(ab')_2$ fragments and DTT/DTNB mixture using preparative size exclusion chromatography (Superdex™ 200 Prep Grade 16/60 HiLoad column).

2.4.3 Protein gel electrophoresis

Sodium dodecyl sulfate polyacrylamide gel electrophoresis (SDS-PAGE) was performed by using precast Mini-Protean® TGX™ polyacrylamide gels. SDS is an anionic detergent. When it is dissolved, its molecules have a net negative charge within a wide pH range. A polypeptide chain binds amounts of SDS proportional to its relative molecular weight. The negative charges on SDS destroy most of the complex structure of proteins, and are strongly attracted toward an anode in an electric field. Because the charge-to-mass ratio is nearly the same among SDS-denatured polypeptides it allows size-dependent separation of the proteins in the range of 5–250 kD.
For analysis 2 μg protein was diluted with sample buffer with or without reducing agent (β-mercaptoethanol). Diluted samples were incubated at 95°C for 5 min. Separation of the proteins was performed at U=200 V. Following electrophoresis, the gel was stained with Roti®-Blue colloidal coomassie staining solution to visualize the proteins. The gel was incubated with staining solution with gentle agitation for 1 h and was then rinsed in a staining tray and destained for 1–3 h with ddH_2O water.

2.4.4 Flow cytometry

Flow cytometry (Fluorescence-activated cell sorting or FACS) measures optical and fluorescence characteristics of single cells or microscopic particles based on their physical properties, internal complexity and surface staining.
In this work flow cytometry was applied using different protocols for several different purposes :

- to measure binding avidity of monoclonal antibodies (characterisation of antibodies)
- to quantify cell surface molecules on different cell lines
- to evaluate expression of certain proteins on the surface of PBL and PBMC
- to determine antibody mediated killing of resting and activated PBMC

2.4.4.1 FACS titration of monoclonal antibodies

For measurement of binding activity, cells (Daudi ($CD20^+$), Jurkat ($CD95^+$), SKW 6.4 ($CD20^+/CD95^+$) or SK-Mel ($CSPG4^+$)) were incubated with appropriate antibodies (or cell culture supernatants) in round-bottom 96 well plates (1.5×10^5 cells/well) for 30 min at 4°C. The cells were washed twice with 200 μL FACS buffer, centrifuged at $561 \times g$ and stained with 50 μL of PE- or APC-conjugated goat-anti-human Fcγ secondary antibodies according to the manufacturer's instructions. After incubation for additional 30 min the cells were washed again and analysed by flow cytometry using a FACSCalibur™ instrument and CellQuestPro Software (BD Biosciences).

2.4.4.2 Quantification of cell surface molecules by FACS analysis

Quantification of CD20 and CD95 expression on different B-lymphoma cell lines used in proliferation inhibition experiments (see 2.5.1.1) was performed using DAKO QIFIKIT®.
Different cell lines (2×10^5 cells/sample) were incubated in duplicates with unconjugated mouse anti-human CD20 (clone 2H7), anti-human CD95 (APO-1) or unrelated antibodies at saturating concentrations (10 μg/mL) for 30 min at 4°C. The cells were then washed twice with 200 μL FACS buffer, centrifuged at $561 \times g$ and stained with 50 μL of FITC-conjugated goat-anti-mouse secondary antibodies according to the manufacturer's instructions. After incubation for additional 30 min, the cells were washed again and analysed by flow cytometry using a FACSCalibur™ instrument and CellQuestPro Software (BD Biosciences).
Data analysis was performed using calibration curve and the following equation:

$$\log x = a \times \log z + b \tag{2.1}$$

a: Linear factor
b: Ordinate intercept
x: Antibody-Binding Capacity
z: Mean fluorescence intensity

Antigen density was calculated based on measured fluorescence intensity of the cells compared to determined fluorescence intensity of the calibration beads.

2.4.4.3 Expression of surface molecules on PBMC

To evaluate expression of certain proteins on the surface of PBMC, Fc receptors were blocked with Flebogamma (50 μg/mL) for 15 min. 1×10^6 cells/sample were stained with directly labelled CD95 antibodies. Gates for different cell populations were determined using FMO ("'fluorescence minus one"') controls in which one experimental antibody within a mixture was replaced by an isotype control labeled with corresponding dye (Tung et al., 2004) (Roederer, 2001). Samples were measured in technical duplicates. AnnexinV expression was measured in activated B- and T-cells within PBMC cultures to assess induction of apoptosis. Cell samples were measured after 4 h of antibody treatment (1 μg/mL). To this end, the cells were incubated with labelled antibodies washed, stained with PE-Annexin V and analyzed by flow cytometry. Acquisitions were performed using the FACSCanto™ II cell analyzer. For data analysis FlowJo software (TreeStar, USA) was used.

2.4.4.4 FACS depletion analysis of human PBMC

For measurement of antibody mediated killing of resting and activated B-cells (described in section 2.5.1.2), different PBMC populations were quantified by flow cytometry. In all FACS experiments binding to Fc receptors was blocked with Flebogamma (50 μg/mL) for 15 min. 1×10^6 cells/sample were stained with mouse anti

human CD4-FITC, CD8-APC and CD19-PacificBlue antibodies for 30 min. Dead cells were excluded by staining with 7-Aminoactinomycin D (7-AAD). The lymphocyte population was defined by light scatter characteristics and the percentage of remaining B- and T-cells after antibody treatment was assessed using compensation particles. By the acquisition of equal numbers of compensation particles (BD Biosciences) in each sample, absolute cell counts could be determined and used to calculate the percentage of remaining B- and T-cells. Samples were measured in technical duplicates. Acquisitions were performed using the FACSCanto™ II cell analyzer. For data analysis FlowJo software (TreeStar, USA) was used.

In some experiments induction of apoptosis in activated B and T cells within PBMC cultures was measured after 4 h of antibody treatment (1 μg/mL). To this end, the cells were incubated with labeled antibodies (CD4-FITC, CD19 PacificBlue) washed, stained with PE-Annexin V and analyzed by flow cytometry.

2.4.5 IgG ELISA

ELISA (Enzyme-linked Immunosorbent Assay) was used for quantification of human IgG secretion by activated B-cells *in vitro*.

To this end, an adapted sandwich procedure was performed. Maxisorp 96 well plates were coated with 50 μL of 1 : 1000 diluted goat anti-human IgGγ or 5 μg/mL Tetanus toxoid in DPBS at 4°C over night. After blocking with 100 μL of 10 % BSA in DPBS for 1 h, ELISA was proceeded by incubation steps with the following reagents, separated by extensive washing: (i) sample dilutions of PBMC supernatants, (ii) 1 : 10000 diluted biotinylated mouse IgG anti-human IgG F(ab')$_2$, (iii) 1 : 5000 diluted poly-HRP Streptavidin and (iv) TMB Microwell Peroxidase Substrate System. Reaction was stopped using 1 M phosphoric acid. Optical density at 450 nm was determined using a Spectra Max 340 ELISA reader. Antibody concentration was calculated using standard curves obtained by diluting human IgG (Flebogamma) or Tetagam P, respectively, in RPMI complete medium.

2.5 Functional immunobiological assays

2.5.1 *In vitro* experiments

2.5.1.1 Proliferation inhibition assay

For the determination of antibody-dependent cellular cytotoxicity (ADCC) lymphoma target cells (SKW 6.4, JY, C1R and Raji) were incubated with varying concentrations of different antibodies with and without PBMC. The cells were incubated for 24 h in 96 well plates and then pulsed with 0.5 μCi/well [methyl-^{3}H]-thymidine. After 20 h cells were harvested on a Printed Filtermate A and the precipitated radioactivity was determined in a liquid scintillation counter. % inhibition of proliferation was calculated according to the formula: 100-($x/x_0 \times 100$), where x and x_0 are counts (cpm) measured in experimental wells (x) and in wells without antibodies (x_0). Each data point represents the mean value of triplicate samples.

2.5.1.2 Inhibition of antibody production by pokeweed mitogen- or antigen-stimulated PBMC

For the verification of B-cell depletion from PBMC cultures upon incubation with antibodies freshly isolated PBMC from healthy donors or from individuals recently immunized with Tetanus toxoid (TT) were stimulated for 6 days with 1 μg/mL pokeweed mitogen (PWM) (Daniel and Krammer, 1994) and 25 ng/mL TT, respectively, as described by Lum et al (Lum and Culbertson, 1985). Cells were washed twice, adjusted to 3.2×10^6 cells/mL in 24 well plates and incubated with antibodies for another 2 days. To prevent detection of the therapeutic antibodies as newly produced human IgG in PWM stimulated cultures, antibody concentrations used were 0.1 μg/mL and 1 μg/mL in cultures stimulated with PWM and TT, respectively. After incubation, cells were analysed by flow cytometry (see 2.4.4.4 on page 52) and panclonal or TT specific human IgG were measured in the cell culture supernatants by ELISA (see 2.4.5 on page 53).

2.5.2 *In vivo* experiments

All animal experiments were performed in accordance with the German animal protection law and approved by the Tübingen Regional Administrative Council (*Regierungspräsidium*); approval numbers: IM 6/08 and IM 2/12.

2.5.2.1 Determination of antibody serum half-life

C57BL/6 mice were purchased from Janvier (Le Genest-Saint-Isle, France). For determination of serum half-life, mice were injected intravenously (i.v.) with 50 µg of the respective antibodies (3 animals per antibody). After 0.5, 1, 2 and 4 hrs (FabSc) or 0.5, 3, 6 and 24 h (IgG-antibodies) mice were bled and serum was obtained. Serum concentrations were measured by incubating SKW 6.4 cells with diluted serum samples. The amount of antibody bound to the cells was determined by flow cytometry and concentration values were calculated using a calibration curve obtained with samples that contained defined amounts of purified antibodies diluted in mouse serum (C57BL/6).

2.5.2.2 Severe combined immunodeficient (SCID) mouse xenograft model

***In vivo* immunotherapy trial**

Immunodeficient male C.B.-17 SCID-mice (CB17/lcr-PrkdcSCID/CRL) were purchased from Charles River (Sulzfeld, Germany). SCID mice were kept under specific pathogen free (SPF) conditions. 4-5 weeks old mice were injected i.v. with a lethal dose of 10^7 SKW 6.4 lymphoma cells in 200 μL DPBS at day 0. As soon as they developed paralysis of the hind legs, animals were sacrificed and SKW 6.4 cells were recovered from the bone marrow of these mice as described in next paragraph. These "SCID-SKW 6.4" cells were expanded and used for all the following experiments with SCID mice.

To determine survival after challenge with tumour cells, groups of 8 C.B.-17 SCID mice were injected at day 0 with 10^7 "SCID-SKW 6.4" cells i.v. Mice treated with monospecific antibodies were injected intraperitoneal (i.p.) with 60 μg of respective

antibody at day 1, animals treated with bispecific antibodies with 20 μg at days 1, 2 and 3. Animals developing visible tumours, sense disturbances or paralysis of the hind legs were sacrificed and tumour growth was confirmed by necroscopy. After termination of the experiment at day 120, surviving mice were sacrificed and subjected to necroscopy and histological examination (Histological examination was performed by Dr. med. vet. M. Wölm, Hamburg).

Isolation of SKW 6.4 cells from mouse bone marrow

For isolation of bone marrow, mice were sacrificed and bone marrow cells were isolated from the hind legs. The femur was dissected from surrounding muscles and excess tissue was removed using sterile forceps and scissors, keeping the ends of the bone intact. The intact bones were soaked in 70% ethanol in a sterile Petri dish for 2 min as disinfection. After rinsing bones in sterile culture medium, both ends of the femurs were trimmed carefully using sterile, sharp scissors to expose the interior marrow shaft. The content of the marrow was flushed with 2 ml of culture medium using a 5 ml syringe with a 29G$\times$1/2 needle. The content was collected into a sterile 50 ml centrifuge tube and washed with media for 5 min at 250 $\times$ *g*. The supernatant was removed and the cell pellet was resuspended in the appropriate amount of RPMI complete medium. The cells were cultivated under standard conditions in a cell incubator.

Chapter 3

Results

To generate recombinant bispecific reagents that selectively stimulate the CD95 death receptor on CD20 positive B-cells, CD95×CD20 bispecific antibodies were developed and characterised in the first part of this work. All new constructs are based on the FabSc format (a F(ab) fragment linked to a Single Chain antibody) as depicted in Fig. 3.2 (Durben et al., 2015). Three expression vectors were used for assembling the new recombinant antibodies: one carrying the sequence for bispecific FLT3×CD3 antibody in the FabSc format (NF-CU$_{N297Q}$ Fig. 2.2) and two for APO-1 antibody heavy (Fig. 2.4) and light (Fig. 2.3) chains. Parts of these vectors were removed or replaced with the sequences for CD95×CD20 bispecific antibodies. The main cloning steps are depicted in Fig. 3.1. An overview of the bispecific FabSc antibodies generated in the first part of this work is depicted in Fig. 3.2.

At the beginning of this work the bispecific CD95×CD20 antibodies will be characterised using standard analytical assays. As a next step, the antibodies will be functionally compared to clinically established monospecific CD20 antibodies used for the treatment of B-cell lymphomas. *In vitro* and *in vivo* experiments using different malignant B-cell lines will be performed to address this question. Since monospecific CD20 antibodies are currently applied not only for haematological, but also for autoimmune diseases, the bispecific CD95×CD20 antibodies will be compared to the monospecific CD20 antibodies also with respect to their capability to deplete normal, activated B-cells and to suppress antibody production.

The generation and characterisation of new fusion proteins stimulating CD95 receptor on antigen-specific activated B-cells will be reported in the last part of this work. Tetanus toxoid (TT) and diphtheria toxoid (DT) antigens were selected for these experiments as model antigens. An expression vector for CD95×CD20 antibodies generated in the first part of this work was used for cloning and construction of the fusion proteins. The CD20 part was replaced with various non-toxic parts of TT and DT. B-cell suppressive activity of these antigen-specific reagents will be compared *in vitro* to the CD95×CD20 antibody and established monospecific CD20 antibodies.

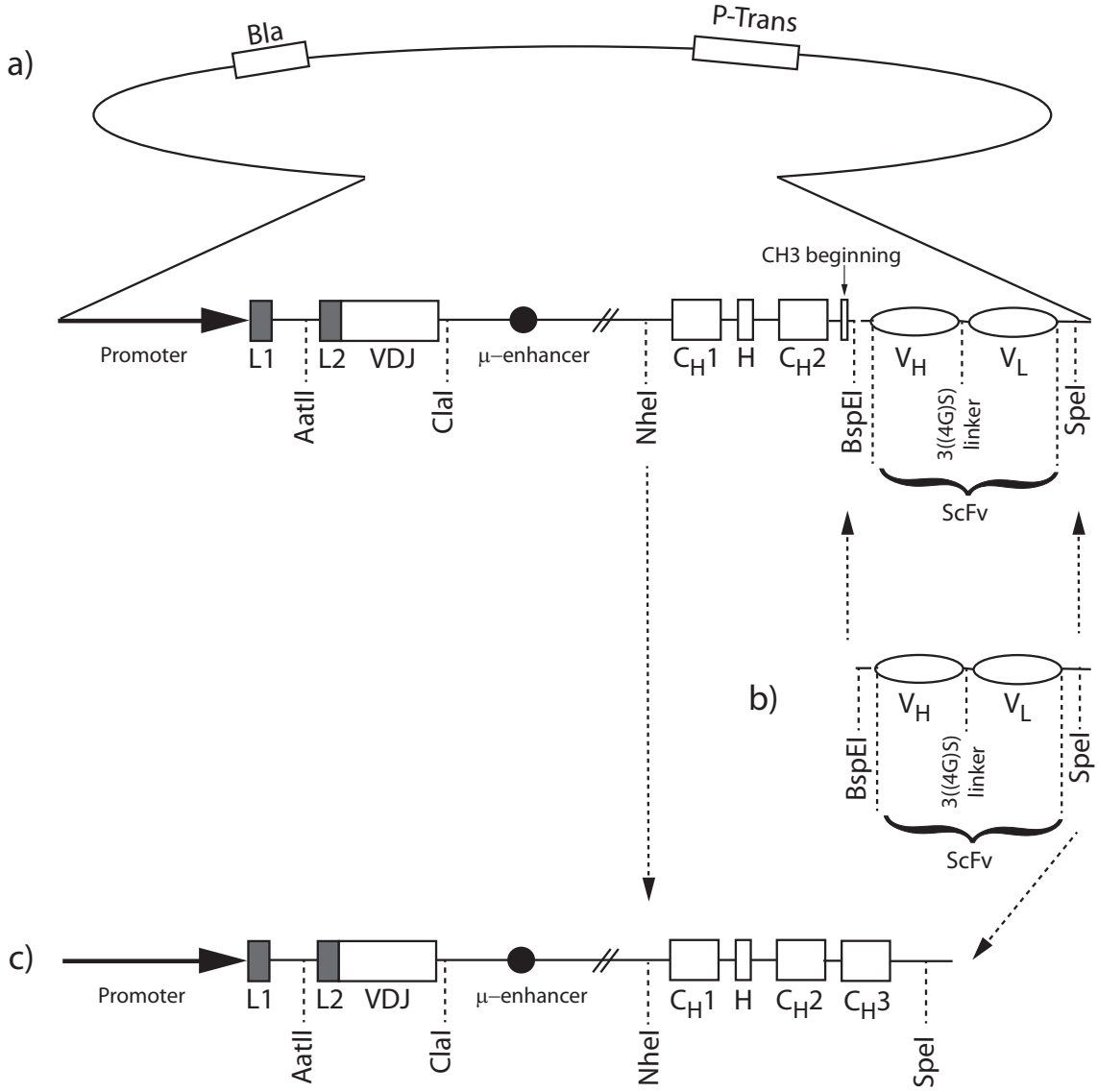

Figure 3.1: **Cloning strategy for the construction of BS9520 and BS2095 antibodies**
(a) Schematically represented NF-CU$_{N297Q}$ heavy chain expression vector (coding for FLT3×CD3 antibody in the FabSc format; all parts of this vector are described in Fig. 2.2 on page 39) was used as a starting material. First ScFv (V$_H$-V$_L$) for UCHT1 antibody at the C-terminus was replaced using BspEI and SpeI restriction sites with the (b) ScFv of desired specificity: ScFv for CD20 antibody (V$_H$-V$_L$) for BS9520 construct or ScFv for CD95 antibody (V$_H$-V$_L$) for BS2095 construct. The whole Fc part of these interim constructs was subsequently transferred into NheI and SpeI digested expression vectors (c) for CD95 heavy chain Fig. 2.4 or expression vector for heavy chain antibody directed against CD20.

3.1 Generation and characterisation of recombinant bispecific antibody constructs

3.1.1 Generation of recombinant bispecific antibodies

For construction of the recombinant bispecific CD95×CD20 antibody, the **FabSc**-format consisting of an N-terminal **F(ab)**-part linked to a C-terminal **S**ingle **c**hain antibody by an Fc-attenuated CH2 domain was used (Durben et al., 2015). Cysteines in the hinge region were replaced by serines (C226S, C229S) and the CH3 domain was removed in order to prevent formation of disulfide bonds and to avoid dimerisation of the molecule. In all constructs 3 amino acids (GQP) from the CH3 domain and an additional serine-glycine linker were inserted between the CH2 domain and the single chain. Usually, the CH2 domain within an IgG molecule is glycosylated at asparagine (N297). In order to abrogate this glycosylation and, subsequently binding to FcγRIIIa receptor (Arnold et al., 2007) or lectin receptors (Sjöwall et al., 2015), asparagine in the CH2 domain was replaced with glutamine (N297Q). Remaining mutations in the CH2 domain (L234V, L235A, G236Δ (Wines et al., 2000), D265G (Sazinsky et al., 2008), A327Q, A330S (Liu et al., 2014)) were implemented in order to prevent binding of the antibody to Fc-receptors.

This backbone was used for production of CD95×CD20 antibodies as well as a control antibody in the FabSc format. The first generated recombinant bispecific CD95×CD20 antibody contained an N-terminal F(ab)-part of a chimeric antibody against human CD20 (χCD20, clone 2H7) linked to a murine single chain antibody against human CD95 (clone APO-1) in V_H-V_L orientation at the C-terminus (Fig. 3.2 a). This construct was designated **BS2095** meaning **Bi**-**S**pecific-CD**20**-CD**95**. The second recombinant bispecific CD95×CD20 antibody, named **BS9520** (Fig. 3.2 b), consisted of the antibody clones mentioned above in the opposite orientation. N-terminal F(ab)-part of a chimeric antibody against human CD95 (χCD95) was linked to a C-terminal mouse single chain antibody against human CD20 in V_H-V_L orientation.

As a negative control for the functional assays, an antibody in the same format with N-terminal F(ab)-part of chimeric antibody against human CD95 and unrelated antibody (melanoma-associated chondroitin sulfate proteoglycan 4 (CSPG4)) on the C-terminus as a mouse single chain in V_H-V_L orientation was generated and designated **BS95Mel** meaning **Bi**-**S**pecific-CD**95**-**Melanoma** (Fig. 3.2 c).

All recombinant antibodies were purified from cell culture supernatant of stably-transfected Sp2/0 cells using KappaSelect affinity chromatography. Eluted proteins were desalted in Dulbecco's phosphate buffered saline (DPBS) by dialysis through a semipermeable cellulose membrane or preparative size exclusion chromatography.

3.1.2 Characterisation of recombinant bispecific antibodies

Characterisation of recombinant antibodies was routinely performed using analytical size exclusion chromatography and SDS-PAGE. Binding properties of bispecific antibodies were analysed by flow cytometry using appropriate cell lines.

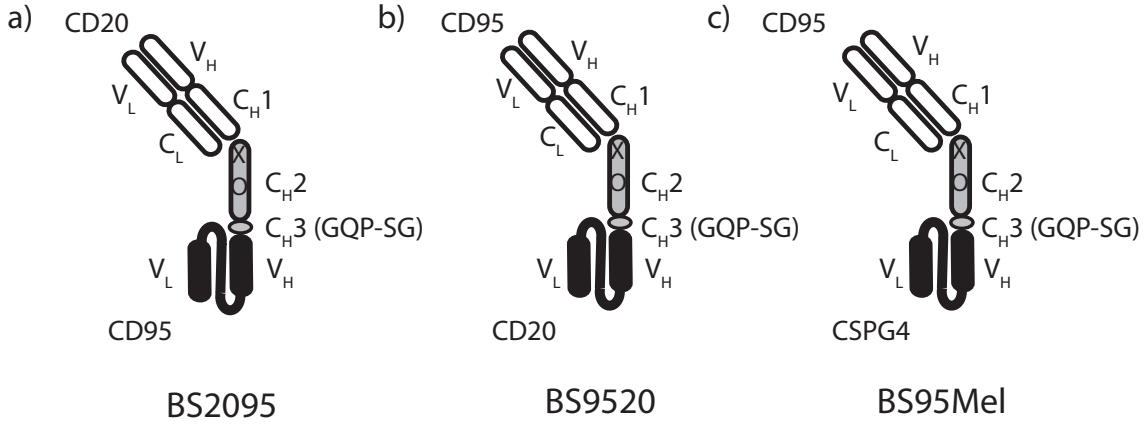

Figure 3.2: **Schematic illustration of the bispecific FabSc antibodies**
CD95×CD20 antibodies: (a) BS2095 and (b) BS9520 and the CD95×CSPG4 antibody (c) BS95Mel.

3.1.2.1 Size exclusion chromatography

10 μg of each protein was loaded onto a Superdex 200 analytical size exclusion chromatography (SEC) column. Elution profiles of the constructs are depicted in Fig. 3.3. The calculated molecular weight of BS2095 and BS9520 is approximately 86 kDa. In the elution profile of BS2095 (containing single chain antibody against CD95) no peak representing this size is detectable (Fig. 3.3 a). Rather, a large amount of aggregated protein appears in the void volume of the column. In contrast, the elution profile of the BS9520 construct (containing CD95 antibody as a N-terminal F(ab)-part) shows only one peak at the expected size (Fig. 3.3 b). Thus it appears that the CD95 antibody as a single chain causes complete aggregation of the BS2095 molecule. Based on these results, BS9520 was chosen for all the following experiments. The same antibody format and orientation was used to generate the control antibody BS95Mel.
Analysis of the purified control antibody BS95Mel was performed on Superdex 200™ increase 10/300 GL column using Dionex™ UltiMate™ 3000 BioRS system[7]. The elution profile of this antibody contains one peak of the expected size (approx. 90 kDa), a small amount of antibody multimers appearing just in front of the main peak and a small amount of antibody fragments behind the main peak (Fig. 3.4). The antibody monomer was separated from the multimer and smaller proteins using a FPLC system (Pharmacia LKB Biotechnology) equipped with a HiLoad™ 16/60 Superdex™ 200 prep grade column (Appendix Fig. 6.1, page 125).

3.1.2.2 SDS-PAGE and verification of amino acid sequence

For further characterisation of BS9520 and BS95Mel antibodies, these reagents were analysed by SDS-PAGE and compared to parental chimeric anti-CD95 monoclonal antibodies (χCD95). Fig. 3.5 represents SDS-polyacrylamide gel electrophoresis of

[7]Dionex™ UltiMate™ 3000 BioRS system equipped with Superdex 200™ increase 10/300 GL column and calibration proteins described in Fig. 3.4 were used in all the following experiments with analytical size exclusion chromatography because of the system replacement in the laboratory.

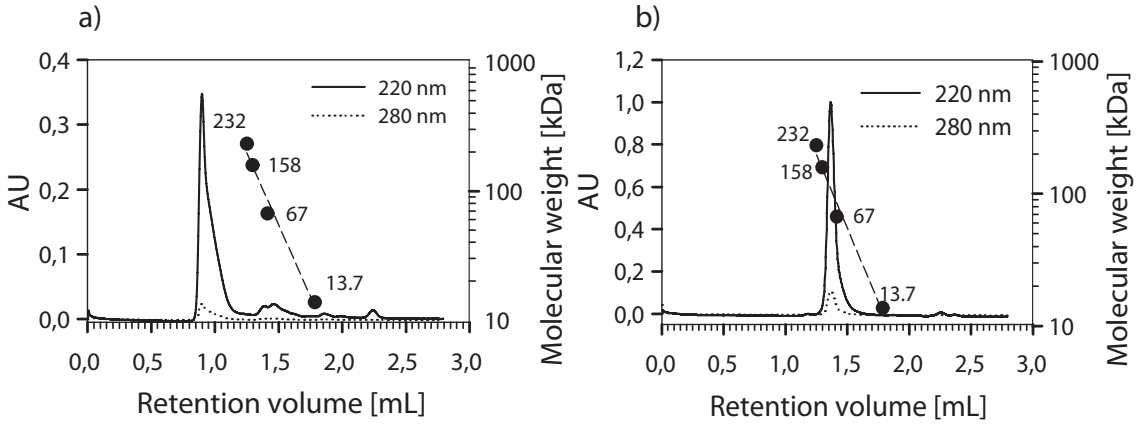

Figure 3.3: **Analytical size exclusion chromatography of BS2095 and BS9520 antibodies**
SEC elution profiles of (a) the recombinant BS2095 and (b) the recombinant BS9520 antibodies. 10 μg of purified antibody were separated using SMART® System equipped with a Superdex 200 column (PC 3.2/30).

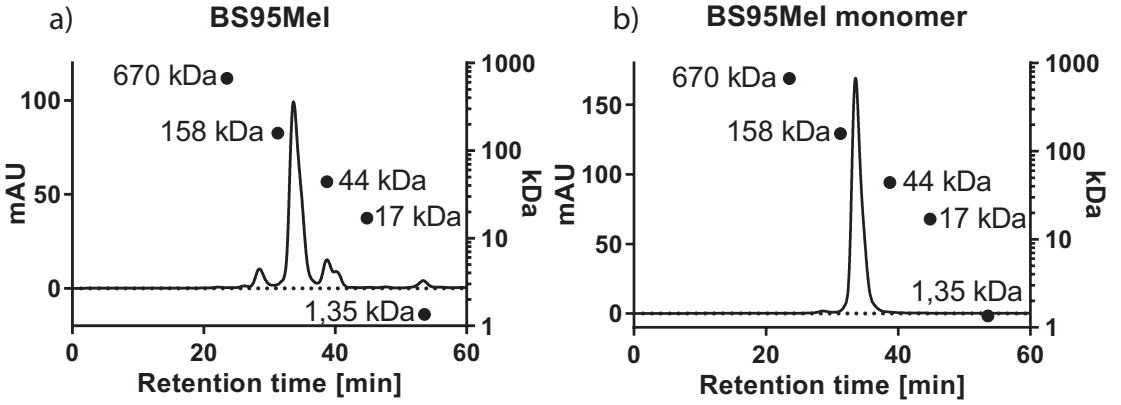

Figure 3.4: **Analytical size exclusion chromatography of BS95Mel**
a) SEC elution profile of the recombinant BS95Mel antibody after a) initial KappaSelect purification and b) additional preparative FPLC separation. 10 μg of purified antibody were separated using a Dionex™ UltiMate™ 3000 BioRS system equipped with Superdex 200™ increase 10/300 GL column.

the antibodies under non-reduced (lanes 2-4) and reduced (lanes 6-8) conditions compared to a pre-stained protein ladder. The upper band in lane 2 (calculated molecular weight 86 kDa) represents the BS9520 antibody. The bands below seem to represent separated heavy and light antibody chains (calculated molecular weight 62.7 kDa and 23.6 kDa respectively). They are comparable to the bands obtained under reduced conditions (lane 6). The upper band in lane 3 (calculated molecular weight 90 kDa) represents BS95Mel antibody. Again, the bands below seem to be monomeric heavy and light chains (calculated molecular weight 66.3 kDa and 23.6 kDa respectively). The (upper) band in lane 4 shows parental chimeric anti-CD95 antibody APO-1 under non-reduced conditions (calculated molecular weight 150 kDa). Under reduced conditions (lane 8) only two bands are visible. The upper band is heavy chain and the band below is the light chain (calculated molecular weight 51 kDa and 23.6 kDa respectively).

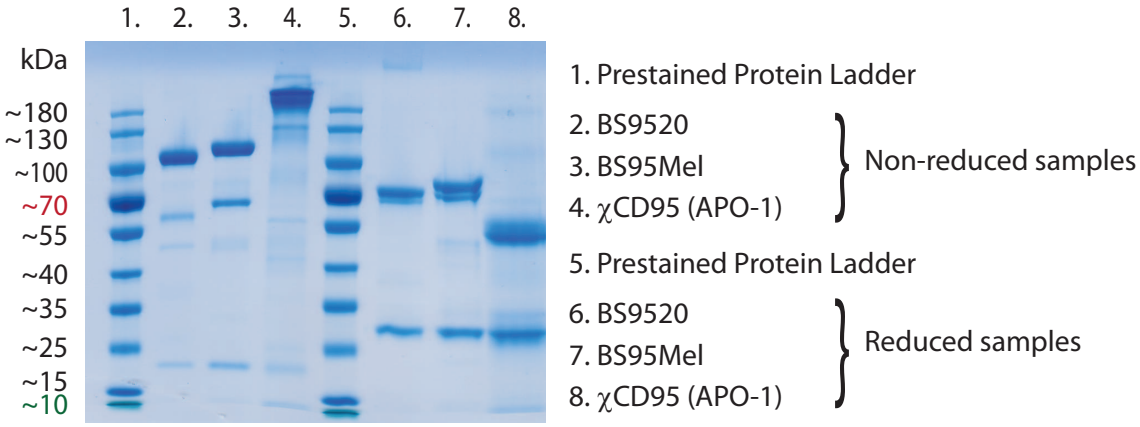

Figure 3.5: **Non-reducing and reducing SDS-PAGE**
Bispecific BS9520 and BS95Mel antibodies were compared to parental monospecific χCD95 antibody under non-reduced (lanes 2-4) and β-mercaptoethanol reduced (lanes 6-7) conditions. Pre-stained protein ladder (lanes 1 and 5) indicates molecular weight in kDa.

Verification of amino acid sequence of bispecific antibodies

In order to verify the antibody mRNA sequence for potential splicing cites and thus, the proper amino acid sequence, mature cytoplasmic mRNA from antibody producing transfected Sp2/0 cells was isolated and transcribed to complementary DNA (cDNA) as described in 2.2.1.2 section on page 42. cDNA sequences coding for the heavy chain of BS9520 and BS95Mel antibodies were amplified, cloned into commercial pJET1.2/blunt vector, sequenced and compared to the theoretical antibody heavy chain sequence. The sequencing results revealed that one part of mRNA coding for the heavy chain of BS9520 as well as BS95Mel constructs was indeed alternatively spliced resulting in a mixture of proteins of the correct size and 1.6 kDa smaller protein lacking the Hinge region (Table 3.1). This may account for the "heavy chain split" observed upon SDS-PAGE analysis (Fig. 3.5, lane 7).

Table 3.1: **Verification of amino acid sequences of FabSc bispecific antibody heavy chains**
Parts of one correct nucleotide and amino acid sequences are compared to alternatively spliced sequences obtained by analysis of cDNA synthesised from mRNA of transfected BS9520 and BS95Mel producing Sp2/0 cells.

		C_H1 domain								Hinge													
Position	...	206								214													
Correct		aac	acc	aag	gtg	gac	aag	aaa	gtt	gag	ccc	aaa	tct	tgt	gac	aaa	act	cac	aca	agc	cca	ccg	agc	cca
		N	T	K	V	D	K	K	V	E	P	K	S	C	D	K	T	H	T	S	P	P	S	P
Spliced		aac	acc	aag	gtg	gac	aag	aaa	gtt	—	—	—	—	—	g–	—	—	—	—	—	—	—	—	—
		N	T	K	V	D	K	K	V															

		C_H2 domain																					
Position	...	229																				250	
Correct		gca	cca	cct	gtg	gca	ggc	ccg	tca	gtc	ttc	ctc	ttc	ccc	cca	aaa	ccc	aag	gac	acc	ctc	atg	atc	
		A	P	P	V	A	G	P	S	V	F	L	F	P	P	K	P	K	D	T	L	M	I	...
Spliced		-ca	cac	ctg	tgg	cat	gac	cgt	cag	tct	tcc	tct	tca	cct	caa	aaa	aga	agg	aca	acc	tca	tga	tct	
		A	P	P	V	A	G	P	S	V	F	L	F	P	P	K	P	K	D	T	L	M	I	...

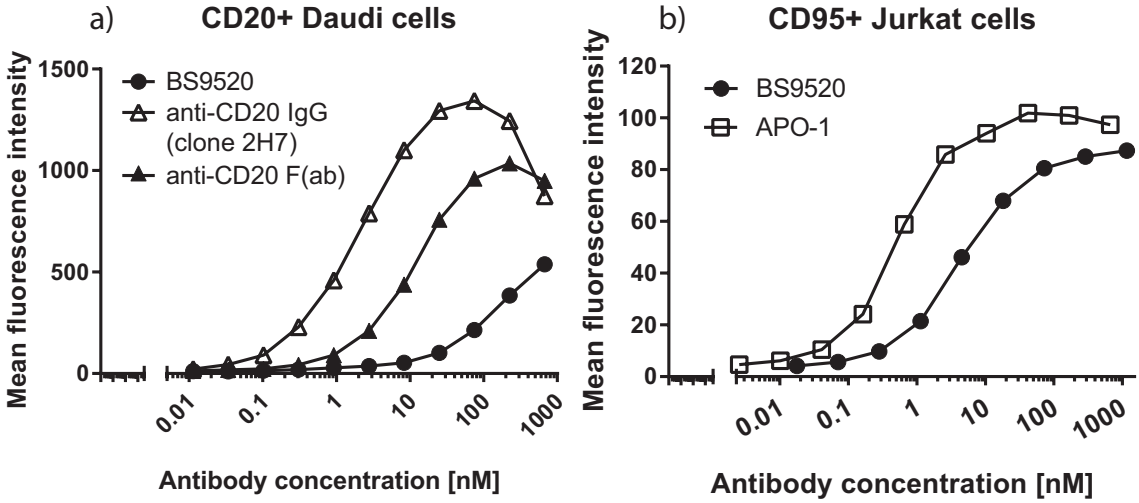

Figure 3.6: **FACS analysis:**
Binding of the recombinant BS9520 antibody (black circle) to (a) $CD20^+/CD95^-$ Daudi cells compared to parental anti-CD20 antibody (open triangle) as well as F(ab') fragment thereof (black triangle) and (b) to $CD95^+/CD20^-$ Jurkat cells compared to parental anti-CD95 antibody (open squares). Detection was performed using a PE-labelled Goat anti-Human Fcγ secondary antibodies.

3.1.2.3 Binding analysis

Binding activity of the **BS9520** antibody was evaluated by flow cytometry as described in section 2.4.4.1 on page 51. The $CD20^+/CD95^-$ Daudi human Burkitt's Lymphoma cell line and the $CD95^+/CD20^-$ Jurkat human acute T-cell leukaemia cell line were used for this purpose.

As depicted in Fig. 3.6 a, expression of the CD20-binding antibody part in the single chain format resulted in a significant loss of affinity compared to the normal, bivalent anti-CD20 antibody (clone 2H7) and to the monovalent F(ab') fragments thereof (prepared as described in section 2.4.2 on page 50). Anti-CD20 antibody 2H7 in IgG format is detectable at concentrations $\geq$0.1 nM and is saturated at the concentration 100 nM. The same antibody as a purified F(ab') fragment is detectable at the concentration $\geq$1 nM and is saturated at the concentration approx. 300 nM. BS9520 is detectable at the concentration $\geq$12 nM and not saturated even at the concentration of 670 nM. In contrast, the activity of BS9520 towards CD95 (Fig. 3.6 b), is only moderately reduced compared to the parental anti-CD95 antibody (APO-1). Binding of the BS9520 antibody on Jurkat cells is detectable at $\geq$0.5 nM and saturated at the concentration of $\geq$100 nM.

Binding of the purified monomeric **BS95Mel** control antibody was also evaluated by flow cytometry. As depicted in Fig. 3.7, BS95Mel antibody is able to bind on both cell lines with a good affinity. Binding on SK-Mel cells was detectable at a concentration of $\geq$0.5 nM and saturated at a concentration $\geq$10 nM. The binding activity of BS95Mel on Jurkat cells is detectable at 0.5 nM and saturated at the concentration of $\geq$10 nM. The binding of BS95Mel detected using $CD95^+$ Jurkat cells correspond to the results obtained with BS9520 antibody (Fig. 3.6).

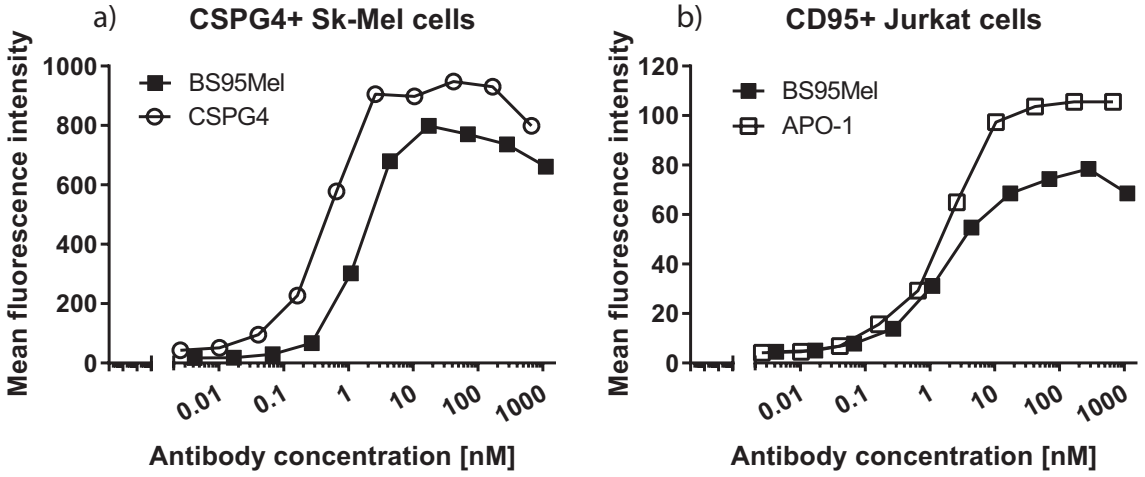

Figure 3.7: **FACS analysis:**
Binding of the recombinant BS95Mel antibodies to (a) $CSPG4^+/CD95^-$ Sk-Mel cells compared to parental anti-CSPG4 antibody and (b) to $CD95^+/CSPG4^-$ Jurkat cells compared to parental anti-CD95 antibody (APO-1). Detection was performed using a PE-labelled Goat anti-Human Fcγ secondary antibodies.

3.2 Induction of apoptosis in B-lymphoma cells

In this section the suppression and depletion of various B-cell lymphoma cell lines by monospecific clinically established CD20 antibodies will be compared to that achieved by the recombinant bispecific BS9520 antibody described in the previous section (Fig. 3.9).

3.2.1 Quantification of CD20 and CD95 expression on various B-lymphoma cell lines

Expression of surface CD20 and CD95 on various B-lymphoma cell lines used in cytotoxicity assays was quantified with QIFIKIT® by flow cytometry using indirect immunofluorescence assay as described in section 2.4.4.2 on page 52. Cell samples were labelled with mouse anti-human CD20 antibody (clone 2H7), mouse anti-human CD95 antibody (clone APO-1) or with mouse anti-human CD3 (clone UCHT1) as an isotype control at saturating concentration (10 μg/mL). Under these conditions, the number of bound primary antibody molecules corresponds to the number of antigenic sites present on the cell surface. To quantify bound primary monoclonal antibodies, the cells were incubated, in parallel with the QIFIKIT® beads, with FITC conjugated polyclonal goat anti-mouse immunoglobulins at saturating concentration. A calibration curve was constructed by plotting the fluorescence intensity of the individual calibration bead populations against the number of antibody binding sites on the beads. The number of antigenic sites on the specimen cells were then determined by interpolation and summarized in table 3.2 with the indicated range for each sample (measurement was performed in duplicates).

Table 3.2: **Quantitative determination of CD20 and CD95 expression on different lymphoma cell lines**

Cells	CD95 expression	CD20 expression (molecules per cell)	CD3 expression
SKW 6.4	$103\,692 \pm 1\,044$	$323\,931 \pm 4\,864$	0
C1R	$36\,547 \pm 373$	$121\,796 \pm 0$	0
JY	$155\,019 \pm 1\,556$	$636\,509 \pm 6\,365$	0
Raji	$20\,872 \pm 108$	$630\,144 \pm 0$	0
Jurkat	$10\,301 \pm 55$	0	$46\,152 \pm 237$

3.2.2 Functional assays *in vitro*

In the initial experiments, specific cytotoxicity of BS9520 antibody was tested on different $CD20^+/CD95^+$ B-cell lymphoma cell lines using a [methyl-^{3}H]-thymidine incorporation assay (Fig. 3.8). Proliferation of SKW 6.4, C1R and JY cell lines was successfully inhibited at concentrations $\geq$100 ng/ml. The cytotoxic activity of BS9520 against Raji cells was marginal, although these cells express CD20 as well as CD95 (Table 3.2).

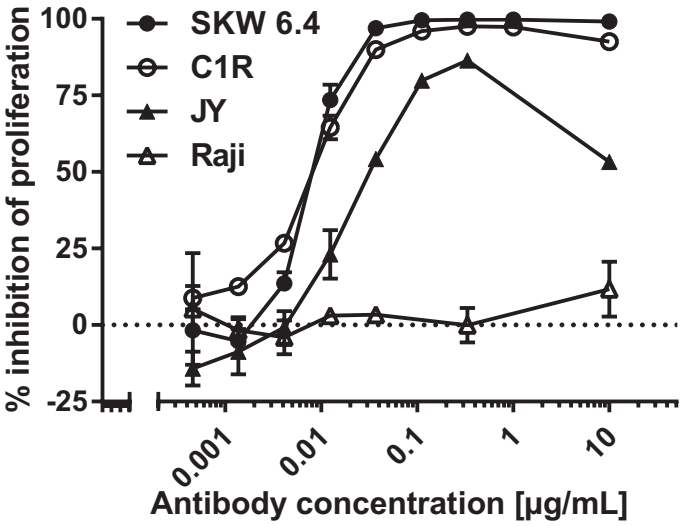

Figure 3.8: **Proliferation of different B-lymphoma cell lines in response to BS9520 antibody**
20 000 cells/well were incubated for 24 h with different antibody concentrations and then pulsed with [methyl-^{3}H]-thymidine. % inhibition of proliferation was calculated as described in section 2.5.1.1 on page 53. Each data point represents the mean value of triplicate samples.

After these initial experiments, the bispecific antibodies (BS9520 and the control antibody BS95Mel depicted in Fig. 3.2 b, c, page 61) were tested in functional assays in comparison to various monospecific anti-CD20 antibodies (Fig.3.9 a, b). One of them is the commercial FDA-approved chimeric anti-CD20 antibody **Rituximab** nowadays used within standard first line treatment regimens for lymphoma. **CH20**

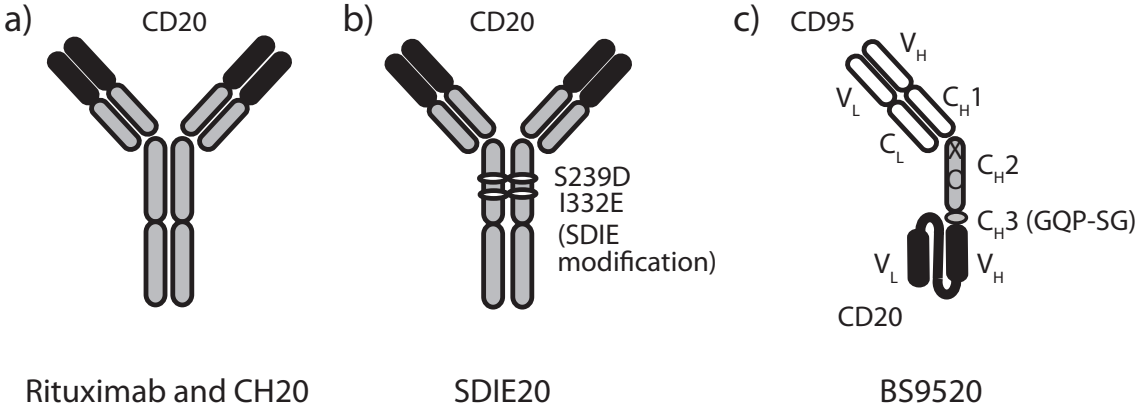

Figure 3.9: **CD20-antibodies compared in this work**
(a) FDA-approved antibody Rituximab and CH20, a chimeric antibody with variable regions derived from the anti-CD20 antibody (clone 2H7), (b) SDIE20, the chimeric anti-CD20 antibody (clone 2H7) with an optimized Fc-part (S239D and I332E in CH2 domain), (c) BS9520, a bispecific molecule in the FabSc-format with an N-terminal CD95-specificity and a C-terminal single chain binding CD20.

is another chimeric, monospecific antibody directed against CD20 (derived from clone 2H7 contained in the commercial antibody Ocrelizumab) and **SDIE20** is an optimised version thereof carrying amino acid modifications S239D and I332E in CH2 domain for enhanced antibody-dependent cell-mediated cytotoxicity (ADCC) activity (Lazar et al., 2006).
Due to the different mode of action of monospecific CD20 antibodies, all further proliferation assays with lymphoma cell lines were performed in the presence of different amounts of PBMC as a source of effector cells for ADCC. The thymidine incorporation assay was termed in this setting "Proliferation inhibition assay" based on the assumption that PBMC do not proliferate and the only cells incorporating [methyl-^{3}H]-thymidine are lymphoma cells.

Fig. 3.10 depicts the anti-proliferative activity of BS9520, CH20, SDIE20 and Rituximab antibodies towards various lymphoma cells in the presence of PBMC as a source of effector cells. At concentrations $\geq$100 ng/ml and a PBMC : target ratio of 5 : 1 (200 000 PBMC and 40 000 target cells) the activity of BS9520 antibody was higher than that of monospecific CD20 antibodies. Rising the PBMC : target ratio to 10 : 1 (200 000 PBMC and 20 000 target cells), however, attenuates this difference. The ADCC activity of Rituximab and CH20 was comparable and clearly less pronounced than that of the Fc-optimized SDIE20 antibody. Cytotoxic activity of BS9520 with PBMC is only marginally diminished compared to results obtained without effector cells (Fig. 3.8).
Whereas this pattern held true for three of the four cell lines tested, Raji cells were different: not only the cytotoxic activity of BS9520 against these cells was marginal, killing by the monospecific antibodies was also markedly reduced.
When we assessed depletion of SKW 6.4 cells (Fig. 3.11) and Raji cells (Fig. 3.12) in a flow cytometry based assay, again at a PBMC : target ratio of 10 : 1, similar observations were made. After 48 hours almost complete depletion of the SKW 6.4 cells

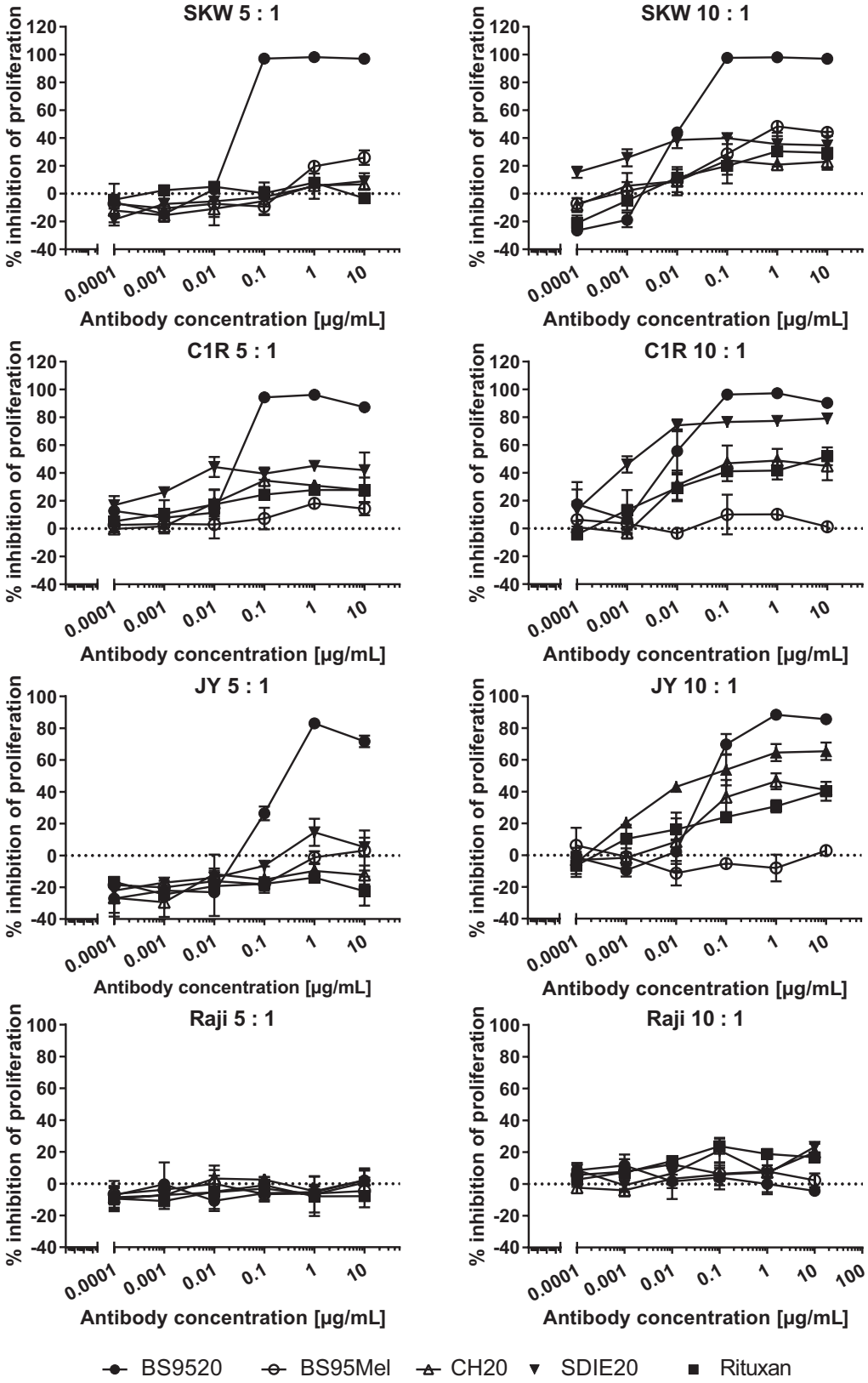

Figure 3.10: **Proliferation inhibition assay**
Antibody dependent cellular cytotoxicity against various lymphoma cell lines. PBMC and target cells were incubated with the indicated antibodies at PBMC : target ratios of 5 : 1 or 10 : 1 and pulsed after 24 h with [methyl-^{3}H]-thymidine. Mean values and standard deviations of triplicate samples are indicated.

by all CD20 targeting antibodies was observed. At low concentrations (≤ 100 ng/ml) the Fc-optimized CD20 antibody was more efficient (Fig. 3.11). If Raji cells were used as targets (Fig. 3.12), the activity of BS9520 and monospecific antibodies was again largely reduced, but it was more pronounced than in the proliferation inhibition assay. Thus, these results confirm in principle the data of the Thymidine-incorporation assay, but with a higher sensitivity. Antibodies, especially SDIE20, were able to decrease the amount of Raji cells at concentrations ≥ 10 ng, but were unable to deplete them completely even at the concentration of 1 μg/mL. Furthermore reduction of monocytes upon incubation with BS9520 but not with the monocpecific antibodies was noticed. In any case, it is notable that normal B-cells remain almost unaffected by the BS9520 construct. In contrast, upon incubation with monospecific antibodies, normal B-cells expressing high amounts of CD19 disappear and a population of "CD19-low" cells remains (Fig. 3.11 and 3.12).

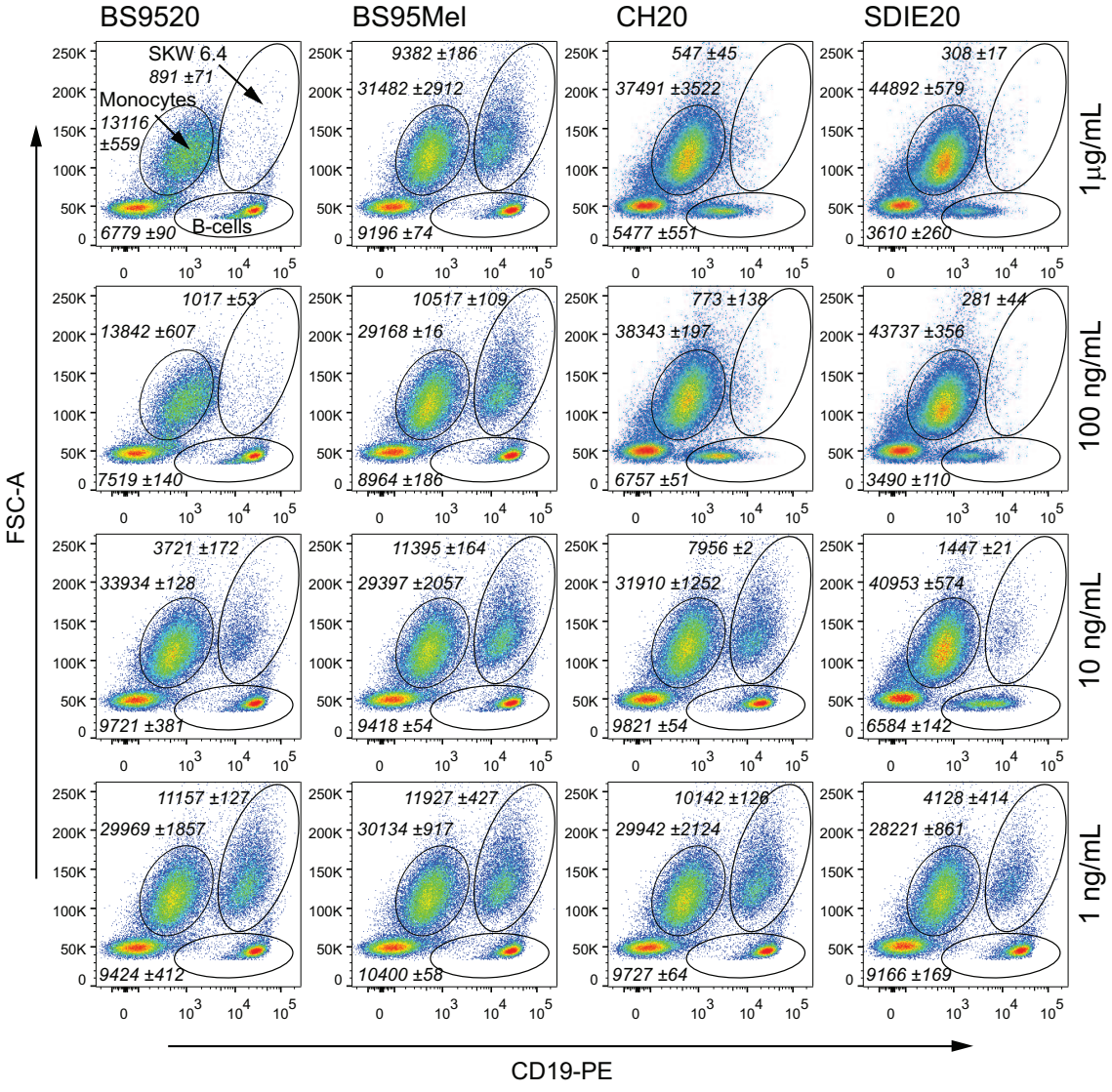

Figure 3.11: **Depletion of SKW 6.4 lymphoma cells in the presence of PBMC**

200 000 PBMC and 20 000 SKW 6.4 were co-cultured in the presence of the indicated antibodies at different concentrations (indicated on the right) and analysed after 48 h by flow cytometry. SKW 6.4 were defined as FSC-A high and $CD19^+$, monocytes as FSC-A intermediate and $CD19^-$, B-cells as FSC-A low and $CD19^+$. Absolute cell numbers (mean and range of technical duplicates) of these populations are indicated on FACS plots as italic numbers.

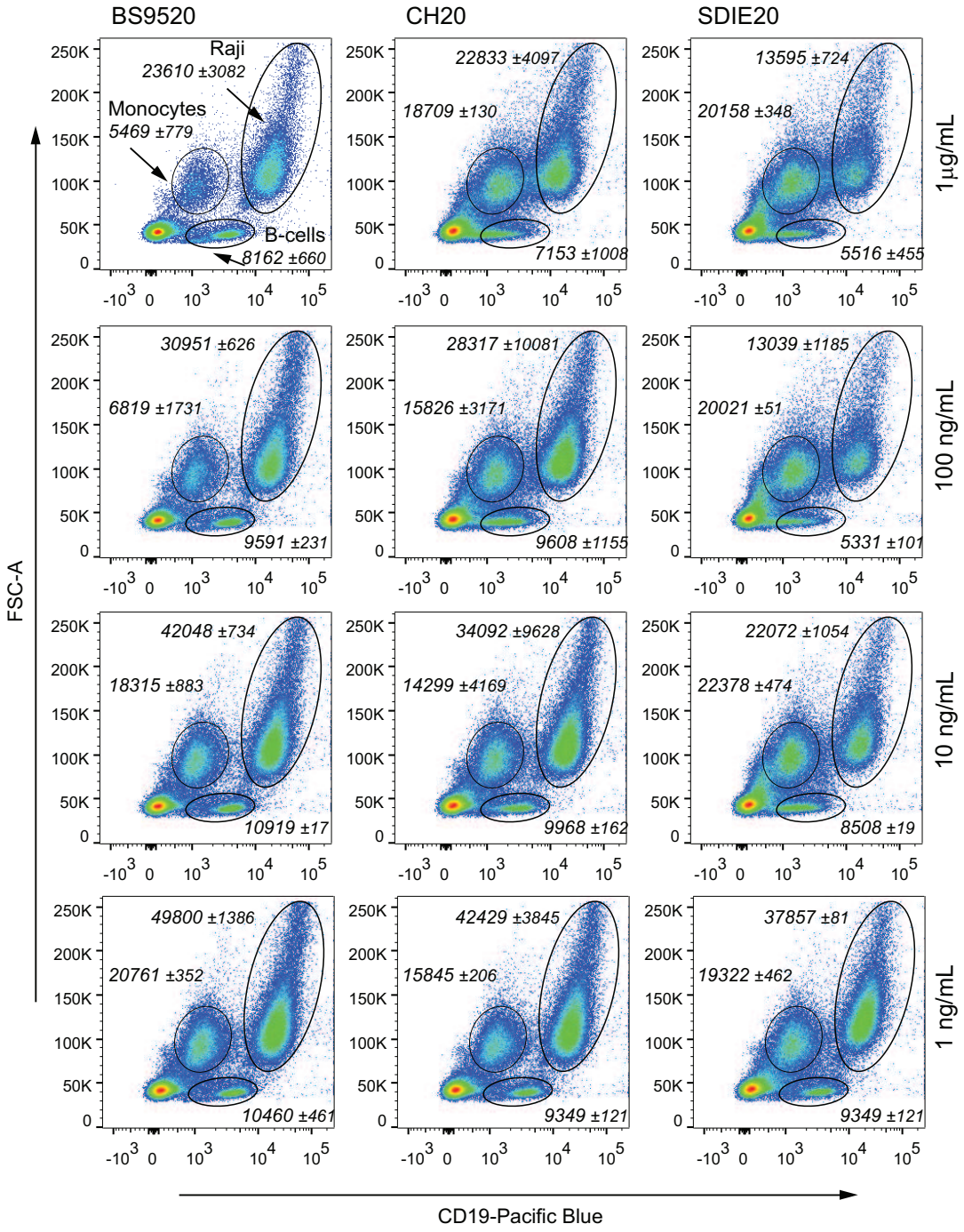

Figure 3.12: **Depletion of Raji lymphoma cells in the presence of PBMC** 200 000 PBMC and 20 000 Raji cells were co-cultured in the presence of the indicated antibodies at different concentrations (indicated on the right) and analysed after 48 h by flow cytometry. Raji cells were defined as FSC-A high and $CD19^+$, monocytes as FSC-A intermediate and $CD19^-$, B-cells as FSC-A low and $CD19^+$. Absolute cell numbers (mean and range of technical duplicates) of these populations are indicated on FACS plots as italic numbers.

3.2.3 Functional assays *in vivo*: determination of antibody half-life in mouse serum

For comparison of bispecific BS9520 antibody kinetics with monospecific anti-CD20 antibodies in mouse serum, C57BL/6 mice were injected with 50 μg of the respective antibody i.v. and blood samples were collected at the indicated time points. The serum concentration of BS9520, CH20 and SDIE20 was determined by FACS analysis.

As depicted in Fig. 3.13, a serum concentration of 15 μg/ml is easily maintained for monospecific antibodies for $\geq$24 h, whereas the concentration of BS9520 falls rapidly below this value within 4 h.

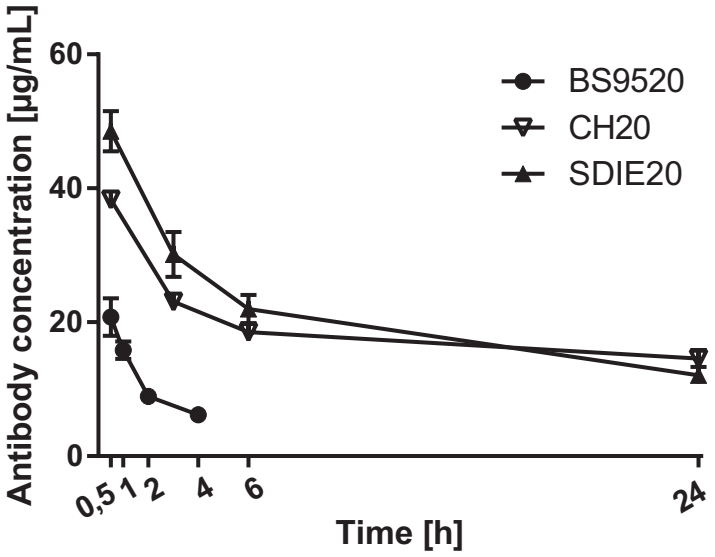

Figure 3.13: **Serum kinetics of anti-CD20 antibodies**
C57BL/6 mice were injected with 50 μg of the respective antibody i.v. and blood samples were taken at the indicated time points. Antibody concentration in mouse serum was determined by FACS analysis. Mean values and standard deviations obtained with three mice per time point are indicated.

3.2.4 Functional assays *in vivo*: SCID mouse xenograft model

In order to compare the anti-tumour activity of mono- and bispecific antibodies *in vivo*, six groups of eight C.B.-17 SCID mice were inoculated with a lethal dose of 1×10^7 SKW 6.4 cells i.v. After 24 h different antibodies in 100 μL DPBS or DPBS alone were applied by intraperitoneal (i.p.) injection. Monospecific antibodies CH20, SDIE20 and anti-epidermal growth factor receptor antibody (EGFR) were applied once (60 μg) at the first day and bispecific antibodies (BS9520 and BS95Mel) were applied 3×20 μg on three consecutive days to compensate for their lower serum half-life (Table 3.3). BS95Mel was used as a control for bispecific BS9520 antibody and anti-EGFR was used as a control for monospecific anti-CD20 antibodies. Mice were observed every day and as soon as they developed paralysis of the hind legs, animals were sacrificed.

Most of untreated (DPBS) and control antibody (BS95Mel and anti-EGFR) treated animals survived only until day 40 (Fig. 3.14). SDIE20 and CH20 were able to prolong survival of 2 mice until day 120. In contrast, BS9520 was found to be the most effective reagent. 6 of 8 animals survived until day 120 when the experiment was terminated.

Table 3.3: **SCID mouse xenograft model experiment schedule**
Respective antibodies were diluted in 100 μL DPBS and applied to the C.B.-17 SCID mice by intraperitoneal (i.p.) injection. Each group consisted of eight mice.

Group	Antibody	Day 1	Day 2	Day 3
1	DPBS	100 μL DPBS	100 μL DPBS	100 μL DPBS
2	BS9520	20 μg	20 μg	20 μg
3	BS95Mel	20 μg	20 μg	20 μg
4	CH20	60 μg		
5	SDIE20	60 μg		
6	EGFR	60 μg		

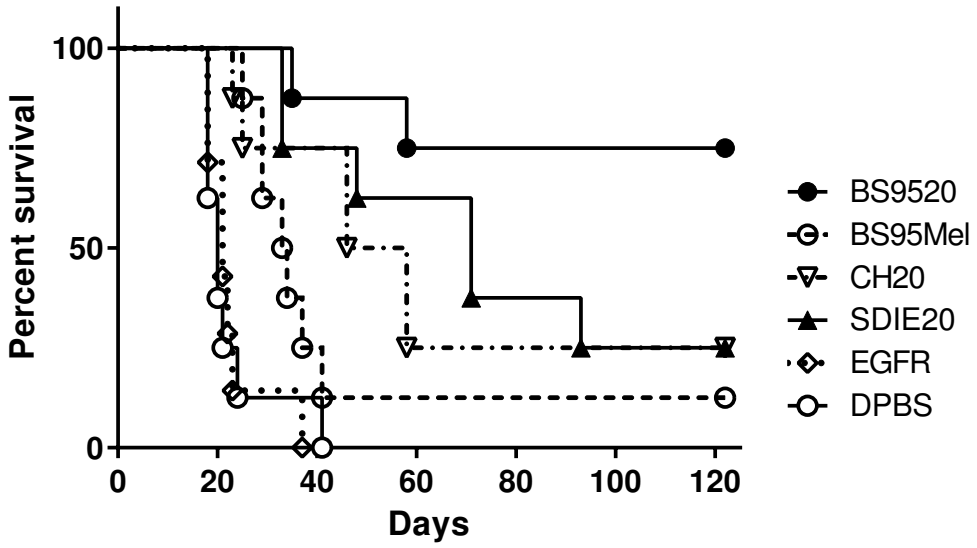

Figure 3.14: **SCID mouse xenograft model survival curves**
Anti-tumour activity of the BS9520 antibody compared to anti-CD20 and control antibodies.

3.3 Induction of apoptosis in normal activated B-lymphocytes

Although the bispecific BS9520 antibody showed promising results against malignant B-cells *in vivo* and *in vitro*, its activity against malignant B-cells in a clinical setting may be limited due to the resistance of the lymphoma cells acquired *in vivo*. In contrast to malignant cells normal B-cells maintain their well established CD95 sensitivity acquired during B-cell activation. Thus, activated and CD95 expressing normal B-cells producing autoantibodies are promising alternative targets for BS9520. Thus, this antibody will be tested in this section against normal and activated B-cells as a model for use in B-cell mediated autoimmune disease.

3.3.1 Expression of CD95 on resting leukocytes

In order to evaluate the expression of CD95 on different normal resting leukocyte populations, peripheral blood leukocytes isolated from heparinized blood samples by red blood cell (RBC) lysis were used. After staining with directly labelled antibodies, specimens were analysed by flow cytometry. Cell populations were determined according to their morphology and surface antigen expression (Fig. 3.15 a-c).

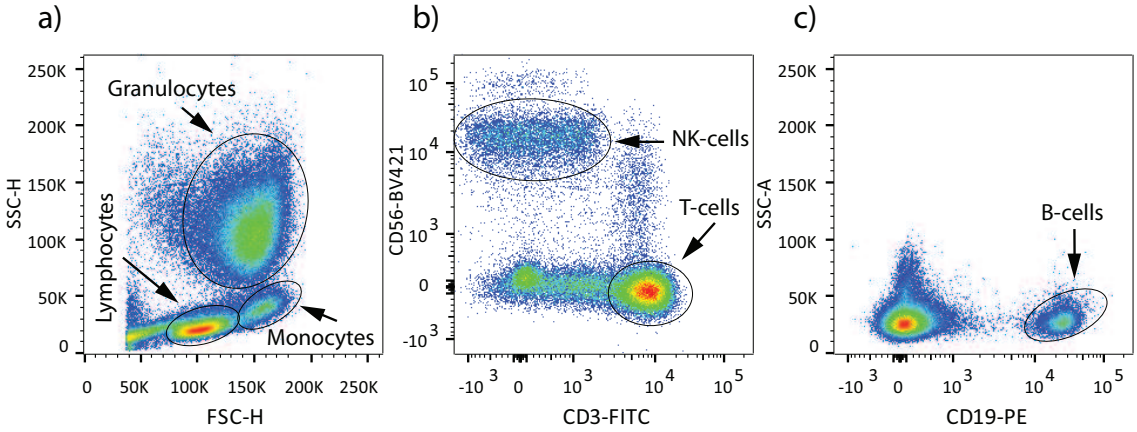

Figure 3.15: **FACS gating strategy for peripheral blood leukocytes**
a) Populations of lymphocytes, monocytes and granulocytes were first identified according to their morphology. b) Populations of T-lymphocytes and NK-cells were determined according to CD3 and CD56 expression on their cell surface. c) B-cells were identified according to CD19 expression.

As depicted in Fig. 3.16 a, expression of CD95 on resting B-cells is marginal. In contrast, almost one half of T-cells are bearing CD95. Some detectable expression of CD95 was also observed on NK cells and this expression varies between different donors (Fig. 3.16). Monocytes and granulocytes were found to be CD95-positive in all of the tested donors.

Plasma cells are B-cells producing immunoglobulins. Thus, CD95 expression was also verified on healthy resting plasma cells to find out whether they could be affected upon BS9520 treatment. To this end fresh bone marrow cells from 5 healthy donors

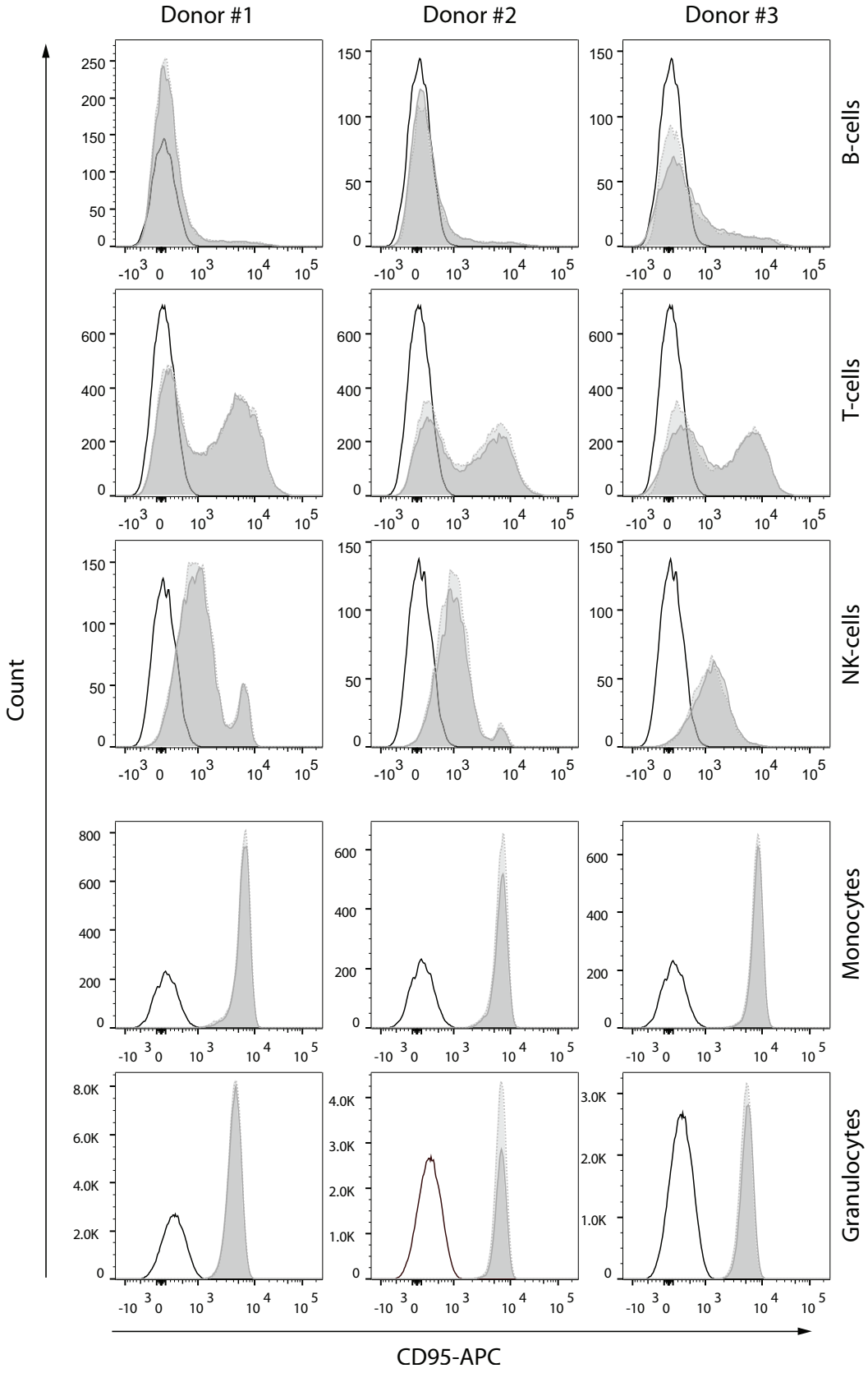

Figure 3.16: **CD95 expression on peripheral blood lymphocytes**
CD95 expression on different leukocyte populations (indicated on the right) from three different donors: empty histograms represent samples stained with APC-labelled isotype control and shaded histograms CD95 staining (samples were analysed in technical duplicates).

(kindly provided by the bone marrow transplantation department in Tübingen) were tested. Red blood cells were removed by RBC lysis. After staining with directly labelled antibodies samples were analysed by flow cytometry. Fig. 3.17 represents the gating strategy (according to (Halliley et al., 2015)) and CD95 expression on CD138$^+$ plasma cells of one representative donor. More than one half of the CD138$^+$ plasma cells in bone marrow were found to express CD95 on the cell surface (Fig. 3.17 d).

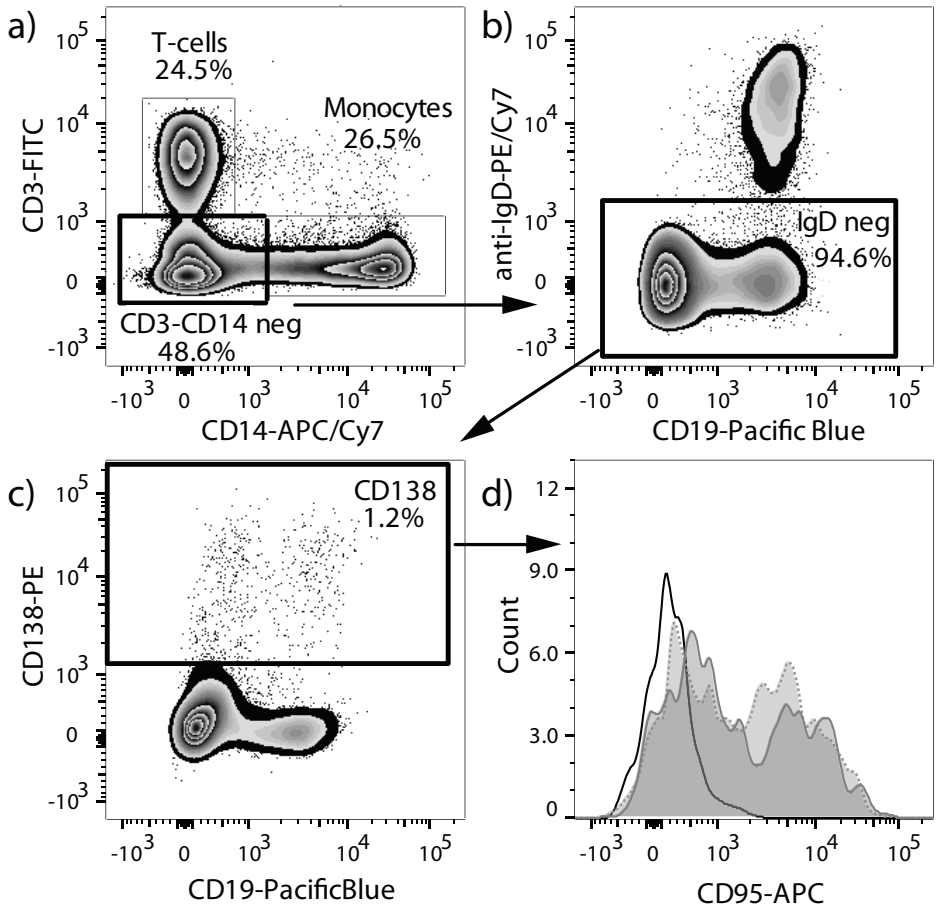

Figure 3.17: **CD95 expression on plasma cells in bone marrow**
Plasma cells isolated from the bone marrow of healthy donors were gated by excluding cells that express CD3, CD14 (a) and IgD (b). Panel (c) represents CD19 negative and positive plasma cells identified by CD138 expression. CD95 expression on CD138$^+$ plasma cells of one representative healthy donor is depicted in the panel (d). Empty histogram represent a sample stained with APC-labelled isotype control and shaded histograms CD95 staining (samples were analysed in technical duplicates).

3.3.2 Kinetics of CD95 expression and antibody production by activated B-cells

As a model for B-cell activation, stimulation of freshly isolated PBMC with pokeweed mitogen (PWM) was performed. PWM is a lectin purified from the plant *Phytolacca americana*. It is frequently used as a T-cell dependent B-cell mitogen to trigger proliferation of B-cells and immunoglobulin secretion *in vitro* (Keightley et al., 1976; Bekeredjian-Ding et al., 2012).

PBMC from healthy donors were stimulated with 1 μg/mL PWM for various times as described by Daniel and Krammer (Daniel and Krammer, 1994). CD95 expression on activated cells was subsequently analysed by flow cytometry. Cell culture supernatants from the same samples were analysed by ELISA for immunoglobulin secretion (as described in 2.4.5 section on page 53). As depicted in Fig. 3.18, the expression of CD95 on CD19$^+$ B-cells was marginal at the initiation of the experiment. It increases significantly after 24 h of PWM stimulation, reaches a maximum at day 3 and remains at this maximum up to 10 days despite removal of PWM at day 6.

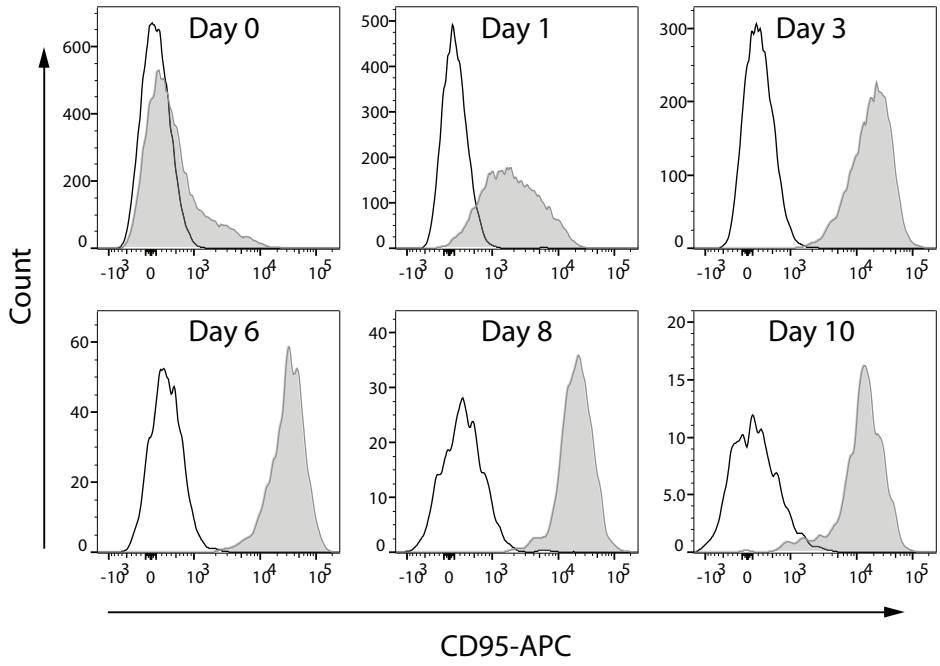

Figure 3.18: **Expression of CD95 on PWM activated human B-cells**
Human PBMC were activated for 1 to 10 days with PWM and then analysed by FACS. CD95 expression on B-cells was determined by gating on the CD19$^+$ population (empty histograms represent samples stained with APC-labelled isotype control antibody and shaded histograms represent CD95 staining).

In contrast to CD95 expression on B-cells, IgG production requires at least 4 days of stimulation to become detectable and, despite washing of the cells at day 6, steadily rises up to day 8, which was the termination point for most of the experiments (Fig. 3.19).

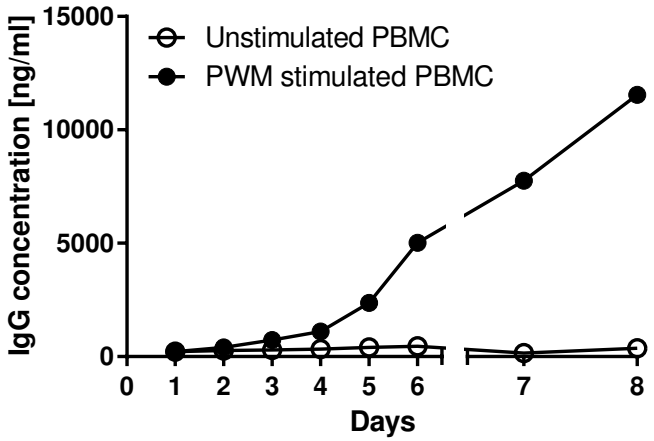

Figure 3.19: **Kinetics of IgG production in PWM activated PBMC cultures**
Cell culture supernatans were taken on indicated days from 24-well plates containing 2×10^6 cells/well/mL of untreated or PWM stimulated PMBC. Supernatants were analysed by ELISA for human IgG secretion as described in 2.4.5 section on page 53.

3.3.3 Induction of apoptosis in activated B-cells *in vitro*

Previous results suggested that anti B-cell activity of BS9520 as well as of the monospecific CD20 antibodies is maximal at concentrations $\geq$100 ng/mL. Thus, BS9520 and BS95Mel were compared in functional assays to the monospecific CD20 antibodies (Fig. 3.9) using this concentration. PBMC cultures that contained either resting cells or cells that had been activated for 6 days with PWM were used as a target cells.

Cytolytic activity of the antibodies against normal resting or PWM-activated B-cells within PBMC cultures was evaluated using a flow cytometry (FACS) based assay as described in 2.4.4.4 on page 52. To illustrate this assay FACS plots of one representative donor are presented in Fig. 3.20. Fig. 3.21 summarizes results obtained with unstimulated PBMC from 4 healthy donors and with PWM-stimulated PBMC from 5 healthy donors. SDIE20 effectively depleted B-cells in resting as well as in activated cultures. The activity of CH20 as well as that of Rituximab was clearly less pronounced and highly variable between different donors, in particular, if resting cells were used. BS9520 is only marginally effective against resting cells, however, it effectively kills B-cells in PWM activated PBMC cultures. Interestingly, we noted that BS9520 in contrast to the monospecific antibodies affected not only B-cells but also $CD4^+$ and $CD8^+$ T-cells present in the PBMC cultures, albeit to a lesser extent. Again, bystander killing of T-cells by BS9520 was observed only in PWM activated cultures.

The pattern of cytolytic activity against activated B- and T-cells described above was also observed when early apoptosis was measured by staining with Annexin V and subsequent analysis by flow cytometry (Fig. 3.22): killing of activated B-cells by the Fc-optimized mono- and the bispecific antibody was comparable, but only the bispecific reagent causes significant apoptosis of activated T-cells.

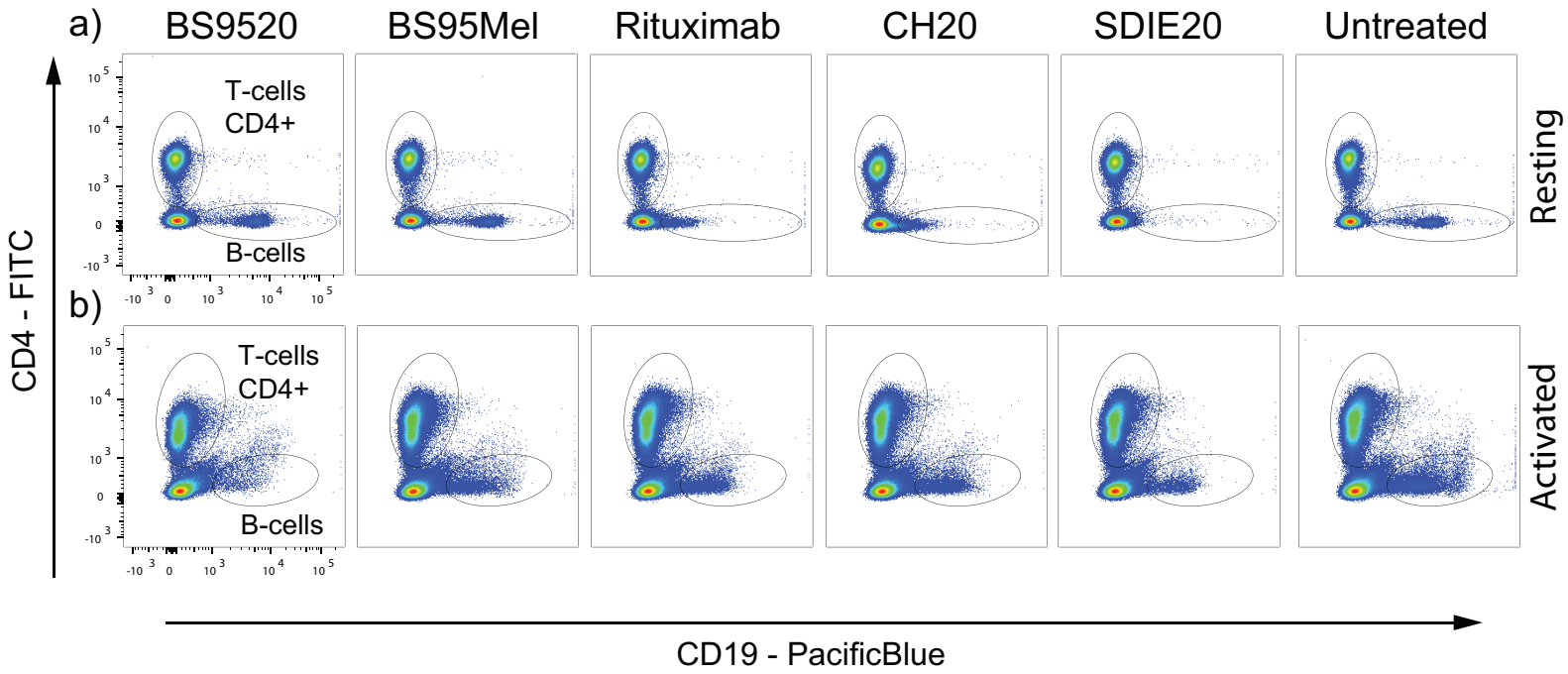

Figure 3.20: **Depletion of B-cells in resting and PWM-activated PBMC cultures.**
PBMC, either untreated (resting) or activated with 1 μg/mL PWM for six days, were incubated for two days with the indicated antibodies (0,1 μg/mL) and analysed by flow cytometry. FACS analysis of B-cell and T-cell depletion within a) resting and b) PWM stimulated PBMC cultures of one donor is shown.

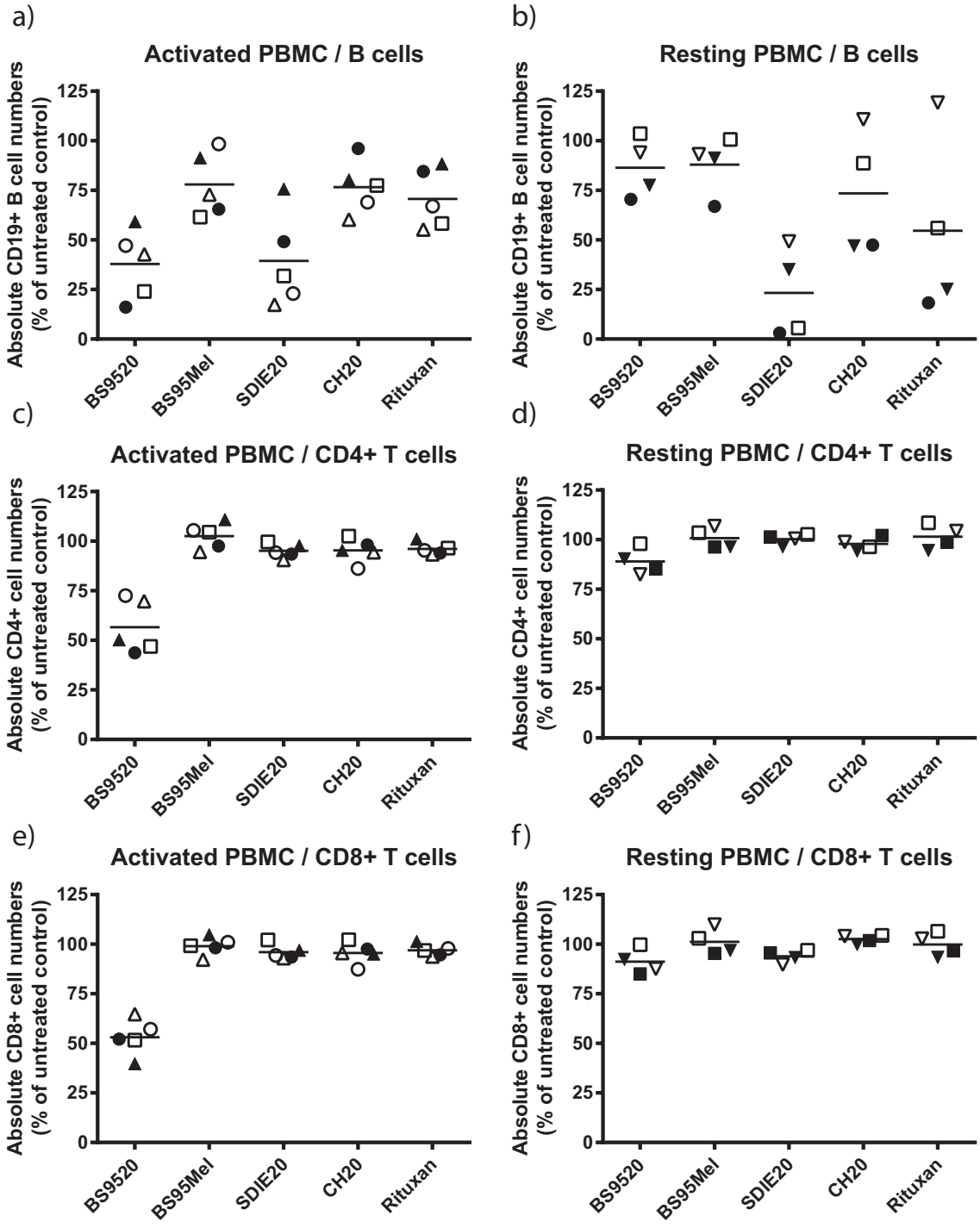

Figure 3.21: **Summarised FACS depletion experiments of activated and resting PBMC**

Depletion of (a, b) B-, (c, d) $CD4^+$ T-cells and (e,f) $CD8^+$ T-cells in PWM-activated and resting PBMC cultures. PBMC, either untreated (resting) or activated with 1 μg/ml PWM for six days, were incubated for two days with the indicated antibodies (0.1 μg/ml) and analysed by flow cytometry. Different symbols indicate the mean values of technical duplicates obtained with PBMC from different healthy donors.

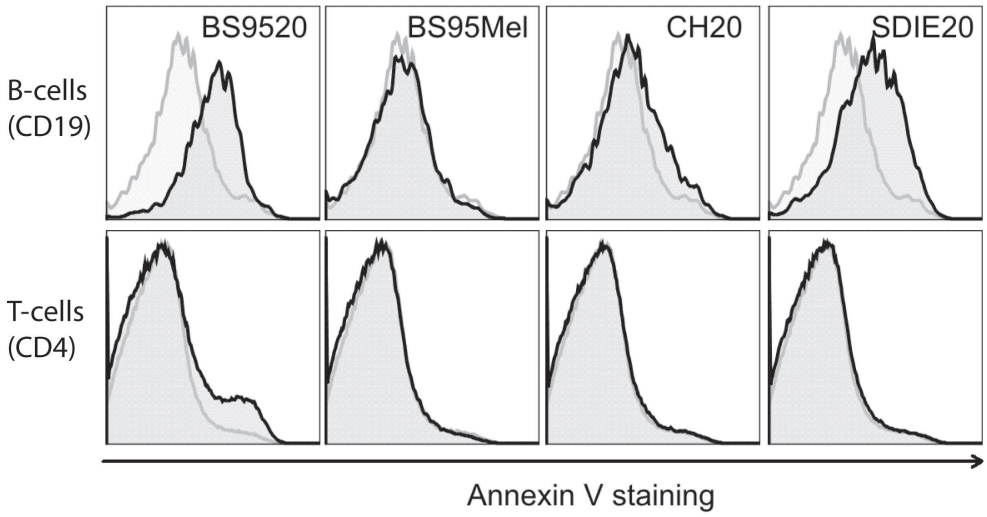

Figure 3.22: **Annexin V staining of activated PBMC after antibody treatment**
$CD19^+$ and $CD4^+$ cells in PWM activated PBMC cultures were incubated with the respective antibodies (1 μg/mL) for 4 h. The cells were stained subsequently with Annexin V and analysed by flow cytometry. One representative experiment of three is shown. Empty histograms represent samples without antibody treatment and filled histograms show Annexin V staining after antibody treatment.

3.3.4 Suppression of PWM-induced IgG synthesis *in vitro*

Next, we investigated the capability of BS9520 to suppress antibody production in PBMC cultures in comparison with anti-CD20 antibodies. To this end, 6 days PWM activated PBMC cultures from 6 healthy donors were incubated with or without 0.1 μg/mL of each antibody for 2 days. Then, cell culture supernatants were analysed by ELISA for human IgG production as described in 2.4.5 section on page 53. Monospecific and bispecific antibodies used in this assay did not interfere with the ELISA detection system at the concentration used (0.1 μg/mL).
Results depicted in Fig. 3.23 a show significant suppression of polyclonal IgG production in PBMC cultures incubated with BS9520, which was superior to that achieved with optimized SDIE20 antibody, although both reagents demonstrated comparable reduction of the B-cells in FACS based depletion assay. Chimeric CH20 antibody as well as Rituximab were not effective in these experiments.

3.3.5 Suppression of TT induced IgG synthesis *in vitro*

The same experimental setting was used to address the question whether BS9520 is also able to suppress IgG production in PBMC cultures stimulated with specific antigen. In this case Tetanus toxoid (TT)-specific IgG was measured in cell culture supernatants using a TT specific ELISA.
As depicted in Fig. 3.23 b, Tetanus-specific antibody production was significantly suppressed by BS9520, SDIE20 induced a marginal suppression. The chimeric anti-CD20 antibody CH20 and Rituximab did not exert significant effects.

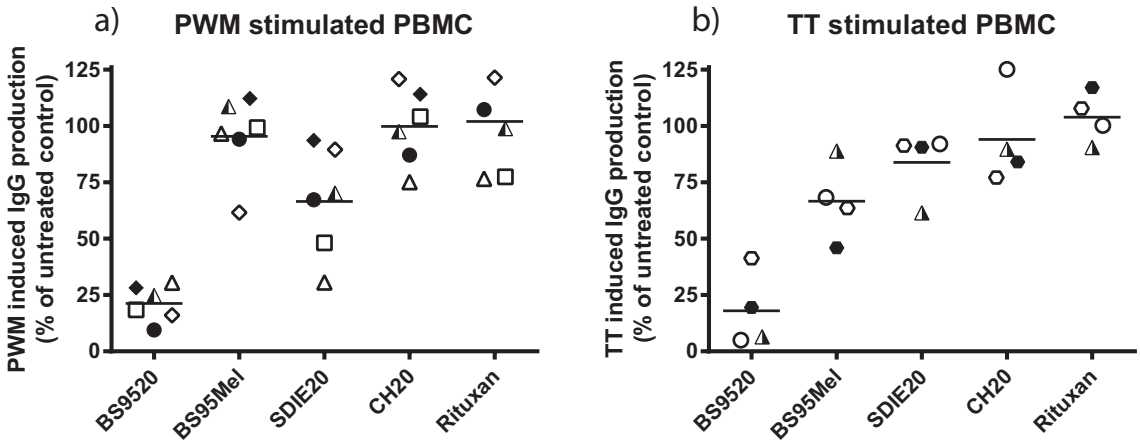

Figure 3.23: **Suppression of IgG production *in vitro***
Suppression of polyclonal and specific IgG production in PBMC cultures by various antibodies. PBMC of different healthy donors were stimulated for six days with PWM (a) and tetanus toxoid (b). Cells were then washed and incubated for two days with the indicated antibodies. Antibody production in the culture supernatants was estimated by ELISA as described in section 2.4.5. Different symbols indicate the mean values of technical ELISA duplicates obtained with PBMC from different healthy donors.

3.4 Generation of recombinant CD95-Ag fusion proteins

The concept of bispecific antibodies depleting activated B-cells and suppressing IgG production via the CD95 death receptor was further developed to increase target-specificity of such reagents. A significant subsequent step of this concept would be suppression and depletion of antigen-specific B-cells.
To this end, novel fusion proteins containing agonistic anti-CD95 antibody and an antigen (Ag) were generated by replacing the C-terminal single chain antibody within the FabSc format by the antigen resulting in a "FabAg-format". In this case CD95-mediated apoptosis is supposed to be induced in activated B-cells carrying a certain antigen-specific B-cell receptor (BCR) and CD95 receptor on their surface. The expected mode of action of such bispecific fusion proteins is depicted in Fig. 3.24.

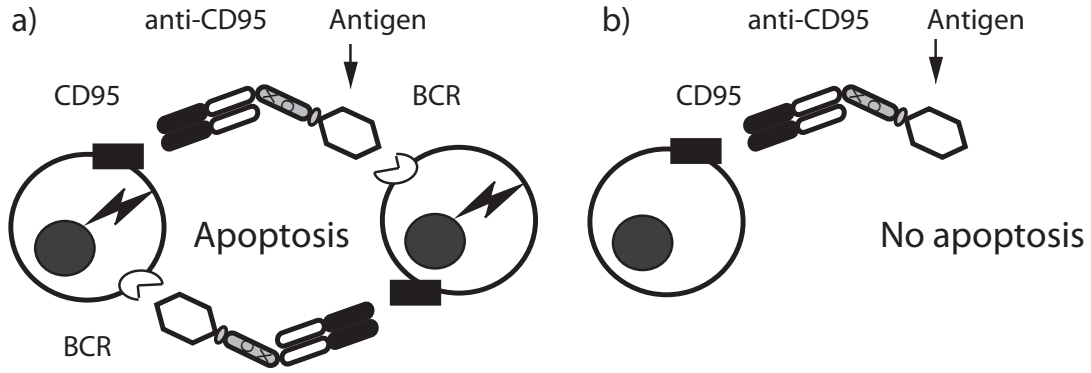

Figure 3.24: **Induction of apoptosis by CD95×Ag fusion proteins**
a) Bispecific CD95×Ag fusion protein binds to Ag-specific BCR and CD95 death receptor on B-cells and induces apoptosis. b) In the absence of the specific BCR apoptosis does not occur.

For proof of principle Tetanus toxoid (TT) and Diphtheria toxoid (DT) were chosen as model antigens. Fusion proteins, generated with these antigens were designated BS95TT and BS95DT, respectively. An expression vector for BS9520 antibody (Fig. 2.4, page 41) developed in the first part of this work was used as a backbone for cloning and transfection of Sp2/0 cells.

3.4.1 Generation and characterisation of BS95TT

The part of the BS9520 vector containing the sequence for the CD20 ScFv was replaced by various truncated sequences for tetanus toxoid (TT) heavy chain. A part of TT heavy chain, also known as Hc or C fragment consists of 451 a.a. (GenBank: #1AF9_A). Three different variants of this fragment capable to induce an immune response in mice (Figueiredo et al., 1995) were linked to CD95 antibody and produced by transfected Sp2/0 cells as fusion proteins in the FabAg format. BS95TT fusion proteins were purified from cell culture supernatant as described in 2.4.1.1 section. Determination of protein concentration was achieved using molar

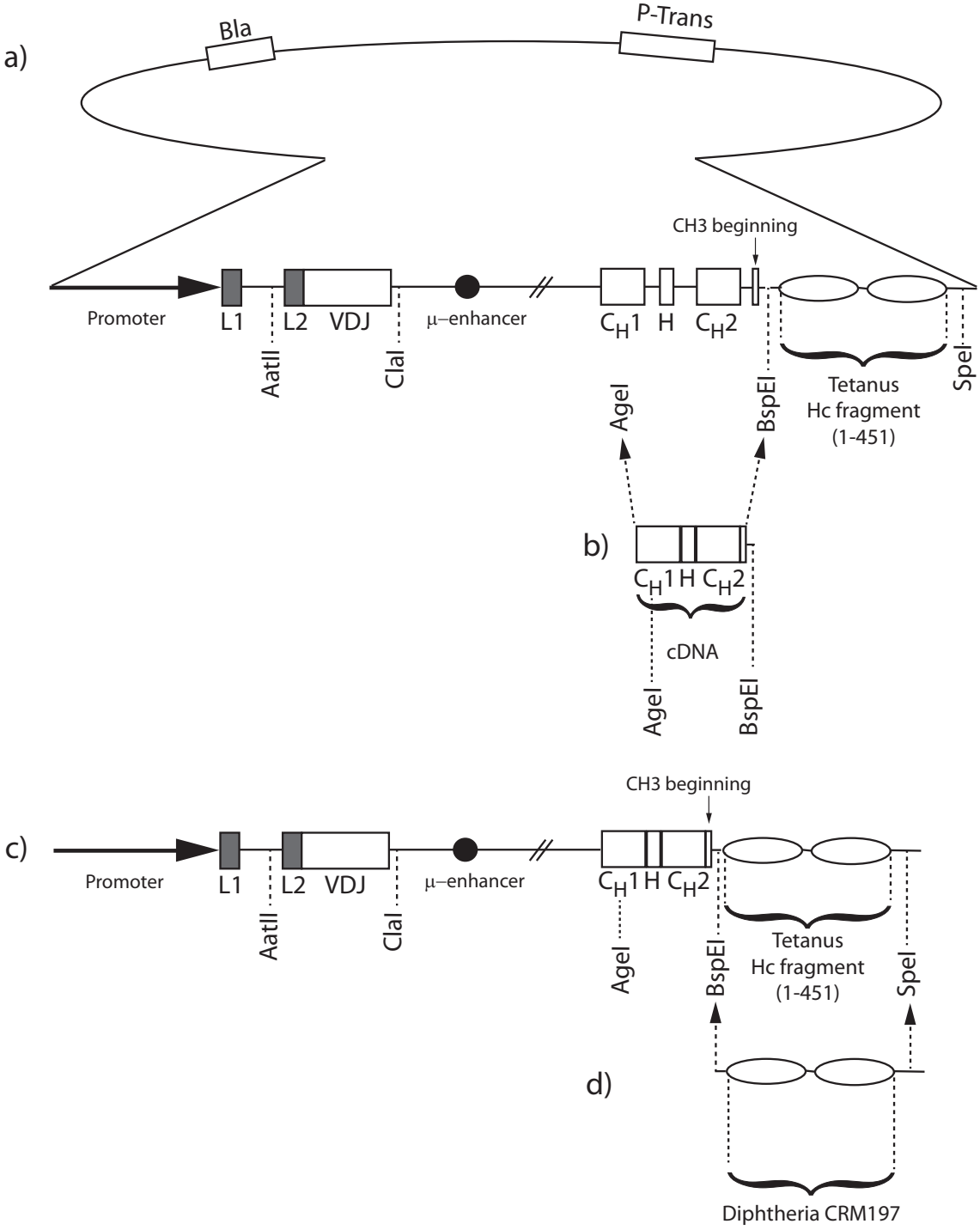

Figure 3.25: **Assembling of improved BS95TT and BS95DT expression vector**

a) BS95TT plasmid containing introns between C_H1 and C_H3 antibody domains. The vector part coding for constant domains, hinge region and introns between C_H1 and C_H3 was removed using AgeI and BspEI restriction sites. DNA sequence without introns (b) was obtained by isolation of cytoplasmic mRNA from Sp2/0 transfected with $BS95TT_{1-451}$ and reverse transcription of the RNA sequence into cDNA. This sequence was inserted into the plasmid c) using AgeI and BspEI restriction sites. Next, TT Hc fragment sequence was replaced with DT sequence (d) using BspEI and SpeI restriction sites.

Table 3.4: **Recombinant BS95TT fusion proteins**
Overview of generated CD95×TT constructs bearing different truncated variants of tetanus Hc fragment, calculated theoretical MW (kDa) and extinction coefficient of the generated proteins.

Construct	TT Hc a.a. in construct	Calculated MW (kDa)	Extinction coef. (M^{-1} cm^{-1}, 280 nm)
$BS95TT_{1-271}$	1-271	89.926	137015
$BS95TT_{80-451}$	80-451	101.996	168875
$BS95TT_{1-451}$	1-451	110.763	177355

extinction coefficients calculated for each protein separately (Table 3.4 [8]).
$BS95TT_{1-451}$ fusion protein capable of folding properly was further improved by modifying the expression vector by removing introns between C_H1 and C_H3 domains of the heavy chain to avoid alternative splicing in the Hinge region as described in the section 3.1.2.2. The main cloning steps leading to improvement of the expression vector are represented in Fig. 3.25. Improved $BS95TT_{1-451}$ (without introns in the expression vector) was produced in Sp2/0 cells and purified from cell culture supernatant using KappaSelect affinity chromatography.

Analytical size exclusion chromatography
Elution profiles of BS95TT constructs are depicted in Fig. 3.26. $BS95TT_{1-271}$ and $BS95TT_{80-451}$ containing truncated parts of Tetanus Hc fragment failed to fold properly. $BS95TT_{1-271}$ (Fig. 3.26 a) showed a non-symmetric main peak and various smaller protein fragments. $BS95TT_{80-451}$ (Fig. 3.26 b) contained a multimerized and aggregated protein. Only one construct containing the whole C-part of TT heavy chain ($BS95TT_{1-451}$) was produced and folded properly (Fig. 3.26 c). Elution profile of the improved $BS95TT_{1-451}$ fusion protein represented in Fig. 3.26 d showed an identical peak compared to that depicted on Fig. 3.26 c. No additional protein fragments or multimers were detectable.

SDS-PAGE analysis
In order to separate BS95TT proteins based on their primary structure SDS-PAGE analysis was performed. Fig. 3.27 depicts gel electrophoresis of generated fusion proteins under non-reduced (lanes 2-5) and β-mercaptoethanol reduced (lanes 7-10) conditions compared to a pre-stained protein ladder.
$BS95TT_{1-271}$ shows multiple bands in the non-reduced sample. In the reduced sample, the heavy chain (upper band) is significantly smaller (approx. 40 kDa) than expected. $BS95TT_{80-451}$ shows more than one band under non-reduced conditions. The upper band might be aggregated protein (according to SEC results in Fig. 3.26 b), the second band is complete $BS95TT_{80-451}$ fusion protein and the bands below could be monomeric heavy and light chains (calculated size 78.2 kDa and 23.6 kDa).

[8] Enumeration of amino acids is assigned to the Tetanus Hc fragment sequence and not to the whole BS95TT fusion protein.

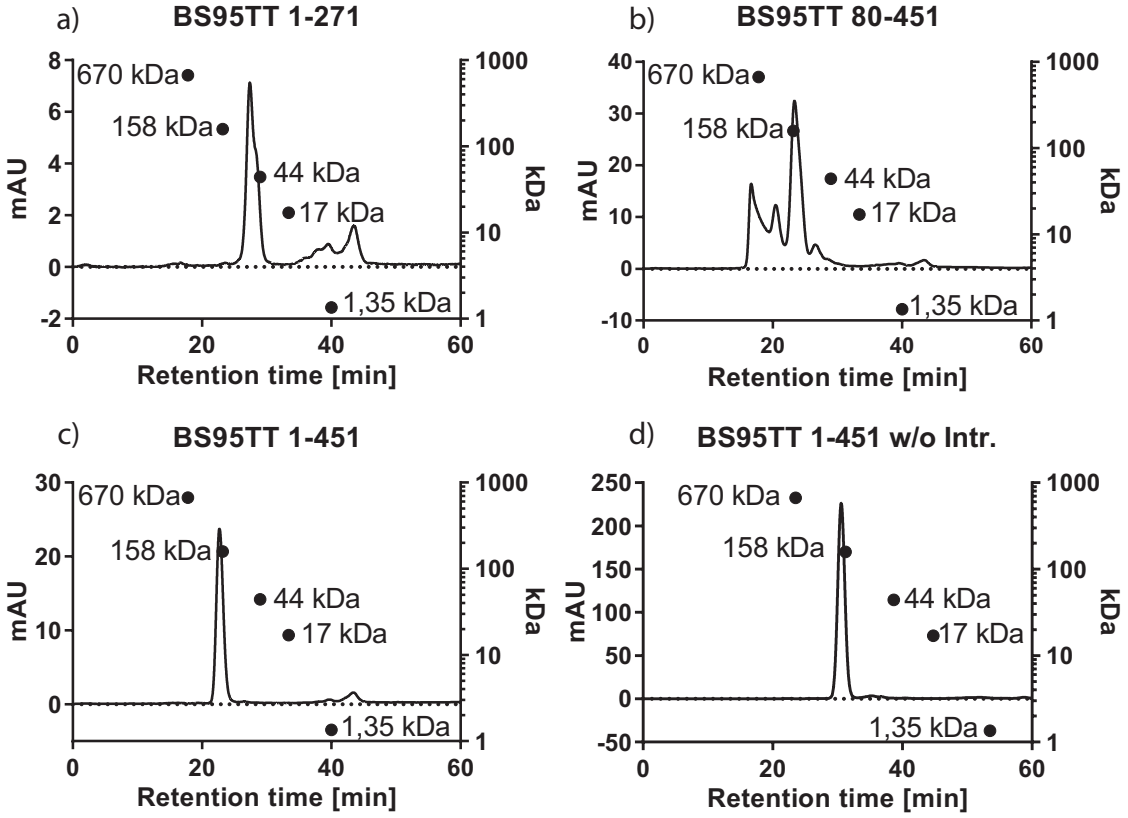

Figure 3.26: **Analytical size exclusion chromatography of different BS95TT fusion proteins**
a) $BS95TT_{1-271}$ fusion protein containing 271 a.a. of Tetanus toxoid on the C-terminus of the heavy chain, b) $BS95TT_{80-451}$ fusion protein containing 371 a.a. (80-451) of Tetanus toxoid, c) $BS95TT_{1-451}$ fusion protein containing 451 a.a. of Tetanus toxoid, d) improved $BS95TT_{1-451}$ fusion protein containing 451 a.a. of Tetanus toxoid. 10 μg of purified fusion proteins were separated using a Dionex™ UltiMate™ 3000 BioRS system equipped with Superdex 200™ increase 10/300 GL column.

Two different variants of one construct – primary and improved $BS95TT_{1-451}$ – are analysed in lanes 4 and 5 as well as in 9 and 10. The upper band in lane 4 represents complete $BS95TT_{1-451}$ fusion protein. The bands below could be monomeric heavy and light chains (calculated size 86.7 kDa and 23.6 kDa, respectively). In contrast, improved $BS95TT_{1-451}$ does not contain any additional bands under non-reducing conditions as depicted in lane 5. Under reduced conditions (lanes 9 and 10) both proteins seems to be identical (calculated molecular weight of the heavy chain 110.7 kDa).

FACS analysis
In order to measure binding activity, $BS95TT_{1-451}$ fusion protein was tested by flow cytometry on SKW 6.4 cells (Fig. 3.28). As expected, $BS95TT_{1-451}$ exhibit very good binding properties on CD95 as well as on TT fusion protein part. Binding on $CD95^+$ SKW 6.4 cells is comparable to that obtained with BS9520 and BS95Mel FabSc constructs.

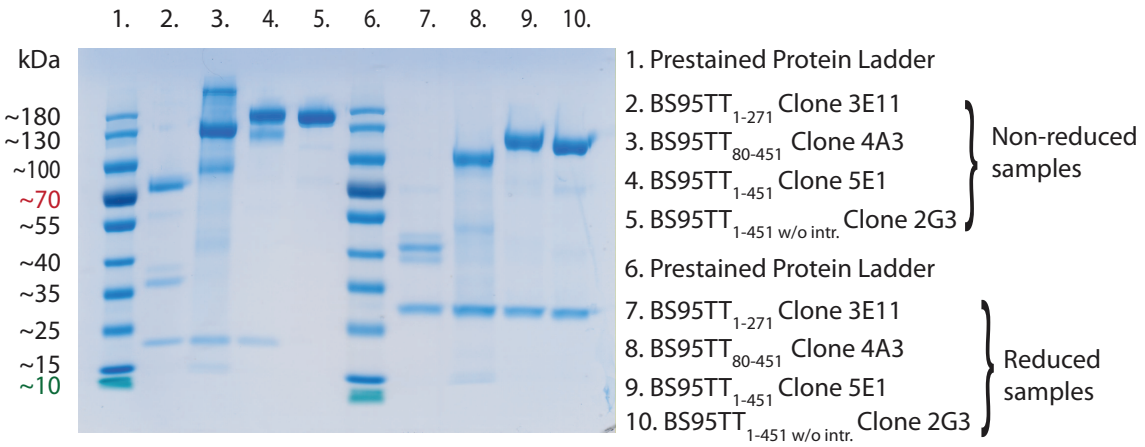

Figure 3.27: **Non-reducing and reducing SDS-PAGE of BS95TT fusion proteins**
2 μg of each antibody pro lane were tested in SDS-PAGE compared to pre-stained protein ladder indicating molecular weight in kDa.

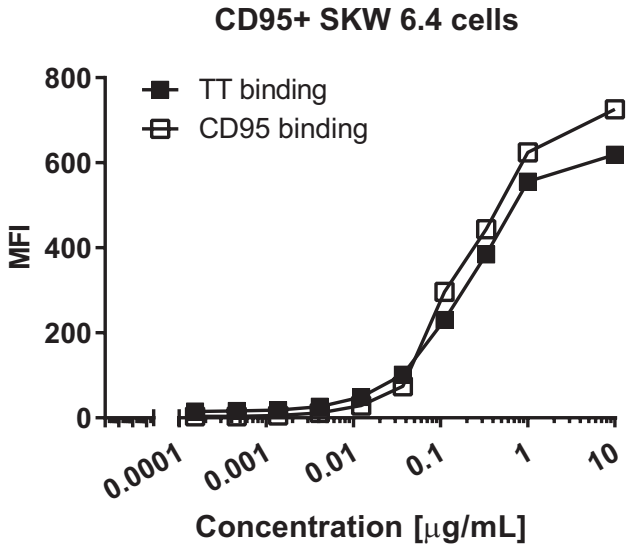

Figure 3.28: **FACS analysis of BS95TT$_{1-451}$ fusion protein on CD95$^+$ SKW 6.4 cells**
Binding to SKW 6.4 cells was detected with Goat anti-Human Igγ-APC secondary antibody (empty squares) and binding to Tetanus part of the fusion protein was detected using anti-Tetanus Hc fragment Rabbit serum, subsequently visualised with Donkey anti-Rabbit Igγ-APC secondary antibody (black squares).

3.4.2 Generation and characterisation of the control protein BS95DT

For construction of the control protein BS95DT the part of the BS95TT vector containing the sequence for Tetanus toxoid was replaced with various truncated sequences of non-toxic Diphtheria toxin Mutant CRM197 (Giannini et al., 1984) using BspEI and SpeI restriction sites (Fig. 3.25 d). First only one part of the DT protein known to be immunogenic (Romaniuk et al., 2012) was coupled to CD95 antibody and produced by transfected Sp2/0 cells as fusion protein. Additionally, constructs with different CRM197 parts and amino acid substitutions were created due to problems concerning protein folding and aggregation. An overview of the generated BS95DT fusion proteins is summarised in the table 3.5.

Table 3.5: **Recombinant BS95DT fusion proteins**
Overview and calculated MW (kDa) of generated CD95×DT constructs bearing different domains (C, T and R) of non-toxic Diphtheria toxin Mutant CRM197.

Construct	CRM197 a.a. in construct	Calculated MW (kDa)	Extinction coef. (M^{-1} cm^{-1}, 280 nm)
BS95DT-TR	194-535	97.864	114555
BS95DT-TR (C201G)	194-535	97.910	114555
BS95DT-CTR (R173Q R193Q)	1-535	119.073	140580
BS95DT-CT (R173Q R193Q)	1-384	103.084	130485
BS95DT-CTR (R173Q R193Q C186G C201G)	1-535	118.981	140455
BS95DT-CT (R173Q R193Q C186G C201G)	1-384	102.390	130360

Size exclusion chromatography
Elution profiles of all generated BS95DT constructs are depicted on Fig. 6.2 in the appendix on page 126. Almost all of them aggregated extensively. Only BS95DT-CT constructs carrying C and T domains (Fig. 6.2 d,f) contained detectable amounts of monomers, which could be separated using preparative size exclusion chromatography. To this end, KappaSelect purified BS95DT-$CT_{R173QR193Q}$ (clone 5B1) fusion protein was loaded onto Superdex™ 200 Prep Grade 16/60 HiLoad column and separated from multimers and smaller protein fragments using ÄKTApure chromatography system. Separated protein was tested again using analytical size exclusion chromatography (Fig. 3.29).

FACS analysis
To measure binding activity, BS95DT-$CT_{R173QR193Q}$ fusion protein and purified monomer thereof were tested by flow cytometry. As depicted in Fig. 3.30 a BS95DT is saturated at the concentration about 1 μg/mL. At the concentrations $\geq 1\,\mu$g/mL unspecific fluorescence increases suggesting the presence of aggregated protein. In contrast, purified monomeric BS95DT does not show this phenomenon (Fig. 3.30 b).

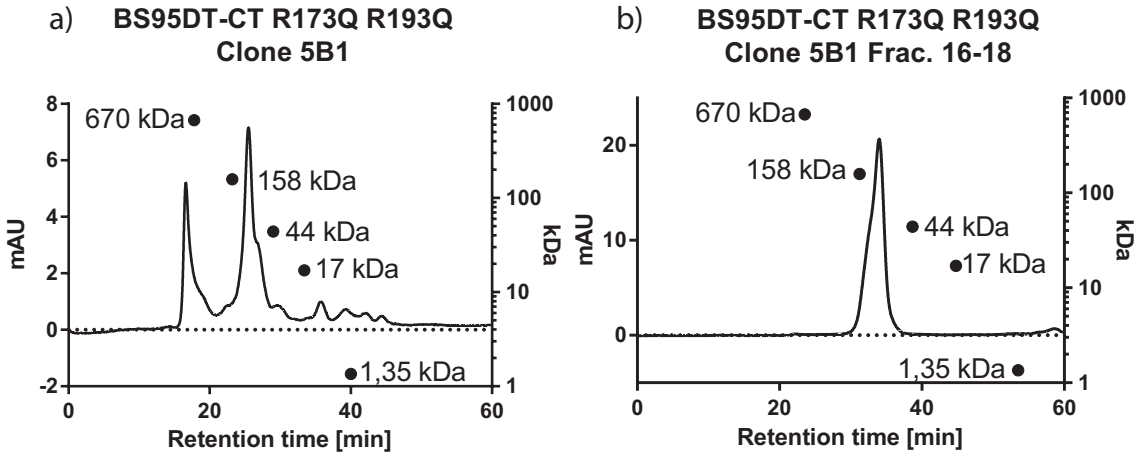

Figure 3.29: **Analytical SEC of BS95DT (clone 5B1) before and after preparative FPLC separation**
a) BS95DT-CT$_{R173Q\,R193Q}$ (clone 5B1) containing C and T domains after initial KappaSelect purification. b) BS95DT-CT$_{R173Q\,R193Q}$ (clone 5B1) preparative FPLC purification using Superdex™ 200 Prep Grade 16/60 HiLoad column. 2 μg of multimeric and monomeric proteins were separated using a Dionex™ UltiMate™ 3000 BioRS system equipped with Superdex 200™ increase 10/300 GL column [10].

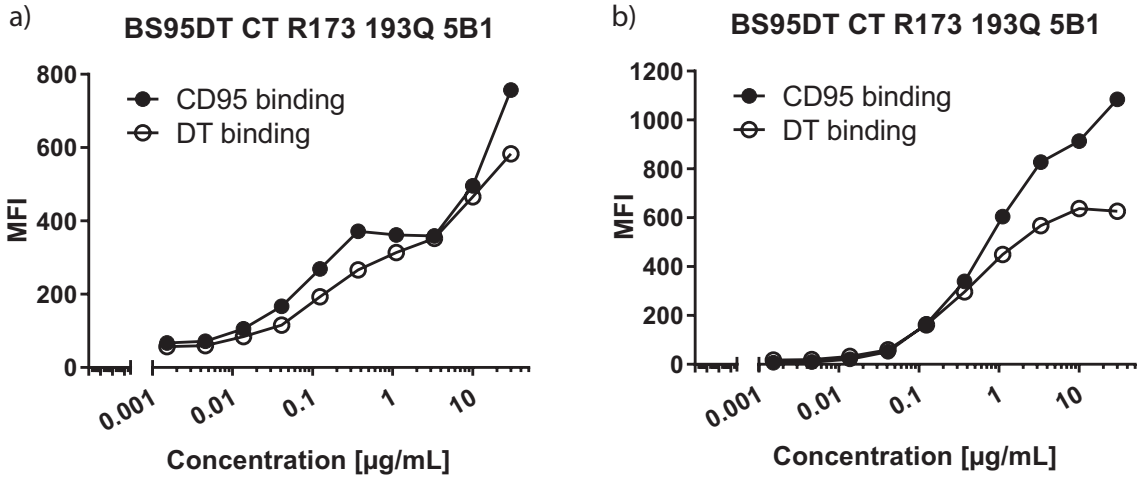

Figure 3.30: **FACS analysis of BS95DT (clone 5B1) before and after preparative FPLC separation**
a) BS95DT-CT$_{R173Q\,R193Q}$ (clone 5B1) containing C and T domains after initial KappaSelect purification. b) BS95DT-CT$_{R173Q\,R193Q}$ (clone 5B1) after preparative FPLC purification. Binding of different BS95DT fusion proteins to SKW 6.4 cells was detected with Goat anti-Human Igγ-APC secondary antibody (black circles) and with anti-Diphtheria rabbit serum, subsequently visualised with Donkey anti-Rabbit Igγ-APC secondary antibody (empty circles).

3.4.3 Suppression of specific IgG production

The induction of *in vitro* anti-tetanus toxoid IgG synthesis was performed according to the protocol described by Lum and Culbertson (Lum and Culbertson, 1985). Freshly isolated PBMC from 6 recently TT/DT immunized donors were stimulated with Tetanus toxoid for 6 days. For an indirect detection of B-cell killing the cells were washed three times and incubated with different antibody- or fusion protein constructs. After two days suppression of specific anti-tetanus IgG production in cell culture supernatants was measured using specific ELISA as described in 2.4.5 section on page 53.
A moderate suppression of tetanus-specific antibody production by BS95TT was observed in 4 of 6 tested donors (Fig. 3.31). It is clearly less efficient than suppression achieved with BS9520. BS95Mel as well as the control fusion protein BS95DT did not exert significant suppressive effects.

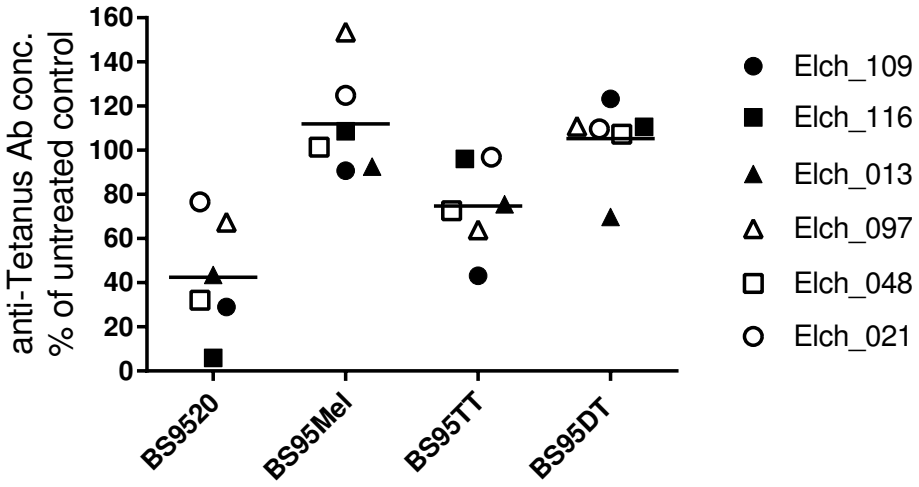

Figure 3.31: **Suppression of anti-TT IgG production *in vitro***
Suppression of specific anti-TT IgG production in TT-stimulated PBMC cultures. Different symbols indicate the mean values of technical ELISA duplicates obtained from 6 different healthy donors.

Chapter 4

Discussion

4.1 Development of the CD95×CD20 antibody

4.1.1 Challenges in protein engineering and production

The selective stimulation of the CD95 death receptor is one of several attractive applications for bispecific antibodies. However, the production of such reagents in pharmaceutical quality and quantity remains a formidable challenge despite considerable progress in recombinant antibody technology (Wörn and Plückthun, 2001; Hust et al., 2007).
The development of the bispecific CD95×CD20 antibody strikingly illustrates this problem: production of a functional bispecific antibody containing the CD95 binding part as a ScFv (single-chain fragment variable) molecule, irrespective of V_H-V_L orientation, was not successful due to extensive aggregation of this moiety. Single chain antibodies can aggregate owing to physical and chemical instabilities that preclude the folding of stable molecules (Perchiacca and Tessier, 2012). It is known that the sequence of CDR loops can significantly impact the folding stability of multidomain antibody fragments. The group of A. Plückthun in Zürich described in 2003 two ScFvs that differed only in the sequence of CDR3 loops in the V_L domain. They provided a striking example of the sensitivity of antibody folding stability to the sequence of CDRs (Ewert et al., 2003; Perchiacca and Tessier, 2012). Thus we speculate, that the CDR regions of the CD95 antibody used in this work are simply not suitable for expression as ScFv.

Despite these problems ScFv fragments serve as an important building block for the construction of bispecific antibodies. The "benchmark" BiTe™ (Bi-specific T-cell engager) format consisting of two ScFv (Bargou et al., 2008) might thus be particularly susceptible to aggregation. This has been demonstrated by Durben et al. comparing otherwise identical antibodies with FLT3×CD3 specificities in the FabSc and BiTe™ format. It was found that the FLT3×CD3 antibody in the FabSc format was superior to the BiTe™ format with respect to:

- affinity to the target antigen,
- production yield by transfected cells,
- the diminished formation of aggregates

In general the FabSc format avoids one of ScFv in the bispecific construct replacing it by a more "physiological" Fab moiety. This moiety can be used if a particular antibody cannot be expressed as a ScFv as observed by the anti-CD95 antibody APO-1.

However, the C-terminal ScFv within the BS9520 FabSc constuct is still a problem: a significant loss of affinity towards CD20 was noticed when compared to intact, monospecific and bivalent CD20 antibodies as well as to monovalent chemically digested anti-CD20 F(ab') fragments (Fig. 3.6). In contrast, the affinity of BS9520 towards CD95 was only moderately reduced when compared to the parental CD95 antibody APO-1 (Fig. 3.6 on page 65). These results demonstrate that monovalency affects the affinity to CD95 only marginal and that the N-terminal F(ab') is less prone to affinity loss than the C-terminal ScFv.

SDS-PAGE analysis revealed that separated heavy and light chains of BS9520 and BS95Mel antibodies are visible if testing proteins under non-reduced conditions (Fig. 3.5 on page 63, lanes 2 and 3). Moreover, the heavy chain under reduced conditions appear as a double band suggesting that two types of the heavy chain are present in the protein solution. mRNA analysis of antibody producing Sp2/0 cells revealed that alternative splicing in the hinge region of the heavy chain results in a heavy chain missing 15 amino acids as shown in section 3.1.2.2 on page 63. This leads to two variants of the protein. Since one cysteine in the hinge-spliced variant is missing, interaction with the corresponding light chain is weaker. It is strong enough to pass purification using KappaSelect affinity chromatography media, but it did not withstand incubation at 95°C for 5 min required for sample preparation in SDS-PAGE analysis. As a result, the association of heavy and light chains is weaker and some separated heavy and light chains are visible in SDS-PAGE even under non-reduced conditions. However, antibodies containing spliced heavy chain were not distinguishable in analytical size exclusion chromatography, suggesting that interaction between heavy and light chain is strong enough to preserve antibody integrity under physiological conditions.

For early development and functional characterisation of BS9520 antibody in this work, the quality of the produced protein was defined as sufficient. However, the use of introns in the expression vector should be avoided during production of this molecule in pharmaceutical quality and quantity.

4.1.2 Depletion of B-lymphoma cells

Monospecific, CD20-targeting antibodies are meanwhile firmly established for the treatment of B-cell malignancies. The chimeric, second generation antibody Rituximab in combination with cyclophosphamide, hydroxydaunorubicin, oncovin (vincristine) and prednisone (R-CHOP) is currently the front-line regimen for diffuse large B-cell lymphoma (Coiffier et al., 2002; Mishima et al., 2012). Nevertheless, the field of CD20-targeting antibodies is developing further. In order to decrease immunogenicity, novel humanized and Fc-optimized anti-CD20 agents were developed. These "third-generation" antibodies are currently undergoing development in numerous clinical trials. The glyco-optimized anti-CD20 antibody Obinutuzumab (GA-101), for instance, was shown to be clearly superior over Rituximab in B-cell chronic lymphocytic leukaemia (B-CLL) patients (Goede et al., 2014; Goede et al., 2015).
Therefore in this work the activity of BS9520 was compared not only to the "gold standard" – Rituximab, but also to a comparable chimeric anti-CD20 antibody (clone 2H7) and in particular to the "third-generation" – Fc-optimized version thereof.

4.1.2.1 BS9520 antibody suppresses growth of lymphoma cells *in vitro*

When comparing the cytotoxic effects of BS9520 to that of the various monospecific anti-CD20 antibodies, the different cytolytic mechanisms used by these reagents had to be taken into account: killing by monospecific antibodies requires the presence

of FcR expressing effector cells, whereas BS9520 acts via CD95-mediated apoptosis in the absence of effector cells. Whereas BS9520 is clearly superior to the most effective monospecific CD20 antibody at a PBMC : target ratio of 5 : 1 these difference in favour of the bispecific antibody is – as expected – diminished at higher PBMC : target ratio of 10 : 1 (Fig. 3.10). In a clinical situation, however, such favourable ratios rarely prevail. Moreover, the amount and activity of FcR expressing effector cells is known to exhibit intra-individual variations affecting monospecific antibody-mediated cytotoxicity. Thus, the complete independence on the presence of effector cells argues in favour of BS9520.

The selectivity of BS9520 towards malignant rather than of resting B-cells is advantageous as well. As demonstrated by FACS analysis, normal B-cells within PBMC cultures remain almost unaffected by the BS9520 construct during co-cultivation with SKW 6.4 or Raji cells. In contrast, upon incubation with monospecific antibodies, malignant as well as normal B-cells are depleted or affected in terms of their CD19 expression (Fig. 3.11 and Fig. 3.12). Resting B-cells expressing high amounts of CD19 disappear and a small population of "CD19-low" cells remains. This phenomenon was explained by D. Jones at al. in 2012. They concluded that the addition of Rituximab to healthy donor PBMCs *in vitro* can result in complement-independent loss of CD19 without causing B-cell death. CD19 is transferred from B-cells to monocytes and neutrophils during shaving of the Rituximab-CD20 complex in an Fc-dependent manner (Jones et al., 2012). These data explain also the shift of CD19 on Raji cells treated with anti-CD20 antibodies (Fig. 3.12) and suggest that therapeutic effect of monospecific, and especially Fc-optimized, anti-CD20 antibodies may be compromised by this activity. In any case, BS9520 spares resting B-cells and thus, side effects such as long term depletion of normal B-cells as observed after clinical application of monospecific CD20 antibodies may be avoidable.

However, there is a challenge rather typical for bispecific CD95-targeting antibody. When PBMC from healthy donors were incubated with SKW 6.4 or Raji cells in the presence of BS9520 and analysed by flow cytometry, a slight bystander killing of monocytes (Fig. 3.11 and Fig. 3.12) was noticed. Thus, CD95 expression was verified in different populations of leukocytes freshly isolated from heparinized blood of healthy donors by red blood cell lysis. As expected, expression of CD95 on resting B-lymphocytes is only marginal. In contrast, almost one half of T-cells and NK-cells express CD95 and this expression varies between different donors. Moreover, entire populations of monocytes and granulocytes were shown to be CD95 positive (Fig. 3.16).

Since monocytes express CD95 their killing in flow cytometry based assay might be explained by bystander lysis induced after trans- binding of BS9520 to the target cells according to a mechanism proposed by Herrmann et al. (Herrmann et al., 2008). The effect of BS9520 on monocytes *in vivo* should be further investigated since human monocytes and monocyte-derived macrophages both express CD95 but are differentially susceptible to CD95-induced apoptosis (Kiener et al., 1997; Perera and Waldmann, 1998; Perlman et al., 1999). A similar consideration applies to granulocytes, since these cells were also found to express CD95. Neutrophils are known to be sensitive to CD95 death receptor signaling *in vitro* (O'Donnell et al., 2015), but it is unknown if CD95-mediated apoptosis could be induced via direct stimulation of the death receptor with agonistic anti-CD95 antibodies.

4.1.2.2 BS9520 antibody suppresses tumour growth *in vivo*

When the pharmacokinetic properties of BS9520 in mouse serum were compared to monospecific CD20 antibodies, it became obvious, that serum half life of BS9520 is much shorter than that of whole IgG molecules. The difference can be explained by the ability of monospecific antibodies to bind *in vivo* to the neonatal Fc receptor (FcRn) preventing antibodies from degradation. The affinity of the **mouse FcRn – human IgG1** interaction is even higher than **mouse FcRn – mouse IgG1** (Ober et al., 2001) making this effect even more pronounced in mice if compared to humans. In contrast, BS9520 antibody is lacking C_H3 domain responsible for IgG-FcRn complex formation and thus, does not interact with FcRn.

When the efficacy of BS9520 antibody was tested in a SCID mouse xenograft model, it became obvious, that the therapeutic effect of BS9520 was clearly superior, even though the dosing schedule did not fully compensate for the markedly lower serum half-life. Monospecific anti-CD20 antibodies known to bind to FcγRIIIA receptors conserved between mouse and human were able to slightly improve survival of the treated mice possibly because of FcγRIIIA expression and ADCC by macrophages, activated monocytes and NK-cells (Hashimoto et al., 1983) present in the SCID mice (Bosma et al., 1983).

4.1.2.3 CD95 resistance in tumour cells

Despite its *in vitro* and *in vivo* activity, BS9520 suffers from a principle weakness also depicted in Fig. 3.8 and Fig. 3.10: if CD95-resistant Raji cells were used as targets, only weak inhibition of proliferation was observed. It has been reported that these cells are deficient in phoshatidylserine externalization resulting in an increased resistance towards apoptosis (Hammond et al., 2007). If Raji cells were used as targets in a more sensitive flow cytometry based kill-assay (Fig. 3.12), the activity of BS9520 in terms of B-cell depletion was again largely reduced as well as cell depletion induced by monospecific antibodies.
It is well established that malignant cells may readily acquire resistance towards CD95-mediated killing by down-regulation of CD95-expression or –sensitivity (Xerri et al., 1998; Bullani et al., 2002; Fulda, 2009). In particular, it has been reported that CD95-sensitivity of malignant lymphoma cells isolated from biopsies is null or weak (Xerri et al., 1998; Plumas et al., 1998). The challenge of CD95 resistance of tumour cells might be met by combining BS9520 with sensitizers for apoptosis such as conventional cytostatic drugs or more specific apoptosis inducing reagents developed more recently (Delbridge and Strasser, 2015).
In contrast to malignant cells, healthy B-cells acquire CD95 expression and- sensitivity during activation (Daniel and Krammer, 1994). This constituted the rationale of using BS9520 for selective depletion of normal B-cells in B-cell mediated autoimmune diseases.

4.1.3 Induction of apoptosis in normal activated B-cells

Since B-cell directed anti-CD20 antibodies such as Rituximab, Obinutuzumab, Ofatumumab, and Ocrelizumab are meanwhile widely used for the treatment of B-cell

mediated autoimmune diseases, is seems to be reasonable to combine these principle of CD20 targeting and the selective mode of action of the CD95-triggering antibodies. Induction of CD95 mediated cell death in B-cells appears to be particularly promising if directed against activated normal (including "autoimmune cells") rather than malignant B-cells since these cells are less likely to develop CD95 resistance and currently there are no data available linking B-cell mediated autoimmunity to the CD95-mediated apoptosis resistance of B-cells. In addition, the specific expression and sensitivity of CD95 on activated rather than resting B- and T-cells offers the perspective of a specific activity towards activated cells. Our observations confirm that BS9520 meets this expectation: it appears to be active primarily against activated B-cells whereas the monospecific anti-CD20 antibodies, including the Fc-optimized, monospecific SDIE20 antibody depletes resting B-cells as well.

4.1.3.1 Suppression of activated B-cells *in vitro*

First we compared the cytolytic activity of BS9520 antibody to that of monospecific antibodies directed to CD20 within PBMC cultures that contained either resting cells or cells that had been activated for 6 days with PWM. We found that BS9520 as well as SDIE20 showed significant reduction of $CD19^+$ B-cells in activated PBMC cultures (Fig. 3.21 a). In contrast, B-cells from the resting PBMC cultures remained unaffected upon BS9520 treatment, whereas SDIE20 and Rituximab demonstrated a significant reduction (Fig. 3.21 b) or CD19 antigen shift (3.20). The variation of activity between different donors (Fig. 3.21), particularly pronounced in the case of the monospecific antibodies, is likely to be due to the known variation of NK cell count and ADCC activity in PBMC cultures of normal healthy donors. These findings confirm independence on the presence of effector cells and the selectivity of BS9520 towards CD95-expressing rather than resting CD95-negative B-cells as demonstrated previously (Fig. 3.11 and Fig. 3.12).

What was unexpected, however, was the superior suppression of antibody production by BS9520 (Fig. 3.23) although the activity of the Fc-optimized CD20 antibody against activated B-cells was comparable. BS9520 was demonstrated to suppress polyclonal (PWM-) as well as antigen-specific (TT) activated B-cell more efficient than monospecific anti-CD20 antibodies. This discrepancy might be due to bystander killing of activated T-cells by BS9520, a phenomenon readily explained by the previously reported bi-cellular binding of bispecific antibodies stimulating CD95. This phenomenon results in the killing of CD95 single positive cells when these cells make contact with CD20-single positive target cells carrying a bispecific antibody as demonstrated by Herrmann et al. (Herrmann et al., 2008). Given the well-established helper function of T-cells during antibody production, it is tentative to speculate, that the killing of activated and $CD95^+$ bystander T-cells enhances the anti-B-cell activity of BS9520. Conceptually, this would constitute an additional advantage of the bispecific vs. the monospecific CD20-targeting antibodies. Since this type of cytolytic activity is restricted to *in vitro* PWM-activated (rather than resting) T-cells (Fig. 3.21 d,f) in neighbouring CD20 expressing B-cells, we do not expect it to result in intolerable T-cell depletion upon *in vivo* application of the reagent.

An additional explanation for the superior suppressive effect of BS9520 on antibody production might be, that the susceptibility of B-cells towards CD95-mediated killing may change during the process of B-cell activation that lasts 6 days in the experiments described here. In this regard, we have noticed in preliminary experiments that the sensitivity of B-cells towards CD95 mediated cell death is steadily increasing in PWM activated PBMC cultures from day 3 to day 6 (data not shown). Moreover, it has been reported that the small subpopulation of peripheral blood B-cells in immunized human subjects capable of producing specific antibody is sensitive to CD95 mediated cell death (Medina et al., 1997). Such cells might be killed by BS9520 induced bystander lysis (Herrmann et al., 2008) even if they have lost CD20 expression during differentiation into antibody producing plasma cells. In any case, the superior suppressive effects of BS9520 on antibody production implies that this reagent may be particularly suitable for the treatment of autoantibody-mediated mediated autoimmune diseases.

4.2 Development of CD95×Ag fusion proteins

The idea of selective therapeutic induction of inhibitory and suppressive function of agonistic CD95 antibodies on normal B-cells was further developed. A significant subsequent step would be antigen-specific B-cell suppression by engaging CD95 death receptor.
The concept of selective targeting of antigen-specific B-cells is intended to eliminate pathogenic B-cells while sparing all unrelated cells. As an attractive option for the treatment of autoantibody-mediated autoimmune diseases, BCR targeting has also been investigated by other groups, using different effector mechanisms. For example, Rammensee et al. investigated targeting of antigen-specific B-cells by cytotoxic T lymphocytes using conjugates of T-cell receptor (TCR) specific antibodies and antigen (Rammensee et al., 1987). Taddeo et al. conjugated an antibody or a F(ab) fragment recognizing the surface markers CD138 or CD44 with the antigen of interest for detection and/or depletion of antigen-specific plasma cells (Taddeo et al., 2015). Ellebrecht et al. engineered autoantigen-based chimeric immunoreceptors (CAAR T-cells) that can direct T-cells to kill autoreactive B-cells through the specificity of the BCR (Ellebrecht et al., 2016). These findings suggest that BCR is in principle suitable as a target molecule despite its physiological property to be internalized after antigen exposure.

The basic idea in this work was to achieve antigen-specific B-cell depletion using CD95×Ag fusion proteins binding to the specific BCR and inducing apoptosis in activated antigen-specific B-cells (Fig. 3.24 on page 84). The BS95TT and BS95DT were generated by replacing the CD20 targeting part of the BS9520 molecule by tetanus and diphtheria toxoids (TT/DT) as a model antigens whereby the DT containing protein served as a negative control. Thus, functional hybrid molecules consisting of an anti-CD95 antibody and immunogenic parts of tetanus or diphtheria toxoid were obtained after overcoming some protein engineering challenges. FabSc format used for the BS9520 antibody was applied for construction of CD95×Ag fusion proteins for the proof of principle of this novel idea.

4.2.1 Suppression of Ag-specific IgG production

Suppression of Ag-specific IgG production in TT activated cultures by the BS95TT fusion protein was analysed in the same way as with BS9520 construct using a specific ELISA. 6 days TT-stimulated PBMC from 6 recently immunised donors were incubated with or without control antibodies and fusion proteins for 2 days. Subsequently, cell culture supernatants were analysed by specific anti-TT IgG ELISA. Using this experimental setting a moderate effect of the BS95TT fusion protein was observed (Fig. 3.31). It was not as pronounced as the effect achieved using BS9520 antibody. It is tentative to speculate that the low frequency of Ag-specific B-cells compared to normal activated B-cells is responsible for this limited effect. It is known that the activity of BS9520 to same extend depends on the density of the target cells (Herrmann et al., 2008). Activated cultures may require higher cell density to achieve more pronounced BS95TT-mediated killing of Ag-specific B-cells. Moreover, the ELISA assay used in this case should be ideally substituted with more sensitive B-cell depletion assays. Direct FACS- or ELISpot-based assays could be further developed for the direct detection and enumeration of specific antibody producing B-cells to further confirm the antigen specific activity of the TT fusion protein.

4.3 Outlook

In the first part of this work a recombinant bispecific CD95×CD20 antibody designated BS9520 was developed. Specific cytotoxicity of this molecule towards CD95-sensitive malignant B-cells and normal activated B-cells was shown to be superior to that achieved using parental monospecific CD20 antibodies, Fc-optimised versions thereof and the FDA-approved anti-CD20 antibody Rituximab *in vitro* and *in vivo*. Nevertheless, using this reagent for the treatment of B-cell malignancies could be limited due to resistance towards the CD95-mediated apoptosis often present in malignant cells. Overcoming this problem will probably need a combination therapy with sensitizing reagents enhancing the susceptibility of tumour cells towards apoptotic cell death. The selective targeting activity of BS9520 should be tested especially in combination with BCL-2 inhibitors, BH3 mimetics and conventional chemotherapeutics. In addition, it may be worth to try alternative anti-CD95 antibody sequences with proper folding as ScFv on the C-terminus of the bispecific antibody in FabSc format. In this case binding to CD20 could be significantly improved by placing the anti-CD20 antibody at the N-terminus of the FabSc molecule. The next step in the development of an optimized molecule will then be GMP-compliant production of the improved molecule.

In the second part of this work a concept for selective antigen specific B-cell suppression was developed and tested. Tetanus (TT) toxoid coupled to the CD95 antibody showed moderate suppression of tetanus specific antibody producing cells. Additional functional assays directly assessing the depletion of antigen-specific cells *in vitro* should be developed. After confirming the activity of the fusion protein using model antigens, a clinically relevant constructs might be developed containing known antigens involved in autoimmune diseases such as acetylcholine receptor (AChR) or desmoglein 3 inducing *Myasthenia gravis* and *Pemphigus vulgaris*, respectively.

Chapter 5

Bibliography

AARDA (2016). Autoimmune statistics. http://www.aarda.org/autoimmune-information/autoimmune-statistics/ (date of request: 05/2016).

Adachi, M., Suematsu, S., Kondo, T., Ogasawara, J., Tanaka, T., Yoshida, N., and Nagata, S. (1995). Targeted mutation in the Fas gene causes hyperplasia in peripheral lymphoid organs and liver. *Nature Genetics*, 11(3):294–300.

Aggarwal, B. B., Singh, S., LaPushin, R., and Totpal, K. (1995). Fas antigen signals proliferation of normal human diploid fibroblast and its mechanism is different from tumor necrosis factor receptor. *FEBS Lett*, 364(1):5–8.

Alderson, M. R., Armitage, R. J., Maraskovsky, E., Tough, T. W., Roux, E., Schooley, K., Ramsdell, F., and Lynch, D. H. (1993). Fas transduces activation signals in normal human T lymphocytes. *J Exp Med*, 178(6):2231–5.

American cancer society (2016). Childhood leukemia. http://www.cancer.org/cancer/leukemiainchildren/detailedguide/childhood-leukemia-how-classified (date of request: 05/2016).

Antibody Society (2015). Approved antibodies. http://www.antibodysociety.org/news/approved_mabs.php (date of request: 09/2015).

Arnold, J. N., Wormald, M. R., Sim, R. B., Rudd, P. M., and Dwek, R. A. (2007). The impact of glycosylation on the biological function and structure of human immunoglobulins. *Annu Rev Immunol*, 25:21–50.

Badros, A. Z., Goloubeva, O., Rapoport, A. P., Ratterree, B., Gahres, N., Meisenberg, B., Takebe, N., Heyman, M., Zwiebel, J., Streicher, H., Gocke, C. D., Tomic, D., Flaws, J. A., Zhang, B., and Fenton, R. G. (2005). Phase II study of G3139, a Bcl-2 antisense oligonucleotide, in combination with dexamethasone and thalidomide in relapsed multiple myeloma patients. *J Clin Oncol*, 23(18):4089–4099.

Bannas, P., Well, L., Lenz, A., Rissiek, B., Haag, F., Schmid, J., Hochgräfe, K., Trepel, M., Adam, G., Ittrich, H., and Koch-Nolte, F. (2014). In vivo near-infrared fluorescence targeting of T cells: comparison of nanobodies and conventional monoclonal antibodies. *Contrast Media Mol Imaging*, 9(2):135–142.

Bargou, R., Leo, E., Zugmaier, G., Klinger, M., Goebeler, M., Knop, S., Noppeney, R., Viardot, A., Hess, G., Schuler, M., Einsele, H., Brandl, C., Wolf, A., Kirchinger, P., Klappers, P., Schmidt, M., Riethmuller, G., Reinhardt, C., Baeuerle, P. A., and Kufer, P. (2008). Tumor regression in cancer patients by very low doses of a T cell-engaging antibody. *Science*, 321(5891):974–7.

Barnhart, B. C., Legembre, P., Pietras, E., Bubici, C., Franzoso, G., and Peter, M. E. (2004). CD95 ligand induces motility and invasiveness of apoptosis-resistant tumor cells. *EMBO J*, 23(15):3175–3185.

Bekeredjian-Ding, I., Foermer, S., Kirschning, C. J., Parcina, M., and Heeg, K. (2012). Pokeweed mitogen requires Toll-like receptor ligands for proliferative activity in human and murine B lymphocytes. *PLoS One*, 7(1):e29806.

Bergsbaken, T., Fink, S. L., and Cookson, B. T. (2009). Pyroptosis: host cell death and inflammation. *Nat Rev Microbiol*, 7(2):99–109.

Bhatt, V. R. and Vose, J. M. (2014). Hematopoietic stem cell transplantation for non-Hodgkin lymphoma. *Hematol Oncol Clin North Am*, 28(6):1073–1095.

Bimboim, H. and Doly, J. (1979). A rapid alkaline extraction procedure for screening recombinant plasmid DNA. *Nucleic acids research*, 7(6):1513–1523.

Boise, L. H., Minn, A. J., Noel, P. J., June, C. H., Accavitti, M. A., Lindsten, T., and Thompson, C. B. (1995). CD28 costimulation can promote T cell survival by enhancing the expression of Bcl-XL. *Immunity*, 3(1):87–98.

Bosma, G. C., Custer, R. P., and Bosma, M. J. (1983). A severe combined immunodeficiency mutation in the mouse. *Nature*, 301(5900):527–530.

Bossen, C. and Schneider, P. (2006). BAFF, APRIL and their receptors: structure, function and signaling. *Semin Immunol*, 18(5):263–275.

Brennan, M., Davison, P. F., and Paulus, H. (1985). Preparation of bispecific antibodies by chemical recombination of monoclonal immunoglobulin G1 fragments. *Science*, 229(4708):81–3.

Bubeník, J. (2003). Tumour MHC class I downregulation and immunotherapy (Review). *Oncol Rep*, 10(6):2005–2008.

Bullani, R. R., Wehrli, P., Viard-Leveugle, I., Rimoldi, D., Cerottini, J. C., Saurat, J. H., Tschopp, J., and French, L. E. (2002). Frequent downregulation of Fas (CD95) expression and function in melanoma. *Melanoma Res*, 12(3):263–70–.

Burnet, F. M. (1976). A modification of Jerne's theory of antibody production using the concept of clonal selection. *CA Cancer J Clin*, 26(2):119–21.

Cang, S., Mukhi, N., Wang, K., and Liu, D. (2012). Novel CD20 monoclonal antibodies for lymphoma therapy. *J Hematol Oncol*, 5:64.

Cao, Y. and Suresh, M. R. (1998). Bispecific antibodies as novel bioconjugates. *Bioconjug Chem*, 9(6):635–644.

Cascino, I., Papoff, G., De Maria, R., Testi, R., and Ruberti, G. (1996). Fas/Apo-1 (CD95) receptor lacking the intracytoplasmic signaling domain protects tumor cells from Fas-mediated apoptosis. *J Immunol*, 156(1):13–17.

Casulo, C., Vose, J. M., Ho, W. Y., Kahl, B., Brunvand, M., Goy, A., Kasamon, Y., Cheson, B., and Friedberg, J. W. (2014). A phase I study of PRO131921, a novel anti-CD20 monoclonal antibody in patients with relapsed/refractory CD20+ indolent NHL: correlation between clinical responses and AUC pharmacokinetics. *Clinical Immunology*, 154(1):37–46.

Chakravarty, R., Goel, S., Valdovinos, H. F., Hernandez, R., Hong, H., Nickles, R. J., and Cai, W. (2014). Matching the decay half-life with the biological half-life: ImmunoPET imaging with (44)Sc-labeled cetuximab Fab fragment. *Bioconjug Chem*, 25(12):2197–2204.

Cheng, J., Zhou, T., Liu, C., Shapiro, J. P., Brauer, M. J., Kiefer, M. C., Barr, P. J., and Mountz, J. D. (1994). Protection from Fas-mediated apoptosis by a soluble form of the Fas molecule. *Science*, 263(5154):1759–1762.

Chow, A. (2010). Cell cycle control by oncogenes and tumor suppressors: driving the transformation of normal cells into cancerous cells. *Nature Education*, 3(7).

Coiffier, B., Lepage, E., Briere, J., Herbrecht, R., Tilly, H., Bouabdallah, R., Morel, P., Van Den Neste, E., Salles, G., Gaulard, P., Reyes, F., Lederlin, P., and Gisselbrecht, C. (2002). Chop chemotherapy plus rituximab compared with chop alone in elderly patients with diffuse large-b-cell lymphoma. *N Engl J Med*, 346(4):235–242.

Coiffier, B., Lepretre, S., Pedersen, L. M., Gadeberg, O., Fredriksen, H., van Oers, M. H. J., Wooldridge, J., Kloczko, J., Holowiecki, J., Hellmann, A., Walewski, J., Flensburg, M., Petersen, J., and Robak, T. (2008). Safety and efficacy of ofatumumab, a fully human monoclonal anti-CD20 antibody, in patients with relapsed or refractory B-cell chronic lymphocytic leukemia: a phase 1-2 study. *Blood*, 111(3):1094–1100.

Cookson, B. T. and Brennan, M. A. (2001). Pro-inflammatory programmed cell death. *Trends Microbiol*, 9(3):113–114.

Creagh, E. M., Conroy, H., and Martin, S. J. (2003). Caspase-activation pathways in apoptosis and immunity. *Immunol Rev*, 193:10–21.

Cruse, J. and Lewis, R. (2010). *Atlas of Immunology, Third Edition*. CRC Press.

Daniel, P. T. and Krammer, P. H. (1994). Activation induces sensitivity toward APO-1 (CD95)-mediated apoptosis in human B cells. *J Immunol*, 152(12):5624–32.

Delbridge, A. R. D. and Strasser, A. (2015). The bcl-2 protein family, bh3-mimetics and cancer therapy. *Cell Death Differ*, 22(7):1071–1080.

Deo, Y. M., Sundarapandiyan, K., Keler, T., Wallace, P. K., and Graziano, R. F. (1998). Bispecific molecules directed to the Fc receptor for IgA (Fc alpha RI, CD89) and tumor antigens efficiently promote cell-mediated cytotoxicity of tumor targets in whole blood. *J Immunol*, 160(4):1677–1686.

Deveraux, Q. L., Roy, N., Stennicke, H. R., Van Arsdale, T., Zhou, Q., Srinivasula, S. M., Alnemri, E. S., Salvesen, G. S., and Reed, J. C. (1998). IAPs block apoptotic events induced by caspase-8 and cytochrome c by direct inhibition of distinct caspases. *EMBO J*, 17(8):2215–2223.

Ding, C., Xu, J., and Li, J. (2008). ABT-874, a fully human monoclonal anti-IL-12/IL-23 antibody for the potential treatment of autoimmune diseases. *Curr Opin Investig Drugs*, 9(5):515–522.

Dotan, E., Aggarwal, C., and Smith, M. R. (2010). Impact of Rituximab (Rituxan) on the Treatment of B-Cell Non-Hodgkin's Lymphoma. *P T*, 35(3):148–157.

Durben, M., Schmiedel, D., Hofmann, M., Vogt, F., Nübling, T., Pyz, E., Bühring, H.-J., Rammensee, H.-G., Salih, H. R., Große-Hovest, L., and Jung, G. (2015). Characterization of a bispecific FLT3 X CD3 antibody in an improved, recombinant format for the treatment of leukemia. *Mol Ther*, 23(4):648–655.

Ehrenschwender, M. and Wajant, H. (2009). The role of FasL and Fas in health and disease. *Adv Exp Med Biol*, 647:64–93.

Ellebrecht, C. T., Bhoj, V. G., Nace, A., Choi, E. J., Mao, X., Cho, M. J., Di Zenzo, G., Lanzavecchia, A., Seykora, J. T., Cotsarelis, G., Milone, M. C., and Payne, A. S. (2016). Reengineering chimeric antigen receptor t cells for targeted therapy of autoimmune disease. *Science*, 353(6295):179–184.

Emmons, C. and Hunsicker, L. G. (1987). Muromonab-CD3 (Orthoclone OKT3): the first monoclonal antibody approved for therapeutic use. *Iowa Med*, 77(2):78–82.

Ewert, S., Huber, T., Honegger, A., and Plückthun, A. (2003). Biophysical properties of human antibody variable domains. *J Mol Biol*, 325(3):531–553.

Fadok, V. A., Voelker, D. R., Campbell, P. A., Cohen, J. J., Bratton, D. L., and Henson, P. M. (1992). Exposure of phosphatidylserine on the surface of apoptotic lymphocytes triggers specific recognition and removal by macrophages. *J Immunol*, 148(7):2207–2216.

Fanger, M. W., Morganelli, P. M., and Guyre, P. M. (1992). Bispecific antibodies. *Crit Rev Immunol*, 12(3-4):101–124.

Favaloro, B., Allocati, N., Graziano, V., Di Ilio, C., and De Laurenzi, V. (2012). Role of apoptosis in disease. *Aging (Albany NY)*, 4(5):330–349.

Feldmann, M. (2002). Development of anti-TNF therapy for rheumatoid arthritis. *Nat Rev Immunol*, 2(5):364–371.

Figgett, W. A., Fairfax, K., Vincent, F. B., Le Page, M. A., Katik, I., Deliyanti, D., Quah, P. S., Verma, P., Grumont, R., Gerondakis, S., Hertzog, P., O'Reilly, L. A., Strasser, A., and Mackay, F. (2013). The TACI receptor regulates T-cell-independent marginal zone B cell responses through innate activation-induced cell death. *Immunity*, 39(3):573–583.

Figueiredo, D., Turcotte, C., Frankel, G., Li, Y., Dolly, O., Wilkin, G., Marriott, D., Fairweather, N., and Dougan, G. (1995). Characterization of recombinant tetanus toxin derivatives suitable for vaccine development. *Infection and immunity*, 63(8):3218–3221.

Fink, S. L. and Cookson, B. T. (2005). Apoptosis, pyroptosis, and necrosis: mechanistic description of dead and dying eukaryotic cells. *Infect Immun*, 73(4):1907–1916.

Fogh, J., Wright, W. C., and Loveless, J. D. (1977). Absence of HeLa cell contamination in 169 cell lines derived from human tumors. *Journal of the National Cancer Institute*, 58(2):209–214.

Freise, A. C. and Wu, A. M. (2015). In vivo imaging with antibodies and engineered fragments. *Mol Immunol*, 67(2 Pt A):142–152.

French, L. E., Hahne, M., Viard, I., Radlgruber, G., Zanone, R., Becker, K., Muller, C., and Tschopp, J. (1996). Fas and Fas ligand in embryos and adult mice: ligand expression in several immune-privileged tissues and coexpression in adult tissues characterized by apoptotic cell turnover. *J Cell Biol*, 133(2):335–43.

Fulda, S. (2009). Tumor resistance to apoptosis. *Int J Cancer*, 124(3):511–515.

Ganjoo, K. N., de Vos, S., Pohlman, B. L., Flinn, I. W., Forero-Torres, A., Enas, N. H., Cronier, D. M., Dang, N. H., Foon, K. A., Carpenter, S. P., et al. (2015). Phase 1/2 Study of Ocaratuzumab, an Fc-Engineered Humanized Anti-CD20 Monoclonal Antibody, in Low-Affinity FcγRIIIa Patients with Previously Treated Follicular Lymphoma. *Leukemia & lymphoma*, 56(1):42–48.

Garg, A. D., Nowis, D., Golab, J., Vandenabeele, P., Krysko, D. V., and Agostinis, P. (2010). Immunogenic cell death, DAMPs and anticancer therapeutics: an emerging amalgamation. *Biochim Biophys Acta*, 1805(1):53–71.

Giannini, G., Rappuoli, R., and Ratti, G. (1984). The amino-acid sequence of two non-toxic mutants of diphtheria toxin: CRM45 and CRM197. *Nucleic Acids Res*, 12(10):4063–4069.

Goede, V., Fischer, K., Busch, R., Engelke, A., Eichhorst, B., Wendtner, C. M., Chagorova, T., de la Serna, J., Dilhuydy, M.-S., Illmer, T., et al. (2014). Obinutuzumab plus chlorambucil in patients with cll and coexisting conditions. *New England Journal of Medicine*, 370(12):1101–1110.

Goede, V., Fischer, K., Engelke, A., Schlag, R., Lepretre, S., Montero, L. F. C., Montillo, M., Fegan, C., Asikanius, E., Humphrey, K., Fingerle-Rowson, G., and Hallek, M. (2015). Obinutuzumab as frontline treatment of chronic lymphocytic leukemia: updated results of the cll11 study. *Leukemia*, 29(7):1602–1604.

Goldenberg, D. M., Morschhauser, F., and Wegener, W. A. (2010). Veltuzumab (humanized anti-CD20 monoclonal antibody): characterization, current clinical results, and future prospects. *Leuk Lymphoma*, 51(5):747–755.

Goldsby, R. A. (2003). *Immunology*. W.H. Freeman, New York, 5th edition.

Grosse-Hovest, L., Hartlapp, I., Marwan, W., Brem, G., Rammensee, H.-G., and Jung, G. (2003). A recombinant bispecific single-chain antibody induces targeted, supra-agonistic CD28-stimulation and tumor cell killing. *Eur J Immunol*, 33(5):1334–1340.

Grosse-Hovest, L., Wick, W., Minoia, R., Weller, M., Rammensee, H.-G., Brem, G., and Jung, G. (2005). Supraagonistic, bispecific single-chain antibody purified from the serum of cloned, transgenic cows induces T-cell-mediated killing of glioblastoma cells in vitro and in vivo. *Int J Cancer*, 117(6):1060–1064.

Guerard, E. J. and Bishop, M. R. (2012). Overview of non-Hodgkin's lymphoma. *Dis Mon*, 58(4):208–218.

Hahne, M., Rimoldi, D., Schröter, M., Romero, P., Schreier, M., French, L. E., Schneider, P., Bornand, T., Fontana, A., Lienard, D., Cerottini, J., and Tschopp, J. (1996). Melanoma cell expression of Fas(Apo-1/CD95) ligand: implications for tumor immune escape. *Science*, 274(5291):1363–1366.

Halliley, J. L., Tipton, C. M., Liesveld, J., Rosenberg, A. F., Darce, J., Gregoretti, I. V., Popova, L., Kaminiski, D., Fucile, C. F., Albizua, I., Kyu, S., Chiang, K.-Y., Bradley, K. T., Burack, R., Slifka, M., Hammarlund, E., Wu, H., Zhao, L., Walsh, E. E., Falsey, A. R., Randall, T. D., Cheung, W. C., Sanz, I., and Lee, F. E.-H. (2015). Long-Lived Plasma Cells Are Contained within the CD19(-)CD38(hi)CD138(+) Subset in Human Bone Marrow. *Immunity*, 43(1):132–145.

Hammond, C. L., Marchan, R., Krance, S. M., and Ballatori, N. (2007). Glutathione export during apoptosis requires functional multidrug resistance-associated proteins. *J Biol Chem*, 282(19):14337–14347.

Hanahan, D. and Weinberg, R. A. (2011). Hallmarks of cancer: the next generation. *Cell*, 144(5):646–674.

Harris, N. L., Jaffe, E. S., Diebold, J., Flandrin, G., Muller-Hermelink, H. K., Vardiman, J., Lister, T. A., and Bloomfield, C. D. (2000). The World Health Organization classification of hematological malignancies report of the Clinical Advisory Committee Meeting, Airlie House, Virginia, November 1997. *Mod Pathol*, 13(2):193–207.

Hashimoto, G., Wright, P. F., and Karzon, D. T. (1983). Antibody-dependent cell-mediated cytotoxicity against influenza virus-infected cells. *J Infect Dis*, 148(5):785–794.

Hendriks, R. W., Yuvaraj, S., and Kil, L. P. (2014). Targeting Bruton's tyrosine kinase in B cell malignancies. *Nat Rev Cancer*, 14(4):219–232.

Herbst, R., Wang, Y., Gallagher, S., Mittereder, N., Kuta, E., Damschroder, M., Woods, R., Rowe, D. C., Cheng, L., Cook, K., Evans, K., Sims, G. P., Pfarr, D. S., Bowen, M. A., Dall'Acqua, W., Dall'Aqua, W., Shlomchik, M., Tedder, T. F.,

Kiener, P., Jallal, B., Wu, H., and Coyle, A. J. (2010). B-cell depletion in vitro and in vivo with an afucosylated anti-CD19 antibody. *J Pharmacol Exp Ther*, 335(1):213–222.

Herrmann, T., Grosse-Hovest, L., Otz, T., Krammer, P. H., Rammensee, H. G., and Jung, G. (2008). Construction of optimized bispecific antibodies for selective activation of the death receptor CD95. *Cancer Res*, 68(4):1221–7.

Horino, K., Nishiura, H., Ohsako, T., Shibuya, Y., Hiraoka, T., Kitamura, N., and Yamamoto, T. (1998). A monocyte chemotactic factor, S19 ribosomal protein dimer, in phagocytic clearance of apoptotic cells. *Lab Invest*, 78(5):603–617.

Hust, M., Jostock, T., Menzel, C., Voedisch, B., Mohr, A., Brenneis, M., Kirsch, M. I., Meier, D., and Dübel, S. (2007). Single chain Fab (scFab) fragment. *BMC Biotechnol*, 7:14.

Huston, J. S. and George, A. J. (2001). Engineered antibodies take center stage. *Hum Antibodies*, 10(3-4):127–42.

Inaba, H., Komada, Y., Li, Q. S., Zhang, X. L., Tanaka, S., Azuma, E., Yamamoto, H., and Sakurai, M. (1999). mRNA expression of variant Fas molecules in acute leukemia cells. *Am J Hematol*, 62(3):150–158.

Irmler, M., Thome, M., Hahne, M., Schneider, P., Hofmann, K., Steiner, V., Bodmer, J. L., Schröter, M., Burns, K., Mattmann, C., Rimoldi, D., French, L. E., and Tschopp, J. (1997). Inhibition of death receptor signals by cellular FLIP. *Nature*, 388(6638):190–195.

Itoh, N., Tsujimoto, Y., and Nagata, S. (1993). Effect of bcl-2 on Fas antigen-mediated cell death. *J Immunol*, 151(2):621–627.

Itoh, N., Yonehara, S., Ishii, A., Yonehara, M., Mizushima, S., Sameshima, M., Hase, A., Seto, Y., and Nagata, S. (1991). The polypeptide encoded by the cDNA for human cell surface antigen Fas can mediate apoptosis. *Cell*, 66(2):233–43–.

Jeong, K. J., Jang, S. H., and Velmurugan, N. (2011). Recombinant antibodies: engineering and production in yeast and bacterial hosts. *Biotechnol J*, 6(1):16–27.

Jones, J. D., Hamilton, B. J., and Rigby, W. F. C. (2012). Rituximab mediates loss of cd19 on b cells in the absence of cell death. *Arthritis Rheum*, 64(10):3111–3118.

Jung, G., Freimann, U., Von Marschall, Z., Reisfeld, R. A., and Wilmanns, W. (1991). Target cell-induced T cell activation with bi- and trispecific antibody fragments. *Eur J Immunol*, 21(10):2431–5.

Jung, G., Grosse-Hovest, L., Krammer, P. H., and Rammensee, H. G. (2001). Target cell-restricted triggering of the CD95 (APO-1/Fas) death receptor with bispecific antibody fragments. *Cancer Res*, 61(5):1846–8.

Kabelitz, D. and Janssen, O. (1997). Antigen-induced death of T-lymphocytes. *Front Biosci*, 2:d61–d77.

Kaczmarek, A., Vandenabeele, P., and Krysko, D. V. (2013). Necroptosis: the release of damage-associated molecular patterns and its physiological relevance. *Immunity*, 38(2):209–223.

Kappos, L., Bates, D., Hartung, H.-P., Havrdova, E., Miller, D., Polman, C. H., Ravnborg, M., Hauser, S. L., Rudick, R. A., Weiner, H. L., O'Connor, P. W., King, J., Radue, E. W., Yousry, T., Major, E. O., and Clifford, D. B. (2007). Natalizumab treatment for multiple sclerosis: recommendations for patient selection and monitoring. *Lancet Neurol*, 6(5):431–441.

Kaveri, S. V., Mouthon, L., and Bayry, J. (2010). Basophils and nephritis in lupus. *N Engl J Med*, 363(11):1080–1082.

Kawai, T. and Akira, S. (2007). TLR signaling. *Semin Immunol*, 19(1):24–32.

Keightley, R. G., Cooper, M. D., and Lawton, A. R. (1976). The T cell dependence of B cell differentiation induced by pokeweed mitogen. *J Immunol*, 117(5 Pt 1):1538–1544.

Kiener, P. A., Davis, P. M., Starling, G. C., Mehlin, C., Klebanoff, S. J., Ledbetter, J. A., and Liles, W. C. (1997). Differential induction of apoptosis by fas-fas ligand interactions in human monocytes and macrophages. *J Exp Med*, 185(8):1511–1516.

Kim, H.-Y., Wang, X., Wahlberg, B., and Edwards, W. B. (2014). Discovery of hapten-specific scFv from a phage display library and applications for HER2-positive tumor imaging. *Bioconjug Chem*, 25(7):1311–1322.

Kirkwood, J. (2002). Cancer immunotherapy: the interferon-alpha experience. *Semin Oncol*, 29(3 Suppl 7):18–26.

Klein, E., Klein, G., Nadkarni, J. S., Nadkarni, J. J., Wigzell, H., and Clifford, P. (1968). Surface IgM-kappa specificity on a Burkitt lymphoma cell in vivo and in derived culture lines. *Cancer Research*, 28(7):1300–1310.

Kleppe, K., Ohtsuka, E., Kleppe, R., Molineux, I., and Khorana, H. (1971). Studies on polynucleotides: XCVI. Repair replication of short synthetic DNA's as catalyzed by DNA polymerases. *Journal of molecular biology*, 56(2):341–361.

Knipping, E., Debatin, K. M., Stricker, K., Heilig, B., Eder, A., and Krammer, P. H. (1995). Identification of soluble APO-1 in supernatants of human B- and T-cell lines and increased serum levels in B- and T-cell leukemias. *Blood*, 85(6):1562–1569.

Köhler, G. and Milstein, C. (1975). Continuous cultures of fused cells secreting antibody of predefined specificity. *Nature*, 256(5517):495–7.

Kontermann, R. E. (2012). Dual targeting strategies with bispecific antibodies. *MAbs*, 4(2):182–197.

Kowalewski, D. J., Schuster, H., Backert, L., Berlin, C., Kahn, S., Kanz, L., Salih, H. R., Rammensee, H.-G., Stevanovic, S., and Stickel, J. S. (2015). HLA ligandome analysis identifies the underlying specificities of spontaneous antileukemia immune

responses in chronic lymphocytic leukemia (CLL). *Proc Natl Acad Sci U S A*, 112(2):E166–E175.

Krammer, P. H., Arnold, R., and Lavrik, I. N. (2007). Life and death in peripheral T cells. *Nat Rev Immunol*, 7(7):532–42–.

Krauss, J. C., PooH., Xue, W., Mayo-Bond, L., Todd, 3rd, R., and Petty, H. R. (1994). Reconstitution of antibody-dependent phagocytosis in fibroblasts expressing Fc gamma receptor IIIB and the complement receptor type 3. *J Immunol*, 153(4):1769–1777.

Kufer, T. A. and Sansonetti, P. J. (2007). Sensing of bacteria: NOD a lonely job. *Curr Opin Microbiol*, 10(1):62–69.

Lalaoui, N., Lindqvist, L. M., Sandow, J. J., and Ekert, P. G. (2015). The molecular relationships between apoptosis, autophagy and necroptosis. *Semin Cell Dev Biol*, 39:63–69.

Lauber, K., Bohn, E., Kröber, S. M., Xiao, Y.-j., Blumenthal, S. G., Lindemann, R. K., Marini, P., Wiedig, C., Zobywalski, A., Baksh, S., Xu, Y., Autenrieth, I. B., Schulze-Osthoff, K., Belka, C., Stuhler, G., and Wesselborg, S. (2003). Apoptotic cells induce migration of phagocytes via caspase-3-mediated release of a lipid attraction signal. *Cell*, 113(6):717–730.

Lawrence, M. S., Stojanov, P., Polak, P., Kryukov, G. V., Cibulskis, K., Sivachenko, A., Carter, S. L., Stewart, C., Mermel, C. H., Roberts, S. A., Kiezun, A., Hammerman, P. S., McKenna, A., Drier, Y., Zou, L., Ramos, A. H., Pugh, T. J., Stransky, N., Helman, E., Kim, J., Sougnez, C., Ambrogio, L., Nickerson, E., Shefler, E., Cortés, M. L., Auclair, D., Saksena, G., Voet, D., Noble, M., DiCara, D., Lin, P., Lichtenstein, L., Heiman, D. I., Fennell, T., Imielinski, M., Hernandez, B., Hodis, E., Baca, S., Dulak, A. M., Lohr, J., Landau, D.-A., Wu, C. J., Melendez-Zajgla, J., Hidalgo-Miranda, A., Koren, A., McCarroll, S. A., Mora, J., Lee, R. S., Crompton, B., Onofrio, R., Parkin, M., Winckler, W., Ardlie, K., Gabriel, S. B., Roberts, C. W. M., Biegel, J. A., Stegmaier, K., Bass, A. J., Garraway, L. A., Meyerson, M., Golub, T. R., Gordenin, D. A., Sunyaev, S., Lander, E. S., and Getz, G. (2013). Mutational heterogeneity in cancer and the search for new cancer-associated genes. *Nature*, 499(7457):214–218.

Lazar, G. A., Dang, W., Karki, S., Vafa, O., Peng, J. S., Hyun, L., Chan, C., Chung, H. S., Eivazi, A., Yoder, S. C., Vielmetter, J., Carmichael, D. F., Hayes, R. J., and Dahiyat, B. I. (2006). Engineered antibody Fc variants with enhanced effector function. *Proc Natl Acad Sci U S A*, 103(11):4005–4010.

Leadbetter, E. A., Rifkin, I. R., Hohlbaum, A. M., Beaudette, B. C., Shlomchik, M. J., and Marshak-Rothstein, A. (2002). Chromatin-IgG complexes activate B cells by dual engagement of IgM and Toll-like receptors. *Nature*, 416(6881):603–7.

Leithauser, F., Dhein, J., Mechtersheimer, G., Koretz, K., Bruderlein, S., Henne, C., Schmidt, A., Debatin, K. M., Krammer, P. H., and Moller, P. (1993). Constitutive and induced expression of APO-1, a new member of the nerve growth

factor/tumor necrosis factor receptor superfamily, in normal and neoplastic cells. *Lab Invest*, 69(4):415–29.

Lühder, F., Huang, Y., Dennehy, K. M., Guntermann, C., Müller, I., Winkler, E., Kerkau, T., Ikemizu, S., Davis, S. J., Hanke, T., and Hünig, T. (2003). Topological requirements and signaling properties of T cell-activating, anti-CD28 antibody superagonists. *J Exp Med*, 197(8):955–966.

Li, Y. R., Zhao, S. D., Li, J., Bradfield, J. P., Mohebnasab, M., Steel, L., Kobie, J., Abrams, D. J., Mentch, F. D., Glessner, J. T., Guo, Y., Wei, Z., Connolly, J. J., Cardinale, C. J., Bakay, M., Li, D., Maggadottir, S. M., Thomas, K. A., Qui, H., Chiavacci, R. M., Kim, C. E., Wang, F., Snyder, J., Flatø, B., Førre, Ø., Denson, L. A., Thompson, S. D., Becker, M. L., Guthery, S. L., Latiano, A., Perez, E., Resnick, E., Strisciuglio, C., Staiano, A., Miele, E., Silverberg, M. S., Lie, B. A., Punaro, M., Russell, R. K., Wilson, D. C., Dubinsky, M. C., Monos, D. S., Annese, V., Munro, J. E., Wise, C., Chapel, H., Cunningham-Rundles, C., Orange, J. S., Behrens, E. M., Sullivan, K. E., Kugathasan, S., Griffiths, A. M., Satsangi, J., Grant, S. F. A., Sleiman, P. M. A., Finkel, T. H., Polychronakos, C., Baldassano, R. N., Luning Prak, E. T., Ellis, J. A., Li, H., Keating, B. J., and Hakonarson, H. (2015). Genetic sharing and heritability of paediatric age of onset autoimmune diseases. *Nat Commun*, 6:8442.

Lim, S. H. and Levy, R. (2014). Translational medicine in action: anti-CD20 therapy in lymphoma. *J Immunol*, 193(4):1519–1524.

Lin, N.-Y., Beyer, C., Giessl, A., Kireva, T., Scholtysek, C., Uderhardt, S., Munoz, L. E., Dees, C., Distler, A., Wirtz, S., Krönke, G., Spencer, B., Distler, O., Schett, G., and Distler, J. H. W. (2013). Autophagy regulates TNFα-mediated joint destruction in experimental arthritis. *Ann Rheum Dis*, 72(5):761–768.

Liu, Z., Gunasekaran, K., Wang, W., Razinkov, V., Sekirov, L., Leng, E., Sweet, H., Foltz, I., Howard, M., Rousseau, A.-M., Kozlosky, C., Fanslow, W., and Yan, W. (2014). Asymmetrical Fc engineering greatly enhances antibody-dependent cellular cytotoxicity (ADCC) effector function and stability of the modified antibodies. *J Biol Chem*, 289(6):3571–3590.

Ljunggren, H.-G. and Malmberg, K.-J. (2007). Prospects for the use of NK cells in immunotherapy of human cancer. *Nat Rev Immunol*, 7(5):329–339.

Lonberg, N., Taylor, L. D., Harding, F. A., Trounstine, M., Higgins, K. M., Schramm, S. R., Kuo, C. C., Mashayekh, R., Wymore, K., and McCabe, J. G. (1994). Antigen-specific human antibodies from mice comprising four distinct genetic modifications. *Nature*, 368(6474):856–859.

Lum, L. G. and Culbertson, N. J. (1985). The induction and suppression of in vitro IgG anti-tetanus toxoid antibody synthesis by human lymphocytes stimulated with tetanus toxoid in the absence of in vivo booster immunizations. *J Immunol*, 135(1):185–191.

Lütje, S., Franssen, G. M., Sharkey, R. M., Laverman, P., Rossi, E. A., Goldenberg, D. M., Oyen, W. J. G., Boerman, O. C., and McBride, W. J. (2014). Anti-CEA antibody fragments labeled with [(18)F]AlF for PET imaging of CEA-expressing tumors. *Bioconjug Chem*, 25(2):335–341.

Major, E. O. (2010). Progressive multifocal leukoencephalopathy in patients on immunomodulatory therapies. *Annu Rev Med*, 61:35–47.

Martin, S. J., Henry, C. M., and Cullen, S. P. (2012). A perspective on mammalian caspases as positive and negative regulators of inflammation. *Mol Cell*, 46(4):387–397.

Martin, S. J., Reutelingsperger, C. P., McGahon, A. J., Rader, J. A., van Schie, R. C., LaFace, D. M., and Green, D. R. (1995). Early redistribution of plasma membrane phosphatidylserine is a general feature of apoptosis regardless of the initiating stimulus: inhibition by overexpression of Bcl-2 and Abl. *J Exp Med*, 182(5):1545–1556.

Martin-Villalba, A., Llorens-Bobadilla, E., and Wollny, D. (2013). CD95 in cancer: tool or target? *Trends Mol Med*, 19(6):329–335.

Matzinger, P. (2002). The danger model: a renewed sense of self. *Science*, 296(5566):301–305.

McCafferty, J., Griffiths, A. D., Winter, G., and Chiswell, D. J. (1990). Phage antibodies: filamentous phage displaying antibody variable domains. *Nature*, 348(6301):552–554.

Medina, F., Segundo, C., Rodríguez, C., and Brieva, J. A. (1997). Regulatory role of CD95 ligation on human B cells induced in vivo capable of spontaneous and high-rate Ig secretion. *Eur J Immunol*, 27(3):700–706.

Mendez, M. J., Green, L. L., Corvalan, J. R., Jia, X. C., Maynard-Currie, C. E., Yang, X. D., Gallo, M. L., Louie, D. M., Lee, D. V., Erickson, K. L., Luna, J., Roy, C. M., Abderrahim, H., Kirschenbaum, F., Noguchi, M., Smith, D. H., Fukushima, A., Hales, J. F., Klapholz, S., Finer, M. H., Davis, C. G., Zsebo, K. M., and Jakobovits, A. (1997). Functional transplant of megabase human immunoglobulin loci recapitulates human antibody response in mice. *Nat Genet*, 15(2):146–156.

Midis, G. P., Shen, Y., and Owen-Schaub, L. B. (1996). Elevated soluble Fas (sFas) levels in nonhematopoietic human malignancy. *Cancer Res*, 56(17):3870–3874.

Milstein, C. and Cuello, A. C. (1983). Hybrid hybridomas and their use in immunohistochemistry. *Nature*, 305(5934):537–40.

Mishima, Y., Terui, Y., Yokoyama, M., Nishimura, N., Sakajiri, S., Ueda, K., Kuboki, Y., Nakano, K., Suzuki, K., Nara, E., Tsuyama, N., Takeuchi, K., Oguchi, M., and Hatake, K. (2012). R-chop with dose-attenuated radiation therapy could induce good prognosis in gastric diffuse large b cell lymphoma. *Exp Hematol Oncol*, 1(1):30.

Morschhauser, F., Marlton, P., Vitolo, U., Lindén, O., Seymour, J. F., Crump, M., Coiffier, B., Foà, R., Wassner, E., Burger, H.-U., Brennan, B., and Mendila, M. (2010). Results of a phase I/II study of ocrelizumab, a fully humanized anti-CD20 mAb, in patients with relapsed/refractory follicular lymphoma. *Ann Oncol*, 21(9):1870–1876.

Mullis, K. B. and Faloona, F. A. (1987). Specific synthesis of DNA in vitro via a polymerase-catalyzed chain reaction. *Methods in enzymology*, 155:335.

Nagata, S. (1999). Fas ligand-induced apoptosis. *Annu Rev Genet*, 33:29–55.

Nicholson, D. W. (1999). Caspase structure, proteolytic substrates, and function during apoptotic cell death. *Cell Death Differ*, 6(11):1028–1042.

Nikolaev, A., McLaughlin, T., O'Leary, D. D. M., and Tessier-Lavigne, M. (2009). APP binds DR6 to trigger axon pruning and neuron death via distinct caspases. *Nature*, 457(7232):981–989.

Nisonoff, A. and Mandy, W. J. (1962). Quantitative estimation of the hybridization of rabbit antibodies. *Nature*, 194:355–9.

Ober, R. J., Radu, C. G., Ghetie, V., and Ward, E. S. (2001). Differences in promiscuity for antibody-FcRn interactions across species: implications for therapeutic antibodies. *Int Immunol*, 13(12):1551–1559.

O'Brien, S. M., Cunningham, C. C., Golenkov, A. K., Turkina, A. G., Novick, S. C., and Rai, K. R. (2005). Phase I to II multicenter study of oblimersen sodium, a Bcl-2 antisense oligonucleotide, in patients with advanced chronic lymphocytic leukemia. *J Clin Oncol*, 23(30):7697–7702.

O'Donnell, J. A., Kennedy, C. L., Pellegrini, M., Nowell, C. J., Zhang, J.-G., O'Reilly, L. A., Cengia, L., Dias, S., Masters, S. L., Hartland, E. L., Roberts, A. W., Gerlic, M., and Croker, B. A. (2015). Fas regulates neutrophil lifespan during viral and bacterial infection. *J Leukoc Biol*, 97(2):321–326.

Oehm, A., Behrmann, I., Falk, W., Pawlita, M., Maier, G., Klas, C., Li-Weber, M., Richards, S., Dhein, J., Trauth, B. C., and et al. (1992). Purification and molecular cloning of the APO-1 cell surface antigen, a member of the tumor necrosis factor/nerve growth factor receptor superfamily. Sequence identity with the Fas antigen. *J Biol Chem*, 267(15):10709–15.

Ogasawara, A., Tinianow, J. N., Vanderbilt, A. N., Gill, H. S., Yee, S., Flores, J. E., Williams, S.-P., Ashkenazi, A., and Marik, J. (2013). ImmunoPET imaging of phosphatidylserine in pro-apoptotic therapy treated tumor models. *Nucl Med Biol*, 40(1):15–22.

Ogasawara, J., Watanabe-Fukunaga, R., Adachi, M., Matsuzawa, A., Kasugai, T., Kitamura, Y., Itoh, N., Suda, T., and Nagata, S. (1993). Lethal effect of the anti-Fas antibody in mice. *Nature*, 364(6440):806–9.

Papoff, G., Cascino, I., Eramo, A., Starace, G., Lynch, D. H., and Ruberti, G. (1996). An N-terminal domain shared by Fas/Apo-1 (CD95) soluble variants prevents cell death in vitro. *J Immunol*, 156(12):4622–4630.

Patel, A. S., Lin, L., Geyer, A., Haspel, J. A., An, C. H., Cao, J., Rosas, I. O., and Morse, D. (2012). Autophagy in idiopathic pulmonary fibrosis. *PLoS One*, 7(7):e41394.

Peracchio, C., Alabiso, O., Valente, G., and Isidoro, C. (2012). Involvement of autophagy in ovarian cancer: a working hypothesis. *J Ovarian Res*, 5(1):22.

Perchiacca, J. M. and Tessier, P. M. (2012). Engineering aggregation-resistant antibodies. *Annu Rev Chem Biomol Eng*, 3:263–286.

Perera, L. P. and Waldmann, T. A. (1998). Activation of human monocytes induces differential resistance to apoptosis with rapid down regulation of caspase-8/flice. *Proc Natl Acad Sci U S A*, 95(24):14308–14313.

Perlman, H., Pagliari, L. J., Georganas, C., Mano, T., Walsh, K., and Pope, R. M. (1999). Flice-inhibitory protein expression during macrophage differentiation confers resistance to fas-mediated apoptosis. *J Exp Med*, 190(11):1679–1688.

Peter, M. E., Budd, R. C., Desbarats, J., Hedrick, S. M., Hueber, A.-O., Newell, M. K., Owen, L. B., Pope, R. M., Tschopp, J., Wajant, H., Wallach, D., Wiltrout, R. H., Zörnig, M., and Lynch, D. H. (2007). The CD95 receptor: apoptosis revisited. *Cell*, 129(3):447–450.

Peter, M. E. and Krammer, P. H. (2003). The CD95(APO-1/Fas) DISC and beyond. *Cell Death Differ*, 10(1):26–35.

Plumas, J., Jacob, M. C., Chaperot, L., Molens, J. P., Sotto, J. J., and Bensa, J. C. (1998). Tumor B cells from non-Hodgkin's lymphoma are resistant to CD95 (Fas/Apo-1)-mediated apoptosis. *Blood*, 91(8):2875–2885.

Porter, D. L., Levine, B. L., Kalos, M., Bagg, A., and June, C. H. (2011). Chimeric antigen receptor-modified T cells in chronic lymphoid leukemia. *N Engl J Med*, 365(8):725–733.

Pulvertaft, R. (1964). Cytology of Burkitt's tumour (African lymphoma). *The Lancet*, 283(7327):238–240.

Rammensee, H. G., Julius, M. H., Nemazee, D., Langhorne, J., Lamers, R., and Köhler, G. (1987). Targeting cytotoxic t cells to antigen-specific b lymphocytes. *Eur J Immunol*, 17(3):433–436.

Ramos, C. A., Savoldo, B., and Dotti, G. (2014). CD19-CAR trials. *Cancer J*, 20(2):112–118.

Ramos-Casals, M., Sanz, I., Bosch, X., Stone, J. H., and Khamashta, M. A. (2012). B-cell-depleting therapy in systemic lupus erythematosus. *The American journal of medicine*, 125(4):327–336.

Rieux-Laucat, F., Le Deist, F., and Fischer, A. (2003). Autoimmune lymphoproliferative syndromes: genetic defects of apoptosis pathways. *Cell Death Differ*, 10(1):124–33.

Roederer, M. (2001). Spectral compensation for flow cytometry: visualization artifacts, limitations, and caveats. *Cytometry*, 45(3):194–205.

Romaniuk, S., Kolybo, D., and Komisarenko, S. (2012). Recombinant diphtheria toxin derivatives: Perspectives of application. *Russian Journal of Bioorganic Chemistry*, 38(6):565–577.

Roopenian, D. C. and Akilesh, S. (2007). FcRn: the neonatal Fc receptor comes of age. *Nat Rev Immunol*, 7(9):715–725.

Rosman, Z., Shoenfeld, Y., and Zandman-Goddard, G. (2013). Biologic therapy for autoimmune diseases: an update. *BMC Med*, 11:88.

Ross, G. D. (1989). Complement and complement receptors. *Curr Opin Immunol*, 2(1):50–62.

Russell, J. H. and Ley, T. J. (2002). Lymphocyte-mediated cytotoxicity. *Annu Rev Immunol*, 20:323–370.

Saiki, O. and Ralph, P. (1983). Clonal differences in response to T cell replacing factor (TRF) for IgM secretion and TRF receptors in a human B lymphoblast cell line. *European journal of immunology*, 13(1):31–34.

Sanders, J., Miguel, R. N., Furmaniak, J., and Smith, B. R. (2010). TSH receptor monoclonal antibodies with agonist, antagonist, and inverse agonist activities. *Methods Enzymol*, 485:393–420.

Sanjuan-Pla, A., Bueno, C., Prieto, C., Acha, P., Stam, R. W., Marschalek, R., and Menéndez, P. (2015). Revisiting the biology of infant t(4;11)/MLL-AF4+ B-cell acute lymphoblastic leukemia. *Blood*, 126(25):2676–2685.

Savill, J. and Fadok, V. (2000). Corpse clearance defines the meaning of cell death. *Nature*, 407(6805):784–788.

Sazinsky, S. L., Ott, R. G., Silver, N. W., Tidor, B., Ravetch, J. V., and Wittrup, K. D. (2008). Aglycosylated immunoglobulin G1 variants productively engage activating Fc receptors. *Proc Natl Acad Sci U S A*, 105(51):20167–20172.

Schlossman, S. F. (1995). *Leucocyte typing V: White cell differentiation antigens: Proceedings of the Fifth International Workshop and Conference, Held in Boston, USA 3-7 November, 1993*. Oxford University Press, Oxford.

Schneider, U., Schwenk, H., and Bornkamm, G. (1977). Characterization of EBV-genome negative "null" and "T" cell lines derived from children with acute lymphoblastic leukemia and leukemic transformed non-Hodgkin lymphoma. *Int J Cancer*, 19(5)(0020-7136 (Linking)):621–626.

Sensi, M. and Anichini, A. (2006). Unique tumor antigens: evidence for immune control of genome integrity and immunogenic targets for T cell-mediated patient-specific immunotherapy. *Clin Cancer Res*, 12(17):5023–5032.

Shin, M. S., Park, W. S., Kim, S. Y., Kim, H. S., Kang, S. J., Song, K. Y., Park, J. Y., Dong, S. M., Pi, J. H., Oh, R. R., Lee, J. Y., Yoo, N. J., and Lee, S. H. (1999). Alterations of Fas (Apo-1/CD95) gene in cutaneous malignant melanoma. *Am J Pathol*, 154(6):1785–1791.

Shulman, M., Wilde, C., and Köhler, G. (1978). A better cell line for making hybridomas secreting specific antibodies. *Nature*, 276:269–270.

Sjöwall, C., Zapf, J., von Löhneysen, S., Magorivska, I., Biermann, M., Janko, C., Winkler, S., Bilyy, R., Schett, G., Herrmann, M., and Muñoz, L. E. (2015). Altered glycosylation of complexed native IgG molecules is associated with disease activity of systemic lupus erythematosus. *Lupus*, 24(6):569–581.

SK Mohanty, K Sai Leela, P. V. K. R. (2008). *TB of Immunology*. Jaypee Brothers.

Spisek, R. and Dhodapkar, M. V. (2007). Towards a better way to die with chemotherapy: role of heat shock protein exposure on dying tumor cells. *Cell Cycle*, 6(16):1962–1965.

Stein, R., Qu, Z., Chen, S., Rosario, A., Shi, V., Hayes, M., Horak, I. D., Hansen, H. J., and Goldenberg, D. M. (2004). Characterization of a new humanized anti-cd20 monoclonal antibody, immu-106, and its use in combination with the humanized anti-cd22 antibody, epratuzumab, for the therapy of non-hodgkin's lymphoma. *Clin Cancer Res*, 10(8):2868–2878.

Storkus, W. J., Alexander, J., Payne, J. A., Dawson, J. R., and Cresswell, P. (1989). Reversal of natural killing susceptibility in target cells expressing transfected class I HLA genes. *Proceedings of the National Academy of Sciences*, 86(7):2361–2364.

Strand, J., Varasteh, Z., Eriksson, O., Abrahmsen, L., Orlova, A., and Tolmachev, V. (2014). Gallium-68-labeled affibody molecule for PET imaging of PDGFRβ expression in vivo. *Mol Pharm*, 11(11):3957–3964.

Strasser, A., Jost, P. J., and Nagata, S. (2009). The many roles of FAS receptor signaling in the immune system. *Immunity*, 30(2):180–92.

Sundarapandiyan, K., Keler, T., Behnke, D., Engert, A., Barth, S., Matthey, B., Deo, Y. M., and Graziano, R. F. (2001). Bispecific antibody-mediated destruction of Hodgkin's lymphoma cells. *J Immunol Methods*, 248(1-2):113–123.

Swaroop, A. and Xu, J. (1993). cDNA libraries from human tissues and cell lines. *Cytogenetic and Genome Research*, 64(3-4):292–294.

Tacke, M., Hanke, G., Hanke, T., and Hünig, T. (1997). CD28-mediated induction of proliferation in resting T cells in vitro and in vivo without engagement of the T cell receptor: evidence for functionally distinct forms of CD28. *Eur J Immunol*, 27(1):239–247.

Taddeo, A., Gerl, V., Hoyer, B. F., Chang, H.-D., Kohler, S., Schaffert, H., Thiel, A., Radbruch, A., and Hiepe, F. (2015). Selection and depletion of plasma cells based on the specificity of the secreted antibody. *Eur J Immunol*, 45(1):317–319.

Takahashi, T., Tanaka, M., Brannan, C. I., Jenkins, N. A., Copeland, N. G., Suda, T., and Nagata, S. (1994). Generalized lymphoproliferative disease in mice, caused by a point mutation in the Fas ligand. *Cell*, 76(6):969–76.

Tang, D., Lotze, M. T., Kang, R., and Zeh, H. J. (2011). Apoptosis promotes early tumorigenesis. *Oncogene*, 30(16):1851–1854.

Tavaré, R., McCracken, M. N., Zettlitz, K. A., Knowles, S. M., Salazar, F. B., Olafsen, T., Witte, O. N., and Wu, A. M. (2014). Engineered antibody fragments for immuno-PET imaging of endogenous CD8+ T cells in vivo. *Proc Natl Acad Sci U S A*, 111(3):1108–1113.

Taylor, R. C., Cullen, S. P., and Martin, S. J. (2008). Apoptosis: controlled demolition at the cellular level. *Nat Rev Mol Cell Biol*, 9(3):231–241.

Thompson, A. J., Giovannoni, G., et al. (2013). Removal of access to alemtuzumab for patients with aggressive multiple sclerosis. *BMJ*, 346.

Traggiai, E., Becker, S., Subbarao, K., Kolesnikova, L., Uematsu, Y., Gismondo, M. R., Murphy, B. R., Rappuoli, R., and Lanzavecchia, A. (2004). An efficient method to make human monoclonal antibodies from memory B cells: potent neutralization of SARS coronavirus. *Nat Med*, 10(8):871–875.

Trauth, B. C., Klas, C., Peters, A. M., Matzku, S., Moller, P., Falk, W., Debatin, K. M., and Krammer, P. H. (1989). Monoclonal antibody-mediated tumor regression by induction of apoptosis. *Science*, 245(4915):301–5.

Tung, J. W., Parks, D. R., Moore, W. A., Herzenberg, L. A., and Herzenberg, L. A. (2004). Identification of B-cell subsets: an exposition of 11-color (Hi-D) FACS methods. *Methods Mol Biol*, 271:37–58.

van Spriel, A. B., van Ojik, H. H., and van De Winkel, J. G. (2000). Immunotherapeutic perspective for bispecific antibodies. *Immunol Today*, 21(8):391–397.

Vardiman, J. W., Thiele, J., Arber, D. A., Brunning, R. D., Borowitz, M. J., Porwit, A., Harris, N. L., Le Beau, M. M., Hellström-Lindberg, E., Tefferi, A., and Bloomfield, C. D. (2009). The 2008 revision of the World Health Organization (WHO) classification of myeloid neoplasms and acute leukemia: rationale and important changes. *Blood*, 114(5):937–951.

Vidal, L., Gafter-Gvili, A., Gurion, R., Raanani, P., Dreyling, M., and Shpilberg, O. (2012). Bendamustine for patients with indolent B cell lymphoid malignancies including chronic lymphocytic leukaemia. *Cochrane Database Syst Rev*, 9:CD009045.

Vugmeyster, Y., Kikuchi, T., Lowes, M. A., Chamian, F., Kagen, M., Gilleaudeau, P., Lee, E., Howell, K., Bodary, S., Dummer, W., and Krueger, J. G. (2004). Efalizumab (anti-CD11a)-induced increase in peripheral blood leukocytes in psoriasis

patients is preferentially mediated by altered trafficking of memory CD8+ T cells into lesional skin. *Clin Immunol*, 113(1):38–46.

Wajant, H. (2006). CD95L/FasL and TRAIL in tumour surveillance and cancer therapy. *Cancer Treat Res*, 130:141–165.

Wakasugi, K. and Schimmel, P. (1999). Two distinct cytokines released from a human aminoacyl-tRNA synthetase. *Science*, 284(5411):147–151.

Watanabe-Fukunaga, R., Brannan, C. I., Copeland, N. G., Jenkins, N. A., and Nagata, S. (1992). Lymphoproliferation disorder in mice explained by defects in Fas antigen that mediates apoptosis. *Nature*, 356(6367):314–7.

Wehrli, P., Viard, I., Bullani, R., Tschopp, J., and French, L. E. (2000). Death receptors in cutaneous biology and disease. *J Invest Dermatol*, 115(2):141–148.

WHO/Europe (2016). Cancer. http://www.euro.who.int/en/health-topics/noncommunicable-diseases/cancer/cancer (date of request: 05/2016).

Wilson, N. S., Dixit, V., and Ashkenazi, A. (2009). Death receptor signal transducers: nodes of coordination in immune signaling networks. *Nat Immunol*, 10(4):348–355.

Wines, B. D., Powell, M. S., Parren, P. W., Barnes, N., and Hogarth, P. M. (2000). The IgG Fc contains distinct Fc receptor (FcR) binding sites: the leukocyte receptors Fc gamma RI and Fc gamma RIIa bind to a region in the Fc distinct from that recognized by neonatal FcR and protein A. *J Immunol*, 164(10):5313–5318.

Wisloff, F., Michaelsen, T. E., and Froland, S. S. (1974). Inhibition of antibody-dependent human lymphocyte-mediated cytotoxicity by immunoglobulin classes, IgG subclasses, and IgG fragments. *Scand J Immunol*, 3(1):29–38.

Wörn, A. and Plückthun, A. (2001). Stability engineering of antibody single-chain Fv fragments. *J Mol Biol*, 305(5):989–1010.

Woyach, J. A., Awan, F., Flinn, I. W., Berdeja, J. G., Wiley, E., Mansoor, S., Huang, Y., Lozanski, G., Foster, P. A., and Byrd, J. C. (2014). A phase I trial of the Fc-engineered CD19 antibody XmAb5574 (MOR00208) demonstrates safety and preliminary efficacy in relapsed CLL. *Blood*, 124(24):3553–3560.

Wucherpfennig, K. W. (2001). Mechanisms for the induction of autoimmunity by infectious agents. *J Clin Invest*, 108(8):1097–104.

Wyllie, A. H., Kerr, J. F., and Currie, A. R. (1980). Cell death: the significance of apoptosis. *Int Rev Cytol*, 68:251–306.

Xerri, L., Bouabdallah, R., Devilard, E., Hassoun, J., Stoppa, A. M., and Birg, F. (1998). Sensitivity to Fas-mediated apoptosis is null or weak in B-cell non-Hodgkin's lymphomas and is moderately increased by CD40 ligation. *Br J Cancer*, 78(2):225–232.

Yonehara, S., Ishii, A., and Yonehara, M. (1989). A cell-killing monoclonal antibody (anti-Fas) to a cell surface antigen co-downregulated with the receptor of tumor necrosis factor. *J Exp Med*, 169(5):1747–56.

Zandman-Goddard, G. and Shoenfeld, Y. (2002). Hiv and autoimmunity. *Autoimmun Rev*, 1(6):329–337.

Zelenetz, A. D., Wierda, W. G., Abramson, J. S., Advani, R. H., Andreadis, C. B., Bartlett, N., Bellam, N., Byrd, J. C., Czuczman, M. S., Fayad, L. E., Glenn, M. J., Gockerman, J. P., Gordon, L. I., Harris, N. L., Hoppe, R. T., Horwitz, S. M., Kelsey, C. R., Kim, Y. H., Krivacic, S., LaCasce, A. S., Nademanee, A., Porcu, P., Press, O., Pro, B., Reddy, N., Sokol, L., Swinnen, L., Tsien, C., Vose, J. M., Yahalom, J., Zafar, N., Dwyer, M. A., Naganuma, M., and , N. C. C. N. (2013). Non-Hodgkin's lymphomas, version 1.2013. *J Natl Compr Canc Netw*, 11(3):257–72; quiz 273.

Zhang, J., Xu, X., and Liu, Y. (2004). Activation-induced cell death in T cells and autoimmunity. *Cell Mol Immunol*, 1(3):186–192.

Chapter 6

Appendix

6.1 List of abbreviations

°C	Degree Celsius
7-AAD	7-aminoactinomycin D
a.a.	Amino acid
ADCC	Antibody-dependent cellular cytotoxicity
AICD	Activation-induced cell death
ALL	Acute lymphocytic leukaemia
AML	Acute myeloid leukaemia
Amp	Ampicillin
APC	Allophycocyanin
BCR	B-cell receptor
BSA	Bovine serum albumin
bp	Base pair
BTK	Bruton's tyrosine kinase
CAR	Chimeric antigen receptors
CDC	Complement dependent cytotoxicity
CDR	Complementarity-determining regions
CIP	Calf Intestinal phosphatase
CLL	Chronic lymphocytic leukaemia
cm	Centimetre
C-Terminus	Carboxy-Terminus
CTLs	Cytotoxic T lymphocytes
CSPG4	Chondroitin sulfate proteoglycan 4
Da	Dalton
DAMPs	Damage-associated molecular patterns
DD	Death domain
ddH_2O	Double-distilled water
DED	Death effector domain
DLBCL	Diffuse large B-cell lymphoma
DMSO	Dimethyl Sulfoxide
DNA	Deoxyribonucleic acid
DPBS	Dulbecco's phosphate buffered saline
DR	Death receptor
dsDNA	Double stranded deoxyribonucleic acid
EDTA	Ethylenediaminetetraacetic acid
EGFR	Epidermal growth factor receptor
ELISA	Enzyme-linked immunosorbend assay
EtBr	Ethidium bromide
FACS	Fluorescence activated cell sorter
FCS	Fetal calf serum
G418	Geneticin
GMP	Good Manufacturing Practice
$\times g$	Times Earth's gravitational force
HRP	Horseradish peroxidase
IMDM	Iscove's Modified Dulbecco's Medium
i.v.	Intravenously

Kan	Kanamycin
kb	Kilobase
kDa	Kilodalton
M	Mol
MCL	Mantle cell lymphoma
MFI	Mean fluorescence intensity
mL	Millilitre
MOPS	3-(N-morpholino)propanesulfonic acid
MW	Molecular weight
MWCO	Molecular weight cut off
μCi	Microcurie
μF	Microfarad
μg	Microgram
μL	Microliter
μM	Micromol
N-Terminus	Amino-Terminus
NHL	Non-Hodgkin's lymphomas
NK	Natural killer cells
nm	Nanometer
O.D.	Optical density
PBMC	Peripheral blood mononuclear cells
PBL	Peripheral blood leukocytes
PMNs	Polymorphonuclear leukocytes
PP	Polypropylen
PS	Polystyrol
PWM	Pokeweed mitogen
RBC	Red blood cells
RPMI	Roswell Park Memorial Institute
ScFv	Single chain Fragment variable
SDS-PAGE	Sodium dodecyl sulfate Polyacrylamide gel electrophoresis
SEC	Size exclusion chromatography
SLE	Systemic lupus erythematosus
PET	Positron emission tomography
TAA	Tumour associated antigen
TAE	Tris-acetate-EDTA
T_{DTH}	Delayed type hypersensitivity T-cells
TLR	Toll-like receptor
TMB	3,3',5,5'-Tetramethylbenzidine
TNF-α	Tumor necrosis factor-α
U	Unit
UV	Ultraviolet
V	Volt
v/v	Volume/Volume
w/v	Weight/Volume

6.2 Single letter amino acid code

A	Alanine
R	Arginine
N	Asparagine
D	Aspartic Acid
C	Cysteine
Q	Glutamine
E	Glutamic Acid
G	Glycine
H	Histidine
I	Isoleucine
L	Leucine
K	Lysine
M	Methionine
F	Phenylalanine
P	Proline
S	Serine
T	Threonine
W	Tryptophan
Y	Tyrosine
V	Valine

6.3 Antibody sequences

Mouse anti-human CD95 (APO-1) V_H:
EVQLVETGGGLVQPKGSLKLSCAASGFTFNTNAMNWVRQAPGKGLEWVA
RIRSKSNNYATYYAESVKDRFTISRDDSQSMLYLQMNNLKAEDTAMYYCVT
DGYYWGQGTTLTVSS

Mouse anti-human CD95 (APO-1) V_L:
DIVLTQSPASLAVSLGQRATISCRASESVEYYGTSLMQWYQQKPGQPPKLLI
YVASNVESGVPARFSGSGSGTDFSLNIHPVEEDDIAMYFCQQSTKVPWTFG
GGTKLEIK

6.4 Supplementary figures

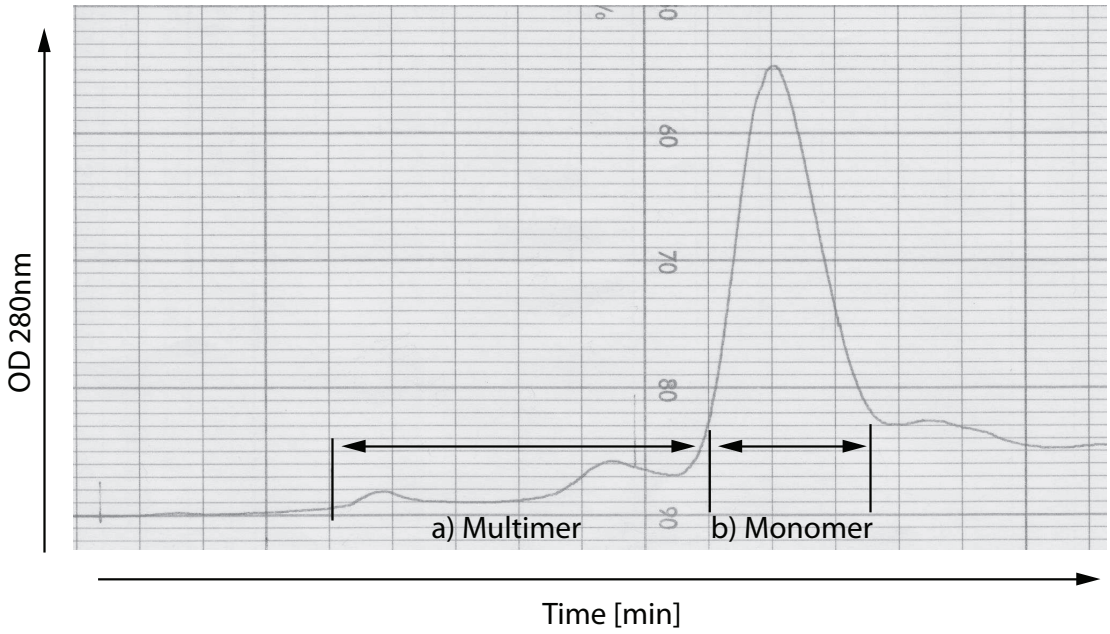

Figure 6.1: **Preparative size exclusion chromatography of BS95Mel**
A representative purification of the recombinant BS95Mel after initial KappaSelect purification. Approx. 2 mg of protein were separated using FPLC system (Pharmacia LKB Biotechnology) equipped with Superdex™ 200 Prep Grade 16/60 HiLoad column as described in section 2.4.1.2 on page 49.

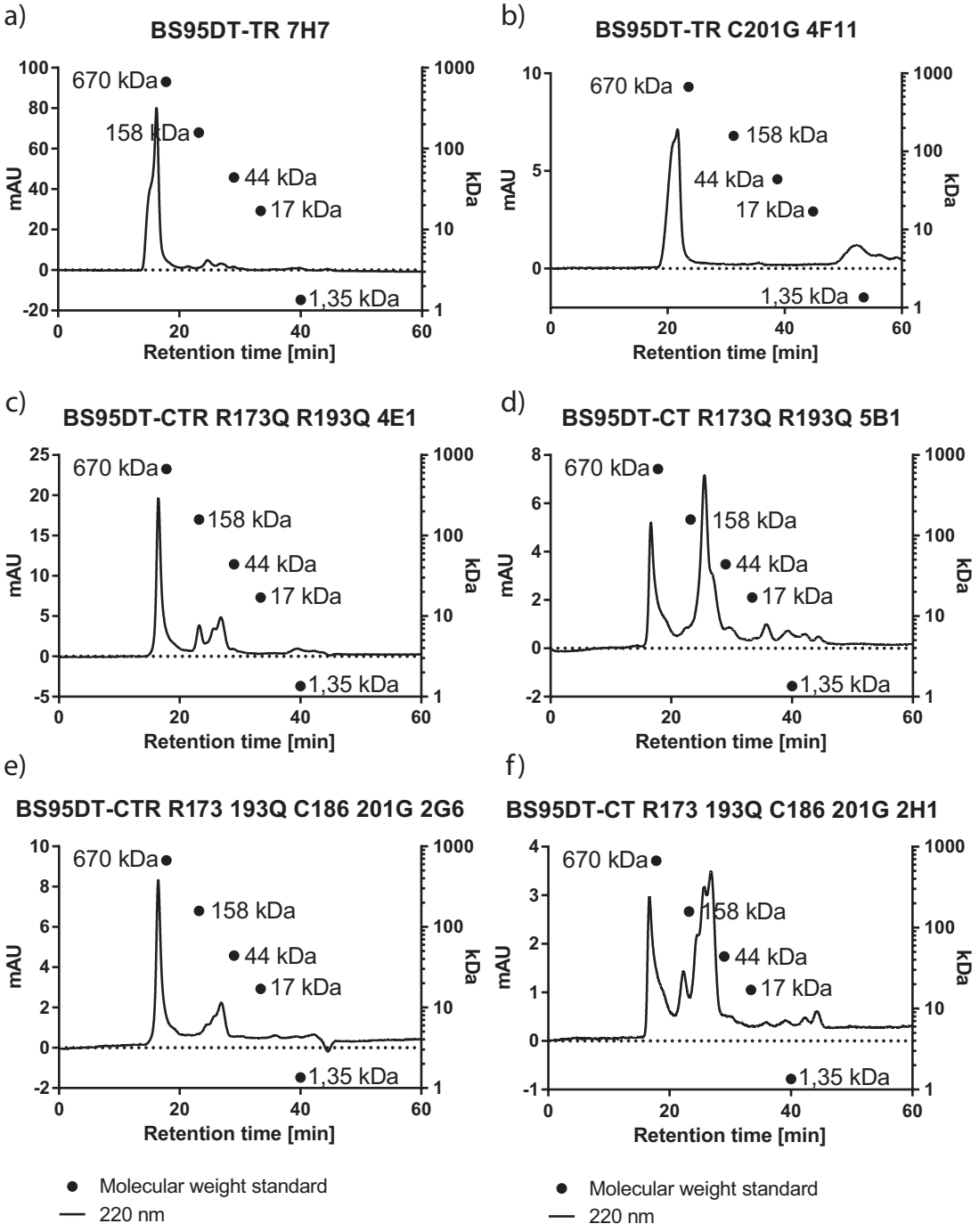

Figure 6.2: **Analytical size exclusion chromatography of different BS95DT fusion proteins after KappaSelect purification**
a) BS95DT-TR (clone 7H7) fusion protein containing T (transmembrane) and R (receptor-binding) domains of Diphtheria toxin mutant CRM197 on the C-terminus of the heavy chain. b) BS95DT-TR$_{C201G}$ (clone 4F11) containing T and R domains. c) BS95DT-CTR$_{R173Q\,R193Q}$ (clone 4E1) containing C (catalytic), T and R domains. d) BS95DT-CT$_{R173Q\,R193Q}$ (clone 5B1) containing C and T domains. e) BS95DT-CTR$_{R173Q\,R193Q\,C186G\,C201G}$ (clone 2G6) containing C, T and R domains. f) BS95DT-CT$_{R173Q\,R193Q\,C186G\,C201G}$ (clone 2H1) containing C and T domains. 10 μg of purified fusion proteins were separated using a Dionex™ UltiMate™ 3000 BioRS system equipped with Superdex 200™ increase 10/300 GL column.

Acknowledgements

First of all I want to express my gratitude to Prof. Hans-Georg Rammensee. Thank You for constructive discussion, suggestions and all the inspiring and demanding ideas. Also thank You for keeping the work atmosphere in this department very productive and friendly.

I do want to thank Prof. Gundram Jung for giving me the opportunity to do my PhD thesis in this laboratory and for providing me with an interesting project. Thank You for the willingness to accept me in Your research group and for Your guidance with helpful ideas and discussions. Thank You also for critically reviewing this thesis and the useful comments and suggestions.

Thanks to Dr. Ludger Grosse-Hovest and Dr. Berit Lochmann for supervising and consulting me in the field of molecular biology and protein engineering.

Special thanks to Dr. Martin Hofmann for introducing me into the world of flow cytometry and consulting me in all the questions regarding experiment performance and evaluation.

I also thank our wonderful technicians: Beate Pömmerl for outstanding animal husbandry, support in cloning experiments and introducing me into the Swabian culture; and Carolin Walker for skilful technical assistance and creating a good mood in the laboratory.

I would not have been able to perform my experiments and write this thesis without a numerous blood donors. Especially, without my "special" tetanus donors! Thanks to all people in the department of Immunology for providing me with blood samples.

Thanks to Dr. Sebastian Haen and to the bone marrow transplantation department in Tübingen for providing me with healthy bone marrow samples.

Finally I want to acknowledge actual and former members of AG Jung: Dr. Berit Lochmann, Dr. Latifa Zekri-Metref, Fabian Vogt, Dr. Martin Pflügler, Timo Manz, Carolin Walker, Lukas Osburg as well as Dr. Gregor Neumann, Dr. Cornelia Lindner, Dr. Martin Hofmann, Dr. Karolin Schwarz and Dr. Michael Durben. Thank you for the support in the lab routine, all the discussions, coffee breaks and for a productive and pleasant working atmosphere.